AD-A043 003 NEW MEXICO UNIV ALBUQUERQUE ERIC H WANG CIVIL ENGINE--ETC F/G 13/2
PAVEMENT EVALUATION SYSTEM.(U)
OCT 76 J P NIELSEN, G T BAIRD F29601-76-C-0015
UNCLASSIFIED CERF-AP-20 AFCEC-TR-76-28 NL

1 OF 2
AD
A043003

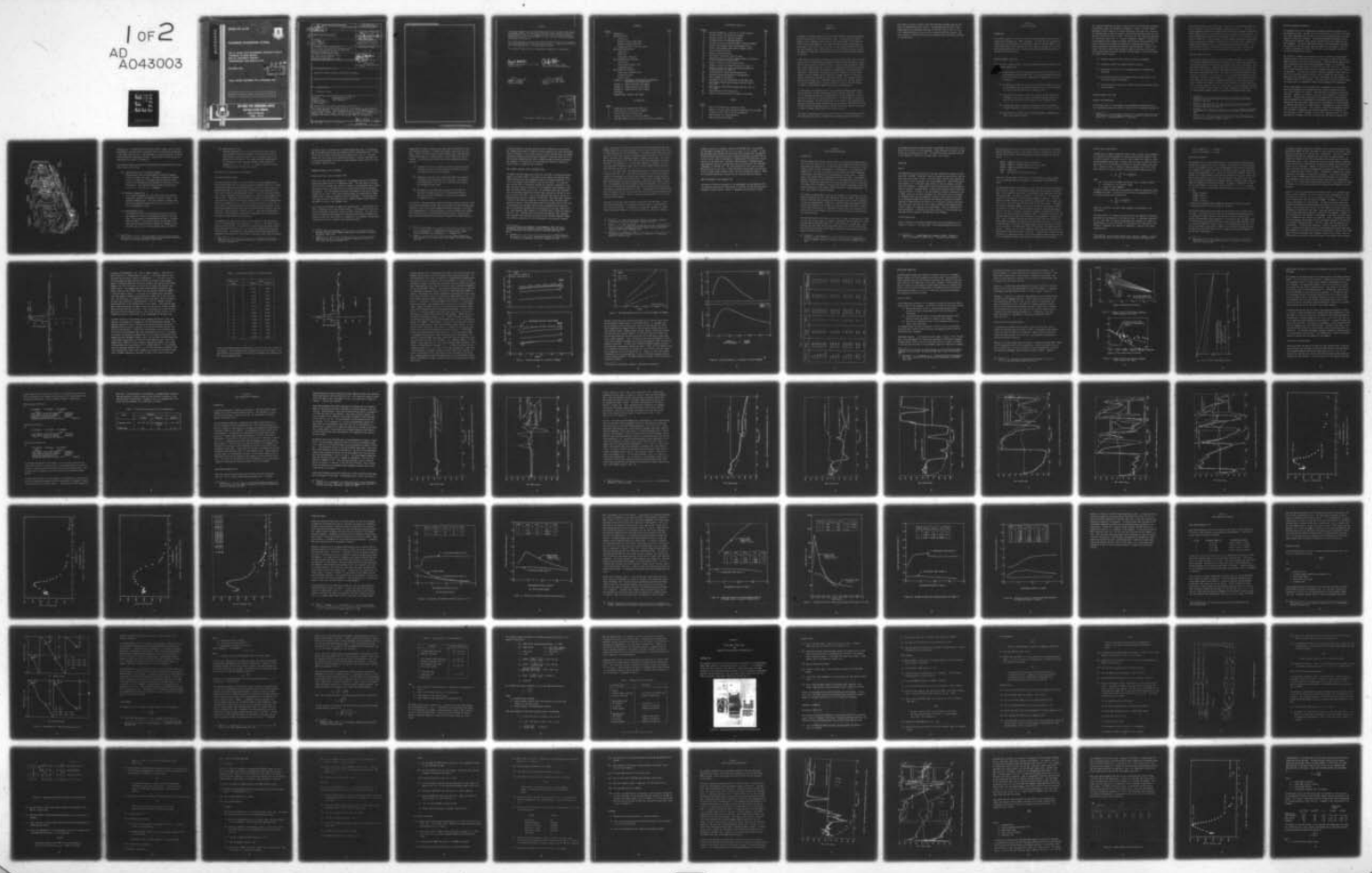

AFCEC-TR-76-28

PAVEMENT EVALUATION SYSTEM

ERIC H. WANG CIVIL ENGINEERING RESEARCH FACILITY
UNIVERSITY OF NEW MEXICO
BOX 25, UNIVERSITY STATION
ALBUQUERQUE, NEW MEXICO 87131

OCTOBER 1976

FINAL REPORT: DECEMBER 1975-SEPTEMBER 1976

Approved for public release; distribution unlimited.

AIR FORCE CIVIL ENGINEERING CENTER
(AIR FORCE SYSTEMS COMMAND)
TYNDALL AIR FORCE BASE
FLORIDA 32403

REPORT DOCUMENTATION PAGE		READ INSTRUCTIONS BEFORE COMPLETING FORM
1. REPORT NUMBER AFCEC TR-76-28	2. GOVT ACCESSION NO.	3. RECIPIENT'S CATALOG NUMBER
4. TITLE (and Subtitle) PAVEMENT EVALUATION SYSTEM		5. TYPE OF REPORT & PERIOD COVERED Final rept. 1 Dec 1975 — 30 Sept 1976 6. PERFORMING ORG. REPORT NUMBER CERF-AP-20
7. AUTHOR(s) John P. Nielsen Glenn T. Baird		8. CONTRACT OR GRANT NUMBER(s) F29601-76-C-0015
9. PERFORMING ORGANIZATION NAME AND ADDRESS Eric H. Wang Civil Engineering Research Facility, University of New Mexico, Box 25, University Station, Albuquerque, NM 87131		10. PROGRAM ELEMENT, PROJECT, TASK AREA & WORK UNIT NUMBERS T.D. 5.01
11. CONTROLLING OFFICE NAME AND ADDRESS Air Force Civil Engineering Center Air Force Systems Command Tyndall Air Force Base, FL 32401		12. REPORT DATE October 1976 13. NUMBER OF PAGES 108 p.
14. MONITORING AGENCY NAME & ADDRESS (if different from Controlling Office)		15. SECURITY CLASS. (of this report) Unclassified 15a. DECLASSIFICATION/DOWNGRADING SCHEDULE --

16. DISTRIBUTION STATEMENT (of this Report)

Approved for public release; distribution unlimited.

17. DISTRIBUTION STATEMENT (of the abstract entered in Block 20, if different from Report)

18. SUPPLEMENTARY NOTES

Available in DDC

19. KEY WORDS (Continue on reverse side if necessary and identify by block number)

Pavements
Pavement Design
Pavement Evaluation
Finite Elements
Nondestructive Testing
Wave Propagation

20. ABSTRACT (Continue on reverse side if necessary and identify by block number)

This report describes the current (1976) Air Force method for load evaluation of airfield pavements. The technique makes use of wave-propagation data and finite-element computer codes to determine the load capacity of pavements. The computer code also provides an estimate of the remaining service life of the pavement from failure criteria for the various layers of the pavement.

400 976

DD FORM 1 JAN 73 1473 EDITION OF 1 NOV 65 IS OBSOLETE

UNCLASSIFIED

SECURITY CLASSIFICATION OF THIS PAGE (When Data Entered)

PREFACE

This report documents work performed during the period 1 December 1975 through 30 September 1976 by the University of New Mexico under contract F-29601-76-C-0015 with the Air Force Civil Engineering Center, Air Force Systems Command, Tyndall Air Force Base, Florida 32401. Lt. Col. George D. Ballentine managed the program for the Center.

This report has been reviewed by the Information Officer (IO) and is releasable to the National Technical Information Service (NTIS). At NTIS it will be available to the general public, including foreign nations.

This technical report has been reviewed and is approved for publication.

George D. Ballentine
GEORGE D. BALLENTINE, Lt. Col., USAF
Project Officer

GUY P. YORK, Lt. Col., USAF
Director of Engineering Materials

ROBERT E. BRANDON
Technical Director

ROBERT M. ITEN, Col., USAF
Commander

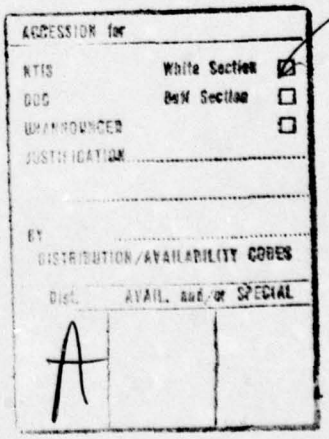

(The reverse of this page is blank)

CONTENTS

ILLUSTRATIONS

ILLUSTRATIONS (Concl'd)

TABLES

SECTION 1
INTRODUCTION

A problem of continual concern to the Air Force relates to determining how new and existing aircraft affect airfield pavements. Two questions are usually asked: (1) can a pavement support the aircraft? and (2) what is the remaining service life of the pavement? The former question concerns the assigned mission capability of a given facility; that is, can a given pavement safely support an assigned aircraft, the B-52 for example? The latter question concerns the number of times the assigned aircraft can safely operate from the pavement in question.

Historically, two different techniques have been used to answer these questions--namely, empirical relationships developed through airfield performance studies, and full-scale testing of pavement sections. Both of these techniques, however, have serious deficiencies for a user who is required to maintain airfield pavements under a wide variety of geotechnical, geographical, and climatological conditions. Additionally, destructive testing is inherent in both of these methods, and thus runways must be closed for extended periods of time while material samples are gathered for laboratory testing. This process, besides being time consuming, has a significant impact on facility use and requires considerable expenditures for testing and analysis; and at best the underlying theory is questionable, though the results are conservative.

To improve upon the situation the Air Force planned a pavement research program to develop a rational pavement evaluation procedure (1967-69). Central to this procedure was the use of nondestructive testing techniques to obtain the in-situ properties of the paving materials. The advantages of such an approach are obvious: test pits do not have to be placed in the pavement, more data can be obtained during equivalent periods of runway closure thus providing a better measure of pavement material characteristics, and testing can be done at night so runways remain open for use during the day.

This report provides documentation on much of the Air Force sponsored research directed toward developing a nondestructive pavement evaluation procedure. It

also serves as a user's manual on the CERF-developed vibratory testing technique for pavement evaluation studies. The equipment and analytical techniques used in this procedure have been transferred (1975) to the Air Force Civil Engineering Center for use in their pavement evaluation program. Current research is concerned with making the nondestructive evaluation equipment air-transportable.

SECTION 2
HISTORICAL REVIEW

INTRODUCTION

This section presents a historical review of the development of the Air Force's nondestructive pavement test (NDPT) procedure. The need for this procedure coincides with the introduction of wide-bodied, jumbo jet aircraft (1967). The research described in the following paragraphs does not include all of the pavement research sponsored by AFWL; only those projects which relate directly to the NDPT project are covered.

RESEARCH PROGRAM (1967-1969)

AFWL outlined a study to evolve a rational pavement evaluation procedure having the following capabilities:

(1) A technique by which the load-supporting capacity of an existing airfield pavement could be determined. The physical parameters required for this evaluation were to be determined by nondestructive testing techniques.

(2) A technique by which the stresses and strains at a general point within the pavement could be determined when the load is applied through the various gear configurations of modern aircraft.

(3) An analytical procedure by which the influence of the strength and thickness of the various pavement components could be compared in terms of the stress and strain response of the pavement system.

(4) An analytical means of evaluating the useful life of an airfield pavement subjected to repetitive loading and mixed aircraft traffic.

(5) Applicability to both rigid and flexible pavements, composite pavements, and pavement overlays.

This study was approached through a critical review of the literature concerned with pavement design and evaluation procedures, a review of the new computer techniques (finite elements) which were emerging at that time, and a review of the new approaches to material modeling (constitutive equations) which were being used in allied fields of science. The results of this study were published in a two-volume report (ref. 1). Volume I contained a summary of flexible and rigid pavement design methods for highways and airfields and an extensive discussion related to the theoretical approaches to pavement evaluation, including computation techniques and material modeling methods. Volume II outlined a five-year research plan intended to meet the objectives of the nondestructive pavement evaluation procedure outlined above. The following areas of reasearch were proposed:

(1) Computer programs for the structural analysis of pavements

(2) Engineering studies for pavement material modeling

(3) Development of vibratory test equipment and data interpretation techniques

(4) Data collection on aircraft characteristics as they relate to the structural response of pavements

(5) Test and evaluation studies to validate the resulting pavement evaluation procedure

RESEARCH PROGRAM (1970-1974)

Computer Code Development

The principal effort on the computer code development was performed at the Civil Engineering Laboratory (formerly the Naval Civil Engineering Laboratory).

---

1. Nielsen, J. P., *Rational Pavement Evaluation - Review of Present Technology*, AFWL-TR-69-9, Air Force Weapons Laboratory, Kirtland Air Force Base, New Mexico, Vol. I, October 1969; Vol. II, May 1970.

The resulting computer code (AFPAV) was a nonlinear, finite-element program capable of treating single and multiwheeled landing gears (ref. 2). The code is actually composed of three main programs--AFPRE (data input and element generation), AFPAV (equation solving), and AFPOST (recovery of results for plot routines). A detailed AFPAV user's manual has been prepared by CERF (ref. 3). Recently, a code known as AFCAN (ref. 4) was prepared to greatly reduce the manhours and potential errors which occur when AFPAV is implemented in its original form. AFCAN is intended to make AFPAV easy to use in routine pavement evaluation studies. The AFCAN Code also contains the results of the fourth study area outlined above. The most recent modifications of the AFPAV Code are presented in section 3.

Material Modeling Studies

A particularly potential aspect of the finite-element technique is its capability to handle generalized constitutive equations. This means, for example, that the nonlinear stress/strain behavior of subgrade soils can be considered in pavement evaluation analyses. Research conducted at the University of Kentucky for AFWL (ref. 5) was concerned with the development of constitutive equations for base course and subgrade materials. The resulting constitutive equation, known as the *Hardin hyberbolic shear/strain equation*, has been incorporated into the AFPAV Code. With this single equation it is possible to define the shear/strain relationship for base course or subgrade materials for a wide range of conditions, including soil density, saturation, and plasticity, and such load parameters as loading rate and number of loading cycles. CERF has rewritten the general form of Hardin's work so that it is simply inputted to the AFPAV Code. This is accomplished by adding simple soil parameters on the AFCAN data cards.

---

2. Crawford, J. E., *An Analytical Model for Airfield Pavement Analysis*, AFWL-TR-71-70, Air Force Weapons Laboratory, Kirtland Air Force Base, New Mexico, May 1972.
3. Nielsen, J. P., *AFPAV Computer Code for Structural Analysis of Airfield Pavements*, AFWL-TR-75-151, Air Force Weapons Laboratory, Kirtland Air Force Base, New Mexico, October 1975.
4. Crawford, J. E., *Software for Everyday Usage of AFPAV*, Technical Memorandum M-51-76-06, Civil Engineering Laboratory, Port Hueneme, California, March 1976.
5. Hardin, B. O., *Constitutive Relationships for Airfield Subgrade and Base Course Materials*, Technical Report UKY 32-71-CE5, College of Engineering, University of Kentucky, Lexington, Kentucky.

Vibratory Equipment Development

The equipment used in the nondestructive pavement evaluation procedure (fig. 1) was developed at CERF. The NDPT van is 8 ft wide and 35 ft long and is divided into three compartments which contain all the test equipment necessary for nondestructive testing of pavements. The forward generator compartment contains a 100-kW diesel generator which supplies 110/220-V electrical energy for the test equipment. The center compartment contains the electromagnetic vibrator, the vibrator oil-cooling system, the power supply for the vibrator field coil, a step-up transformer to convert 220 V to 440 V, and a hydraulic system for raising and lowering the vibrator.

The vibrator is lowered by two hydraulic jacks into position on the pavement through a hatch in the floor of the van. A large mass is used to keep the vibrator baseplate in contact with the pavement. The mass/vibrator system weighs 6750 lb and comes into contact with the pavement through a 12-in-diameter baseplate. The vibrator consists of armature coils and field coils. The electrical field moves the armature, which is connected through three load cells to the baseplate. The load cells are used to measure the dynamic load, which can be varied sinusoidally about the static load up to 5000 lb, peak to peak. A sweep oscillator servomechanism is used to continuously vary the frequency of the dynamic load from 10 to 3500 Hz. The output from a velocity pickup located in the baseplate is integrated to obtain the displacement of the baseplate.

The aft compartment of the van contains the instrumentation, recording and monitoring equipment, and the power amplifier console and sweep oscillator servo, which control the vibrator. Instrumentation is provided for measuring the force, frequency, acceleration, velocity, and displacment of the vibrator baseplate. The vertical acceleration of the pavement at selected distances from the baseplate can be measured by accelerometers which are epoxied to the pavement and the phase angle between any two accelerometers can be determined by inputting the signals to a phase computer. Geophones can be used to obtain data on the deflection basin. The recording and monitoring equipment consists of a 14-channel, FM magnetic tape recorder/reproducer, an X-Y recorder, an oscilloscope, a digital voltmeter, and a digital frequency counter. A servomechanism on the sweep oscillator is used to hold the load or frequency at a

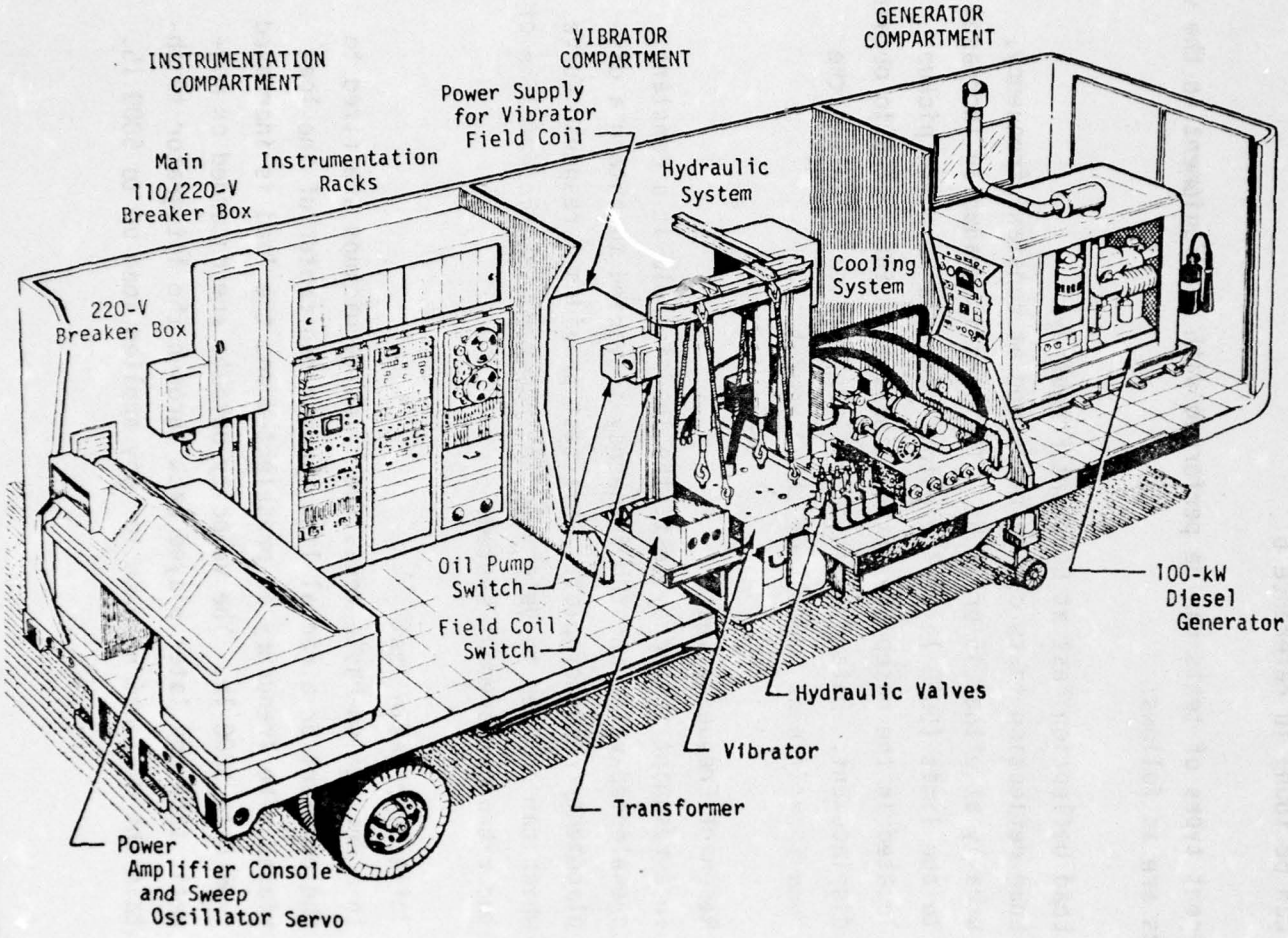

Figure 1. Nondestructive Pavement Test (NDPT) Van

desired level. The power amplifier console contains readout units for load, displacement, and acceleration, and panel meters to observe any malfunctions in the power amplifier unit. The compartment is also equipped with a heating/cooling system for temperature control. Further details on the van and its operation can be found in reference 6.

Four different types of tests can be performed with the equipment in the van. These tests are as follows:

(1) Load Deflection Test at Constant Frequency

Load deflection tests can be performed at constant frequency, usually at either 15 or 25 Hz. The load is gradually increased to the limit (5000 lb). The output from the velocity pickup located in the baseplate of the vibrator is integrated to obtain displacement. Data from this test are used to calculate the *dynamic stiffness modulus* of the pavement.

(2) Resonant Frequency Test

In a resonant frequency test, the load is held at a constant, preselected value and the frequency is varied to obtain a displacement/frequency plot. This test provides a response curve which can be used to determine the *resonance characteristics* of the vibrator/pavement system.

(3) Deflection-Basin Test

In a deflection-basin test, the velocity pickups are fixed to the pavement on a radial line through the center of the load plate. The frequency is preselected and the load is increased from 0 to 5000 lb. The velocity outputs are recorded on magnetic tape and later played back through the integrator to obtain the *deflection basin* for any applied load up to 5000 lb.

---

6. Baird, Glenn T., et al., *Instruction Manual for Mobile Nondestructive Vibratory Test Equipment*, AFWL-TR-74-301, Air Force Weapons Laboratory, Kirtland Air Force Base, New Mexico, August 1975.

(4) Wave Propagation Test

The wave propagation test is the principal test used in the Air Force pavement evaluation procedure. In this test the load is held constant, usually at 1000 lb, and a frequency sweep is conducted from 10 to 3500 Hz. The signals from the accelerometers are recorded and later processed through a phase computer to produce a *phase angle/frequency plot*, which is used to construct a dispersion curve for each test station.

See section 4 for details on data reduction.

Test and Evaluation Studies

Test and evaluation studies to verify the NDPT procedure proceeded slowly. The principal reason for this cautious approach concerned the use of a concept (vibratory testing) which had the theoretical potential of being useful but had only been used in a limited manner in pavement studies and often with either conflicting or noninterpretable results. An initial evaluation effort (ref. 7) was concerned with the construction of a special test pavement at the CERF facility. Three test sections were built--one of Portland cement concrete and two of asphalt concrete over a deep uniform silty clay subgrade with a CBR in the range of 8 to 12. These test sections served as a facility on which vibratory testing procedures with the NDPT van were formalized. Phase velocity/wavelength relationships were determined from the vibratory data and these were used to construct dispersion curves. These tests indicated the usefulness of the vibratory procedure and suggested certain modifications in equipment and data interpretation techniques.

Subsequently, the test van was taken to seven airbases in the southwest for test and evaluation under field conditions. A series of CERF letter reports summarizes these studies. This road tour revealed certain equipment problems--mainly the inability of the *bench stock* electronic components to withstand road vibrations. On the positive side the tour verified the suggested test procedures and revealed that interpretable dispersion curves could be obtained.

---

7. Rao, H. A. B., *Nondestructive Evaluation of Airfield Pavements (Phase I)*, AFWL-TR-71-75, Air Force Weapons Laboratory, Kirtland Air Force Base, New Mexico, December 1971.

Two other field test programs which provided useful data later in the development of the NDPT program were the pavement distress investigation (ref. 8) and the WES multiple-wheel, heavy gear-load pavement tests (ref. 9). The major objective of the former was to establish parameters to predict remaining life in an existing pavement; the latter provided subgrade failure criteria for the wide-bodied, jumbo aircraft.

PAVEMENT RESEARCH (1974 TO PRESENT)

Program Evaluation (July to October 1974)

Before July 1974, the various elements of the pavement evaluation development program proceeded primarily as independent tasks. This was necessary because each of the five program areas called for research and development which pushed the state-of-the-art and thus called for creative and original technological developments. With the apparent successful development of the various program elements by July 1974, efforts were directed toward the organization of these elements into a composite pavement evaluation procedure. This program direction occurred nearly simultaneously with a complete change in CERF technical personnel in the soils and pavements area.

For the new CERF personnel to comply with the directive, it was necessary for them to thoroughly review the previous efforts. Initial work was directed toward a review and evaluation of some of the NDPT field data. This was a particularly important task because conflicting results had been informally presented and there was some concern as to whether or not vibratory testing could effectively be used for pavement load evaluation studies.

---

8. O'Brien, Ken, and Associates, *Distress Criteria for Pavement Systems*, AFWL-TR-73-226, Air Force Weapons Laboratory, Kirtland Air Force Base, New Mexico, April 1974.
9. Hammitt, G. M., et al., *Multiple-Wheel Heavy Gear Load Pavement Tests*, AFWL-TR-70-113, Vol. IV, Air Force Weapons Laboratory, Kirtland Air Force Base, New Mexico, November 1971.

Another area of concern related to the shear moduli obtained from vibratory testing on pavements; in general the modulus values were much too large. After a review of these and other problem areas, CERF presented a briefing at AFWL late in August 1974 to discuss some of the project findings. The following significant points were presented during this briefing:

(1) A review of test data collected at Altus Air Force Base indicated that the data could be organized to conform to that of a forced vibrator with viscous damping.

(2) Theoretical considerations revealed that NDPT data should be corrected before shear moduli are calculated. (This would yield lower moduli; but, the form of the correction factors was not known at that time.)

(3) Differences in the NDPT data collected with the CERF van and that collected by WES (ref. 10) could be explained on the basis of certain theoretical considerations presented by Lysmer (ref. 11).

As a result of the above points, some of the former concerns relative to NDPT testing were eliminated and CERF took the position that sufficient data were available to form a provisional pavement evaluation procedure. The procedure recommended was a structural approach in which nondestructive pavement testing would provide in-situ material properties data. These data and the aircraft load characteristics would be inputted to the AFPAV Code for

---

10. Hall, J. W. and Green, J. L., *Nondestructive Vibratory Testing of Airport Pavements, Vol. I, Evaluation Methodology and Experimental Test Results*, FAA Report, U.S. Department of Transportation, Federal Aviation Administration, Washington, D.C., December 1973.

11. Lysmer, J., *Vertical Motion of Rigid Footings*, Contract Report No. 3-115, University of Michigan, ORA Project 05366, Ann Arbor, Michigan, June 1975.

structural analysis, and then certain critical stresses and strains would be reviewed with respect to material failure properties to predict permitted aircraft coverages. Also in the briefing,* certain problem areas that needed additional review were outlined and an approach to meet the directive of organizing the program elements into a workable pavement evaluation procedure was suggested. Following this briefing CERF was directed to formulate a specific plan to accomplish this objective.

NDPT Program (October 1974 to November 1975)

In October 1974 CERF negotiated a work unit with AFWL to continue the development of the NDPT project. The thrust of this effort was directed toward organizing the provisional pavement evaluation procedure suggested as a result of the previous three months of work on the project. This new work unit directed CERF to thoroughly evaluate the electronic components in the NDPT van and to replace with more reliable components those equipment items which had often failed on road trips. An additional effort was concerned with the detailed evaluation of the NDPT data collected on the earlier evaluation trips (circa 1973). This review indicated that some of the earlier data were poor because of equipment malfunctions. More importantly, however, a review of the good data suggested a procedure by which the shear moduli could be corrected. CERF also demonstrated that the NDPT data could be used in conjunction with the AFPAV Code to predict pavement deflections which were in substantial agreement with those measured on the test runways (ref. 8). CERF presented these findings in a briefing report to AFWL on January 2, 1975 (ref. 12). Although these results were encouraging, CERF suggested that a second field evaluation trip would verify the data reduction scheme and provide an opportunity to test and evaluate a wide range of pavement

*This briefing was also presented to the Commander, AFCEC and the Directorate of Engineering Materials, Tyndall Air Force Base on October 17, 1974 because of the planned transfer of AFWL/DEZ activities to AFCEC.

12. Nielsen, J. P., *Develop Pavement Evaluation System*, Progress Report No. 3 (T.D. 5.11/00), Civil Engineering Research Facility, University of New Mexico, Albuquerque, New Mexico, December 30, 1974.

types. For example, the previous surveys did not include pavements with stabilized base courses, complex pavement cross-sections involving multiple layers, or those resulting from overlay operations. Accordingly, CERF submitted a test plan (ref. 13) to AFWL to perform pavement evaluation studies at six Air Force Bases: Williams, Luke, Holloman, Laughlin, Cannon, and Kirtland. This plan was approved on February 23, 1975; the field work was completed by the end of May, 1975. The analyses of these data were completed in November, at which time the authors presented a paper (ref. 14) which summarized the results of the field tests at the *Symposium on Nondestructive Test and Evaluation of Airport Pavements* held at WES. An enlarged discussion of these results was published in 1976 (ref. 15). These tests demonstrated an excellent correlation between field-measured deflections (under actual aircraft loading) and those predicted by the AFPAV Code with NDPT data. These results suggested that the data-interpretation and correction procedures were valid and, thus, a reasonably valid pavement evaluation procedure could be formulated. As a result of the successful evaluation of the NDPT data from the second field trip, plans were made to transfer the NDPT van to AFCEC. Accordingly, AFCEC personnel were given training on the use of the van and the van was officially transferred to AFCEC on October 9, 1975. AFCEC is currently using the NDPT van in its pavement evaluation program.

One area of particular concern was the reduction of the NDPT data. During the field testing phase of a pavement evaluation study, a large amount of data is easily acquired. The reduction of these data represents a significant investment of manhours, so much so that CERF was directed to develop

---

13. Nielsen, J. P., CERF letter to Major George D. Ballentine, AFWL/DEZ, Kirtland Air Force Base, New Mexico, February 20, 1975.

14. Nielsen, J. P., and Baird, Glenn T., *Air Force System for Nondestructive Testing of Pavements*, Symposium on Nondestructive Test and Evaluation of Airport Pavements, Waterways Experiment Station, Corps of Engineers, Vicksburg, Mississippi, November 1975.

15. Nielsen, J. P., and Baird, Glenn T., *Nondestructive Pavement Load Rating*, Thirteenth Paving Conference, University of New Mexico, Albuquerque, New Mexico, January 1976.

computer routines for automatic reduction of the NDPT data. This problem was thoroughly reviewed with the *Analog-to-Digital Section* of AFWL. It soon became evident that although the field data could be digitized, no automatic (computer-based) techniques existed or could be developed to provide the *engineering judgment* which is necessary to interpret the field data prior to computation by the AFPAV Code. Therefore, CERF developed a laboratory-based, data-reduction electronic package which can be used to reduce the field data independent of the NDPT van. This setup permits the field crews to gather NDPT data with the van, while a laboratory-based crew proceeds with the preparation of phase angle/frequency plots used in the evaluation studies. Appendix A contains operational instructions for the data reduction package.

NDPT Developments Since November 1975

The thrust of the work subsequent to the developments through November 1975 has been concerned with the finalization of the NDPT test and data evaluation procedures and the orderly transfer of equipment and technology to AFCEC.

SECTION 3
AFPAV CODE MODIFICATIONS

INTRODUCTION

The AFPAV Code, which performs stress/strain calculations on pavements subjected to aircraft loading (ref. 16), has been used extensively by CERF during the development and evaluation of the NDPT procedure. AFPAV is a nonlinear, finite-element program in which the pavement is represented as a two-dimensional extended solid. The code is capable of treating both single and multiwheeled landing gears; tire loadings are represented by a Fourier series. A preprocessor code, AFPRE, formats pavement and load data for AFPAV. Unfortunately, however, preparation of the AFPRE data is a very cumbersome, error-prone task. Therefore, to make the code easier to use and to provide a means of predicting the fatigue life of pavements, two major modifications were added to the AFPAV Code--a preprocessor code known as AFCAN and material fatigue subroutines. The latter were placed in subroutine RESULT.

The computer program AFCAN, written by John Crawford of CEL provides a simpler means of obtaining the input data required for AFPRE and AFPAV. As originally written, AFCAN was used to generate the AFPRE data cards which were subsequently used to implement AFPAV. AFCAN also contained a data check subroutine which insured that reasonable and complete data were introduced into AFPRE. However, before AFCAN could be used for operational studies, the values assigned to its variables had to be reviewed to assure the user that realistic stress analyses were being performed.

The code modifications described in this report include the enlargement of AFCAN to cover more aircraft than it originally covered and the incorporation of AFCAN into the code so that AFPAV would operate efficiently as a single code. Thus, AFCAN permits the highly sophisticated AFPAV Code to be used for routine pavement evaluation work when a large number of AFPAV runs must be made for a wide range of military aircraft.

---

16. Crawford, J., and Pichumani, R., *Finite-Element Analysis of Pavement Structures Using AFPAV Code (Nonlinear Elastic Analysis)*, AFWL-TR-74-71, Air Force Weapons Laboratory, Kirtland Air Force Base, New Mexico, April 1975.

Any pavement evaluation program includes both pavement load rating and an estimate of the fatigue life of the pavement. AFPAV performed the former, but the latter had to be added to the code. The material fatigue considerations used in this addition to AFPAV are also described in this section.

AFCAN CODE

General

The AFCAN Code increases efficiency in the data preparation required to implement AFPRE and AFPAV. AFCAN has a series of subroutines which contain the constants for a particular aircraft: tire print data, aircraft load characteristics, Fourier series parameters, and finite-element data. Other AFCAN subroutines generate all of the data cards relative to node and element locations and print statements. Although AFCAN significantly decreases the engineering effort required to implement AFPRE, it does so by assigning constant values to the many variables in AFCAN, to the mesh geometry variables subsequently used in AFPRE, and to the locations (elements) for which stress data are printed. To implement AFCAN, the user prepares a series of cards (one for each layer of the pavement system) which indicate the thickness and material property data and an identification card which calls a particular aircraft subroutine. These few cards constitute the entire input to AFCAN, which generates data (cards or tape) for a complete run through AFPAV. Since the AFCAN data are easily prepared by a technician, decisions relative to finite elements and nonlinear material property considerations are eliminated.

Finite-Element Mesh

Details relative to the AFCAN and AFPAV Codes are fully documented in references 3, 4, and 17. The data preset in the AFCAN subroutines consist of

---

17. Crawford, J. E., Unpublished user's manual on AFCAN. Contract report to be prepared for AFCEC by CEL. Publication date unknown.

mesh generation instructions and aircraft loading characteristics, including data for the Fourier series. Each aircraft listed in AFCAN has its own subroutine, which contains the following code variables (constant for each aircraft):

NUMCOS = number of Fourier series cosine terms
NELOAD = number of elements under the tire (x-y plane)
NUMELX = number of elements along the x-axis
WLOAD = wheel load
ZLEN = half-period of the Fourier series

These are fixed variables; others such as layer thickness, material properties, and nonlinear material parameters are introduced on the AFCAN data cards.

The AFPAV Code treats the pavement as a solid with the surface of the pavement lying in the x-z plane; the x-y plane contains the cross-section of the pavement. The thickness of each layer is read directly into AFCAN from cards prepared by the user. The depth of the mesh is set at 144 in. This depth was arbitrarily selected, and it can easily be changed if necessary. The half-width of the mesh (XLEN) was also arbitrarily established. For a single wheel load, XLEN is set at 25 times the half-width of the tire (XLEND). The number of columns of elements (NUMELX) is set in each aircraft subroutine in AFCAN. The selection of values for these variables, which are concerned with the geometry of the mesh, is based on engineering judgment, consideration of the accuracy of the stress results, and computer costs. In general, the size of the elements should be such that the flexibility of the pavement is properly modeled. This is achieved by making the elements small; but, this results in a large number of elements and computer costs which are excessive. As the size of each element is increased, the system becomes less flexible and the computer costs decrease. No theoretical guidance is available for making these decisions. Computer runs on typical pavements must be made and the results compared before a satisfactory mesh is achieved. The selection of values for mesh variables is a subjective matter. Values which produce satisfactory stress results at reasonable computer fees have been assigned to these variables.

Fourier Series Load Function

In AFPAV the tire loads are applied normal to the x-z plane. Gear assemblies are situated to produce symmetrical loading conditions with respect to the x-y and y-z planes. A Fourier series is used to model tire loads for single and multiwheeled landing gears. However, the tire loads are replaced with an equivalent set of forces which are applied to the nodes directly under each tire. Because the gear is located to produce symmetry, the Fourier series takes the form of an even function in which the coefficients are given by

$$a_n = \frac{2}{p} \int_0^p f(z) \cos\left(\frac{n\pi}{p}\right) z dz$$

where

$f(z)$ = tire pressure (PSINOM) defined over the tire length (ZLENLD)

p = half-period of the function (ZLEN)

n = number of terms (NUMCOS)

The Fourier series coefficients are generated in AFPRE for prescribed values of NUMCOS and ZLENLD. The Fourier series functional representation of the tire pressure takes the following form:

$$F_{u_i} = \sum_{n=1}^{n} a_n \cos\left(\frac{n\pi}{p}\right) z$$

where F_{u_i} is the force at node i which produces a displacement in the y-direction.*

The force vector, {F}, contains a nodal force for each degree-of-freedom for each node for each harmonic of the Fourier series. In the above expression for F_{u_i}, the z-term in $\cos(n\pi/p)z$ represents the z-station (x-y plane) at which results are to be calculated; in the expression for the Fourier coefficient, z represents the interval of integration. Note for this latter expression that

*This does not strictly follow Fourier series concepts. NUMCOS = 1 corresponds to $1/2a_0$, the first term of the series, not the first cosine term.

$f(z) = PSINOM$ if $0 \leq z \leq ZLENLD/2$

$f(z) = 0$ if $ZLENLD/2 < z \leq ZLEN$

Selection of Constants

The technique used to select AFCAN constants is best outlined by detailing the procedure for a particular aircraft. However, the analysis is fully applicable to all single-wheeled aircraft. Each multiwheeled aircraft must be considered as a separate case in which selection of the AFCAN constants is more subjective than in the single-wheeled case. Values for tire pressure (PSINOM), wheel load (WLOAD), tire length (ZLENLD), and half-width (XLENLD) are based on landing gear data for the particular aircraft at maximum take-off gross weight (ref. 18). These are included in AFCAN as the standard constants; however, other values for WLOAD and PSINOM can be entered into AFCAN. If WLOAD and PSINOM are not entered, the code defaults to the values for the aircraft at *basic mission* weight. For the F-4 aircraft, the following standard constants are listed or calculated in AFCAN:

WLOAD = 27,000 lb

PSINOM = 265 psi

XLENLD = 4.43 in

ZLENLD = 11.50 in

If other values of WLOAD and/or PSINOM are entered into AFCAN, new values of XLENLD and ZLENLD will be calculated by the code.

Selection of the variables associated with the Fourier series requires careful study. The Fourier series is used so that multiwheeled landing gears can be considered in AFPAV and stress calculations in the x-y plane at any z-station (z-coordinate) can be determined. To accomplish this, the wheel loads are considered to be periodic functions, and the tire-pressure diagrams in the y-z plane are modeled by a Fourier series. As indicated above, the tire pressure is considered to be uniform. However, any functional distribution could be modeled with the AFPAV Code; this is a potential of the AFPAV Code which has not been investigated.

---

18. Hay, D. R., *Aircraft Characteristics for Pavement Design and Evaluation*, AFWL-TR-69-54, Air Force Weapons Laboratory, Kirtland Air Force Base, New Mexico, October 1969.

The primary variables which play a dominate role in the tire-pressure diagram modeling are NUMCOS and ZLEN--the number of cosine terms in the Fourier series and the half-period of the load function, respectively. There are no general guidelines available for assigning numerical values to these variables. A suggested maximum value for ZLEN can be obtained by considering the aircraft landing gear layout. From a theoretical point of view the degree to which the Fourier series fits or describes the tire-pressure diagram can be evaluated by several *fitness* techniques. However, an excessively large number of cosine terms is required to achieve a mathematically satisfactory fit because the *duty cycle* (ratio of ZLENLD to ZLEN) is small. Additionally, computer costs become excessive as the number of cosine terms increases. To solve this apparent dilemma, values for NUMCOS and ZLEN were selected on the basis of the response of the pavement to the Fourier load function, rather than by a mathematical measure of fit. Before explaining the approach used to select values for these variables, a brief discussion concerning the interaction of NUMCOS and ZLEN is necessary.

Figure 2 is a plot of the Fourier load series for ZLEN = 15 x (ZLENLD/2) and various values of NUMCOS. For the F-4 aircraft, this corresponds to a numerical value for ZLEN of 86.22 in, or a period of 172.44 in. In this plot the load is normalized to the tire pressure (PSINOM). If NUMCOS = 1, the load function corresponds to a step function. The addition of more cosine terms increases the normalized load and narrows the length of the first half-cycle. Ideally, this distance should be half the tire length and the pulse should be rectangular as indicated in the figure. Note that negative load values occur; these indicate that tension (uplift) is applied to the pavement. However, in each case the total load applied to the pavement is the same (twice the integral of PSINOM over the interval 0 to ZLENLD/2). With a large number of terms the series becomes concave about the axis of symmetry because of the addition of the higher frequency harmonics. The fit is good, but the computer costs are excessive. To improve this situation, a smaller value may be used for ZLEN. A review of the equation given for the Fourier coefficients shows that the argument of the cosine varies inversely with p(ZLEN). The term $n\pi/p$ is the angular velocity; therefore, the frequency is n/2p, or n/2 x ZLEN. Thus, as ZLEN decreases, the values of the coefficients of the Fourier series increase

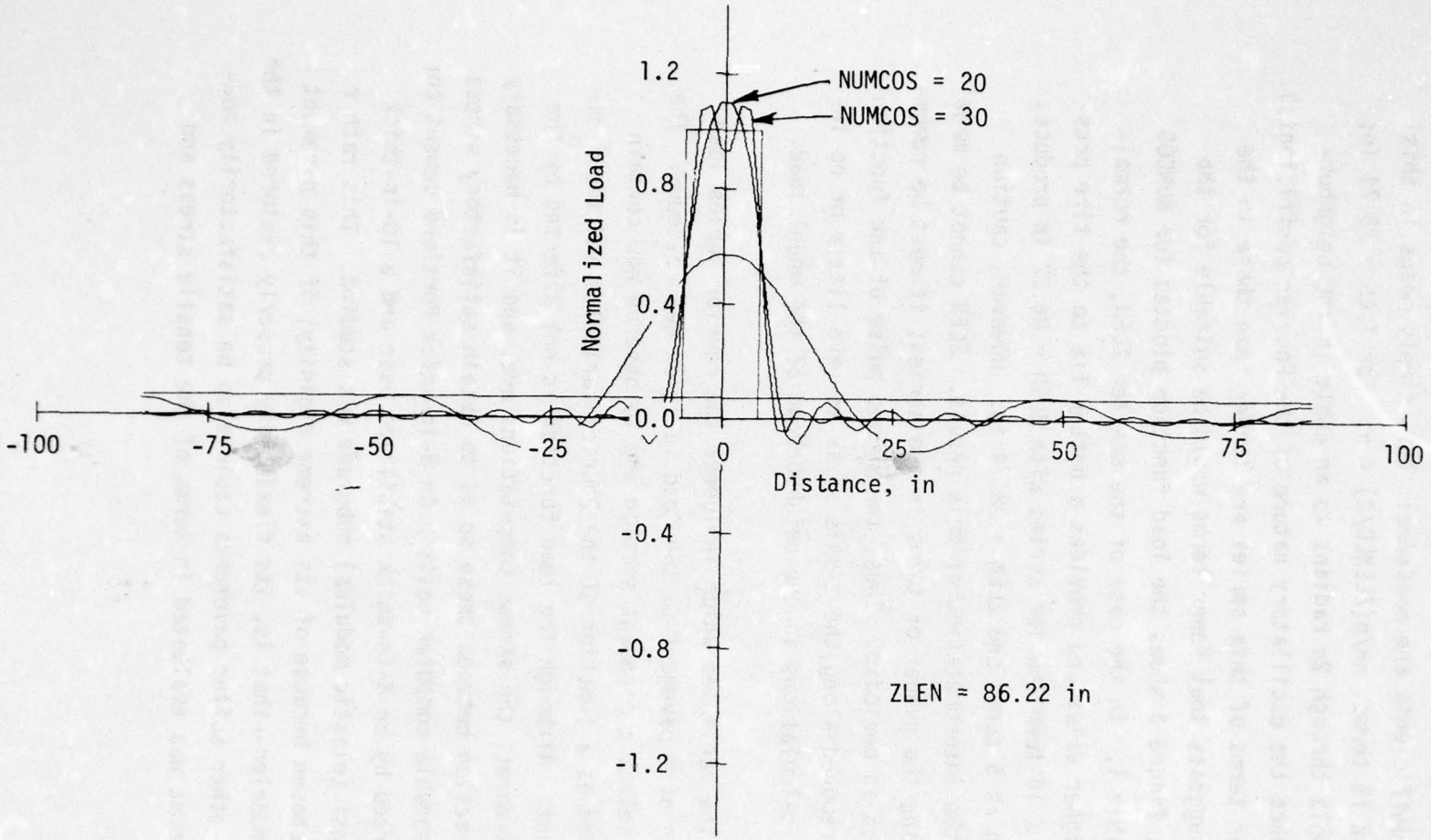

Figure 2. Fourier Series as a Function of NUMCOS

as long as $n\pi/p(ZLENLD/2) \leq \pi/2$. This is shown in table 1. Note that for ZLEN = 86.22 in, all coefficients are *positive*. This simply means in this case that for the first 15 terms, $n\pi/p(ZLENLD/2) < \pi$. For ZLEN = 28.74 in, 15 terms extend the angle through 2π radians to an angle in the neighborhood of 3π radians (hence the oscillatory nature of the Fourier coefficients). However, the first four terms of this series are larger than those in the former series. This suggests that fewer terms would be suitable for the smaller value of ZLEN; figure 3 shows the load function plotted for NUMCOS = 5 and the data in table 1. In the case of the smaller ZLEN, the normalized load reaches a higher value and provides a better fit to the tire pressure. For this case, a 15-term Fourier series with ZLEN = 86.22 in produces the same load function as 5 terms and ZLEN = 28.74 in. However, caution must be exercised in the interpretation of this result. ZLEN cannot be made small simply by reducing the number of terms in the series; it must be remembered that the function is periodic. Thus, the second pulse of the function must be sufficiently removed along the z-axis so as to have little or no influence on the stress calculations in the neighborhood of the wheel load.

To select values for the variables which influence the Fourier series load function, the response of a pavement to the load function was reviewed. The approach used was to select a pavement section and to observe how certain computed results varied as a function of the Fourier variables and the flexibility of the pavement. Although the load function is not affected by the flexibility of the pavement, the stress computations are, and it is necessary to consider the interaction between these so as to obtain satisfactory stress computations and reasonable computer costs. An 8-in-thick Portland cement concrete pavement supported by an 8-in-thick stabilized base and a 10-in-thick subbase over a 5000-psi (elastic modulus) subgrade was studied. This rather strong pavement was chosen because of its extreme rigidity; if this pavement could be reasonably modeled--that is, its flexibility properly captured in the finite-element mesh--other softer pavements could also be satisfactorily modeled. Pavement response was evaluated in terms of the tensile stress and

Table 1. Fourier Coefficients as a Function of ZLEN

Coefficient Number	ZLEN	
	86.22 in	28.74 in
1	0.067	0.200
2	0.132	0.374
3	0.130	0.303
4	0.125	0.202
5	0.118	0.093
6	0.110	0.000
7	0.101	-0.063
8	0.091	-0.086
9	0.079	-0.076
10	0.063	-0.042
11	0.055	0.000
12	0.043	0.034
13	0.031	0.051
14	0.020	0.046
15	0.009	0.027

strain in the wearing course and the normal stress and compressive strain in the subgrade. These parameters were selected because they are needed in the application of this program--the load rating of pavements from nondestructive test (wave propagation) data.

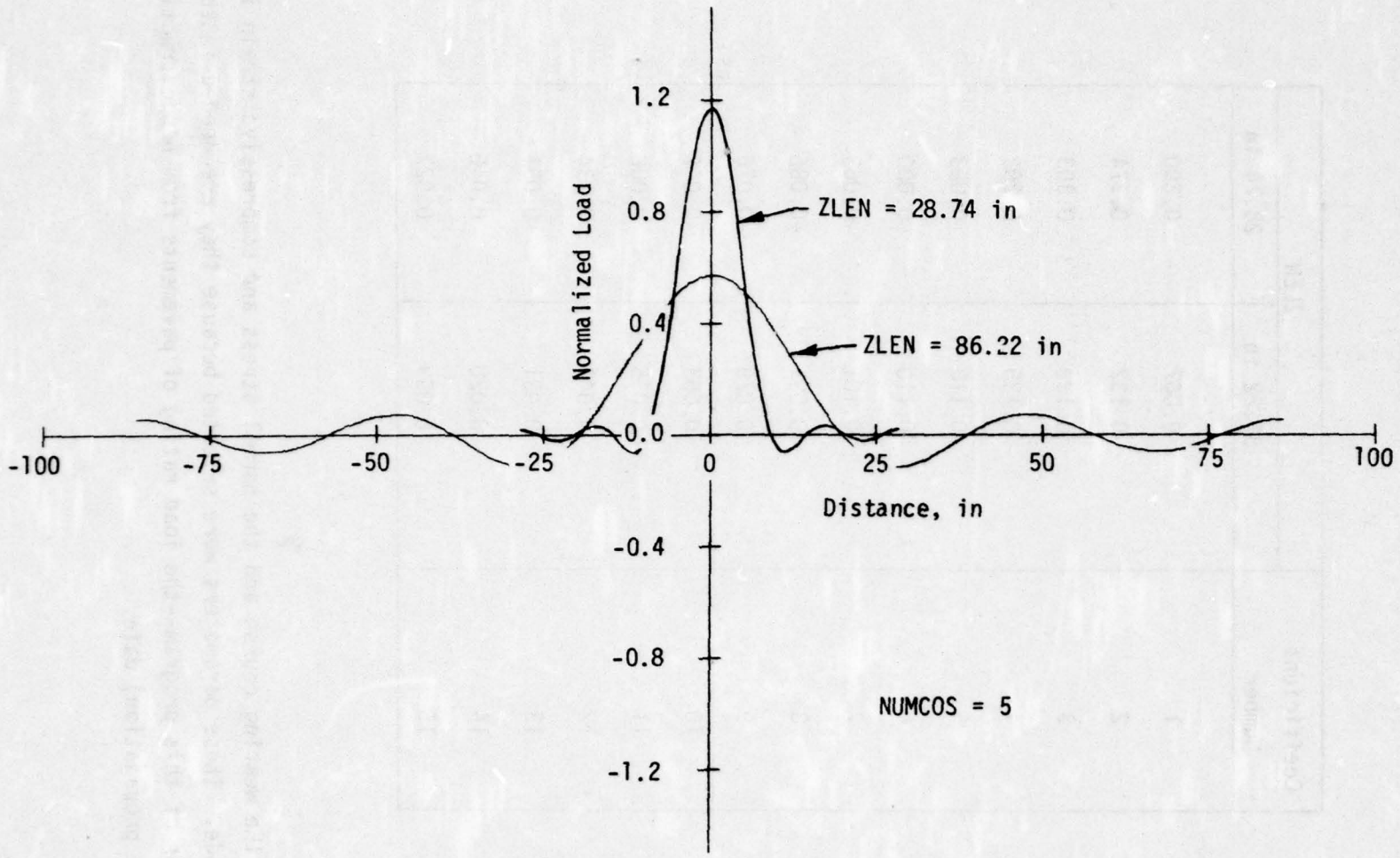

Figure 3. Fourier Load Function Versus ZLEN

Pavement flexibility is influenced by the number of elements along the x-axis (NUMELX) and the number of rows of elements within each material layer. As explained earlier this latter consideration is accomplished by AFCAN without any input from the user; however, the variable NUMELX is in each aircraft subroutine. Figure 4 indicates how the concrete tensile stresses and strains under the centerline of the load (F-4 aircraft) vary with NUMELX and NUMCOS for the case of ZLEN = 86.22 in. The stress variations are easily explained by reviewing the characteristics of the Fourier load function as NUMCOS increases. Low stresses and strains correspond to low normalized loads; these occur when a few Fourier terms are used and at higher numbers of terms. Ten cosine terms yield the highest stresses for the variables plotted for ZLEN = 86.22 in. The effect of increasing NUMELX from 10 to 18 is an approximate 4-percent increase in the computed tensile stress for all values of NUMCOS shown. However, as shown in figure 5, the computer costs increase significantly with increasing values for both NUMELX and NUMCOS. It was an objective of this study to organize the code so that the cost per run per aircraft would not exceed $10.00 on the CDC-7600 computer. NUMELX was set at 14 because the boundary stresses, σ_x and σ_y, were very small and because the bending-stress diagram within the concrete layer was nearly symmetrical. However, for NUMCOS = 10 and NUMELX = 14 the cost per run was nearly $15.00. In order to reduce the run time, the problem was studied further. As discussed earlier, the Fourier load series is a function of the variable ZLEN. Figure 6 is a plot of the argument of the Fourier series 2 x ZLEN/ZLENLD versus the concrete tensile stress and strain. As discussed above, NUMELX = 14 appeared to sufficiently model the flexibility of the pavement. According to figure 5 fewer than seven cosine terms would be required to keep the cost below $10.00 per run for NUMELX = 14. Therefore, NUMELX = 14 and NUMCOS = 5 were used (fig. 6). This figure indicates that the tensile stress reaches a maximum when the argument is 7.5. For the F-4 aircraft this corresponds to ZLEN = 43.11 in. Figure 4 shows that although this lower value of ZLEN produces a 5-percent increase in tensile stress and a smaller increase in the tensile strain, the computer costs are reduced to $5.50 per run. Subgrade normal stresses and compressive strain are affected by ZLEN, NUMELX, and NUMCOS in a manner similar to that for concrete tensile stresses and strains.

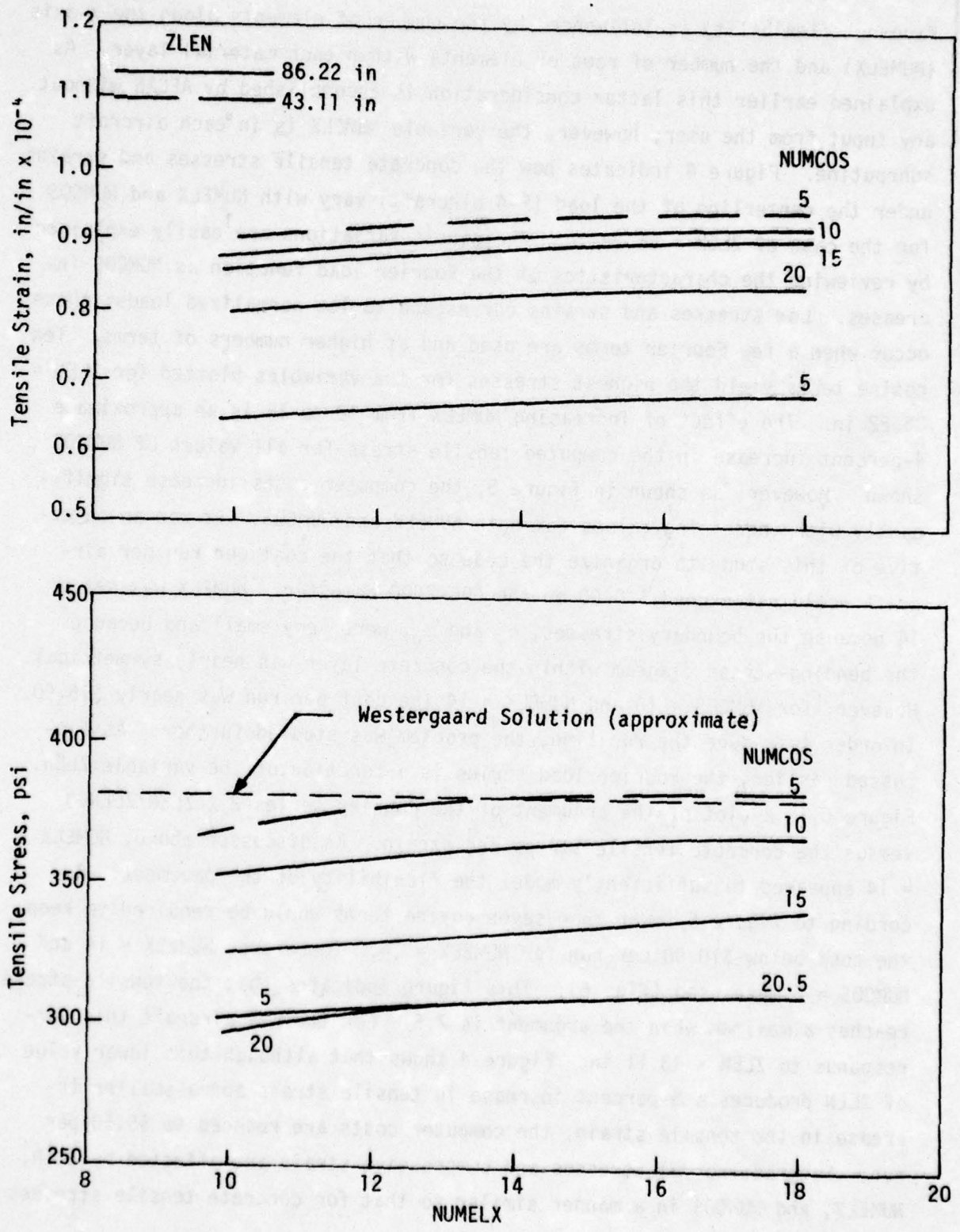

Figure 4. Concrete Response as a Function of NUMELX

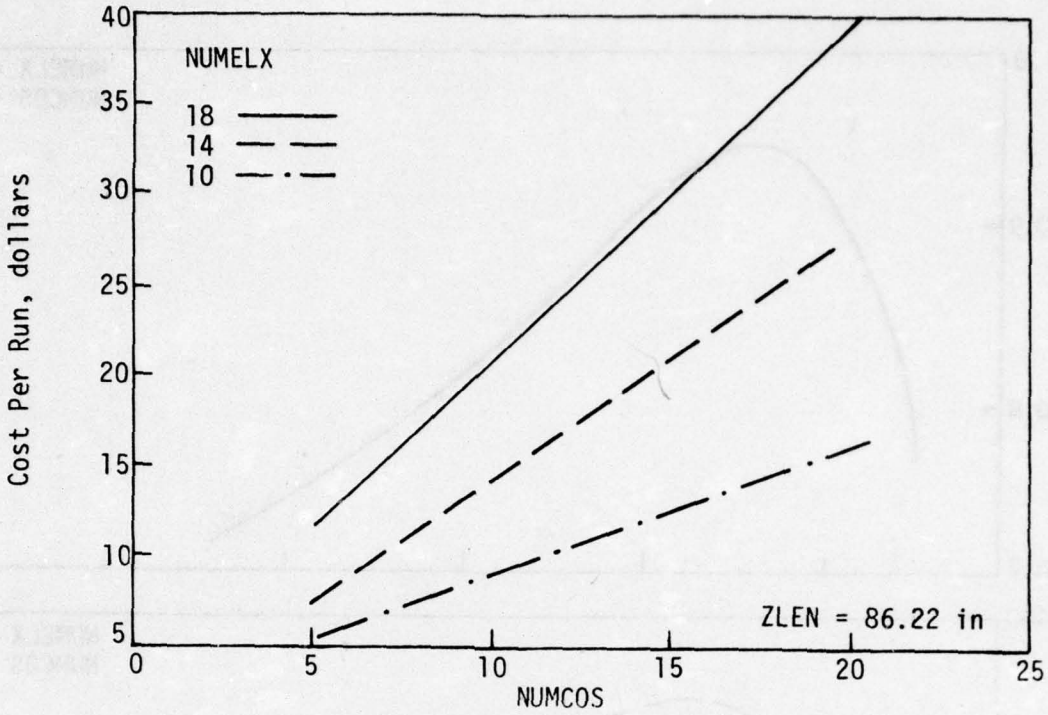

Figure 5. CDC-7600 Computer Costs as a Function of NUMELX and NUMCOS

Analyses of the type outlined above were made for all aircraft (both single and multiwheeled landing gears) in the AFCAN library. As indicated, the values assigned to the variables were selected to provide data for the Air Force nondestructive pavement test and load evaluation program and to minimize computer costs. Although these variables produce satisfactory results from the structural analysis (AFPAV), the decisions which led to their selection were subjective and these values may not be the same as those selected by another engineer. This is especially true with multiwheeled aircraft, since larger numbers of elements are required to adequately model the aircraft/pavement interaction. In these cases trade-offs between pavement response, load modeling, and boundary stresses were made in order to limit computer costs to an average of $25.00* per run, except for the C-5A which, even for conservative modeling, costs about $50.00 per run. However, at this time further refinements do not seem appropriate, at least until better pavement fatigue criteria become available. The AFCAN constants assigned to each aircraft are tabulated in table 2.

* The cost for the CDC-7600 computer at $610.00 per system-hour.

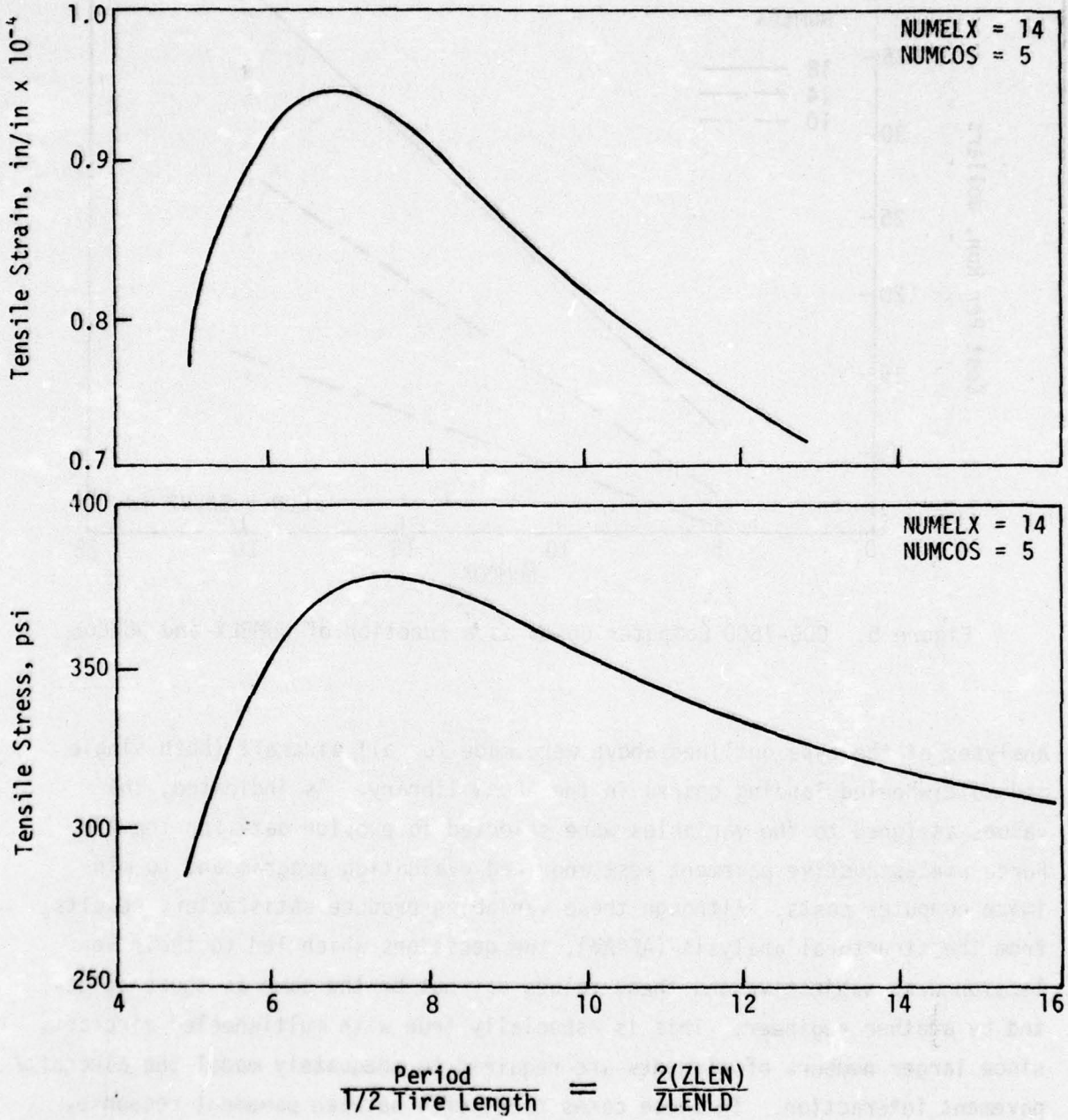

Figure 6. Concrete Response as a Function of Fourier Argument

Table 2. Summary of Aircraft and Load Function Constants Used in AFCAN

Aircraft	WLOAD, lb	PSINOM, psi	NUMCOS	ZLEN, in	Cycles per Coverage	
					Taxiways	Runways/Aprons
F-4	27,000	265	5	43.12	7.36	13.38
F-15	23,400	260	5	40.52	7.73	14.13
F-16	15,000	275	5	31.55	9.56	17.79
F-105	23,400	220	5	44.08	7.26	13.19
F-111	47,000	150	5	75.61	4.77	8.21
FB-111A	54,000	215	5	67.68	5.16	9.00
B-1	40,500	195	9	92.00	2.45	3.50
B-52	67,100	285	9	118.00	1.12	2.85
B-57	27,700	152	5	57.66	5.85	10.37
B-747	41,600	204	10	90.00	2.57	3.63
C-5	30,100	115	15	285.00	1.35	1.66
C-9A	25,800	148	10	60.00	4.43	6.75
C-130	41,900	95	12	102.00	2.12	3.58
C-141	37,400	180	10	62.00	2.25	3.31
KC-97	44,500	180	10	70.00	4.43	6.75
KC-135	35,500	155	8	90.00	2.24	3.24
T-38	5,650	250	5	20.30	14.11	26.89

LOAD RATING SUBROUTINE

The AFPAV Code provides for a complete structural analysis of a pavement. However, before an airfield pavement can be load rated,* known material fatigue characteristics must be considered along with the results of the structural analysis. The capability to load rate a pavement is the principal objective of the Air Force research and development program for pavement evaluation. With the successful development of the NDPT van and the associated data-reduction schemes, a *provisional* load-rating technique for pavements was formulated and placed in AFPAV.

Failure Criteria

In any load-rating procedure, it is necessary to establish the most probable failure modes for the pavement. The following failure criteria were selected:

(1) The maximum tensile strain in the bituminous wearing course should not exceed a prescribed level of strain expressed in microinches.

(2) The maximum tensile stress in a Portland cement wearing course should be below the modulus of rupture of the concrete.

(3) The vertical compressive strain in the subgrade should not exceed a prescribed level.

To implement these structural procedures, failure criteria for bituminous surface courses, Portland cement concrete, and subgrade materials were extracted from the literature.

Bituminous Concrete. -- The fatigue criteria shown in figure 7 (ref. 19) were used in the development of a load-rating procedure for bituminous pavements. Although several other criteria are available, those in figure 7 are useful in that the tensile strain in the bituminous layer for a particular pavement

---

*Load rating is the process of indicating what aircraft and how many annual movements of each aircraft can safely be made from a given airfield pavement.

19. Monismith, C. L., and McLean, D. B., "Structural Design Considerations," *Proceedings*, Association of Asphalt Paving Technologists, Cleveland, Ohio, 1966.

and aircraft loading can be determined from a structural analysis. The elastic modulus, E, is determined from the nondestructive field test. With these data it then becomes a simple matter to determine from figure 7 the number of load repetitions required to cause failure in the bituminous wearing course for a particular aircraft.

Concrete. -- The Portland Cement Association failure criteria for Portland cement concrete (ref. 20) were adopted for concrete pavements. A graphical representation of the concrete failure criteria is shown in figure 8.

Subgrade. -- Figure 9 is a graphical representation of the fatigue criteria selected for the subgrade materials. These relationships were taken from data presented by WES from its test section studies of conventional and heavy, multiwheeled aircraft, from Shell Oil Company suggested criteria, and from data presented by The Asphalt Institute. Three fatigue relationships have been used to cover the conditions of Portland cement concrete pavements and strong bituminous pavements ($E > 350{,}000$ psi), weak bituminous pavements ($E \leq 200{,}000$ psi), and heavy, multiwheeled aircraft (B52, C5A, etc.).

Code Revisions for Fatigue Analysis

To incorporate a pavement fatigue analysis into the AFPAV Code, certain changes and additions had to be made to AFPAV. To accomplish these changes a new code, known as PREDICT, was prepared. PREDICT performs structural analyses on many problems (up to 20) and it also contains a subroutine to perform mixed traffic analysis.

PREDICT is a single program which in essence is composed of AFCAN, AFPRE, AFPAV, and the fatigue and mixed traffic subroutines. Some of the capabilities present in AFPAV (ref. 3), such as formating of data for RESPON (the plot packages DEFLEC and CONTOUR), have not been included in PREDICT. However,

---

20. Packard, R.G., "Design of Concrete Airport Pavement," *Engineering Bulletin*, Portland Cement Association, 1973.

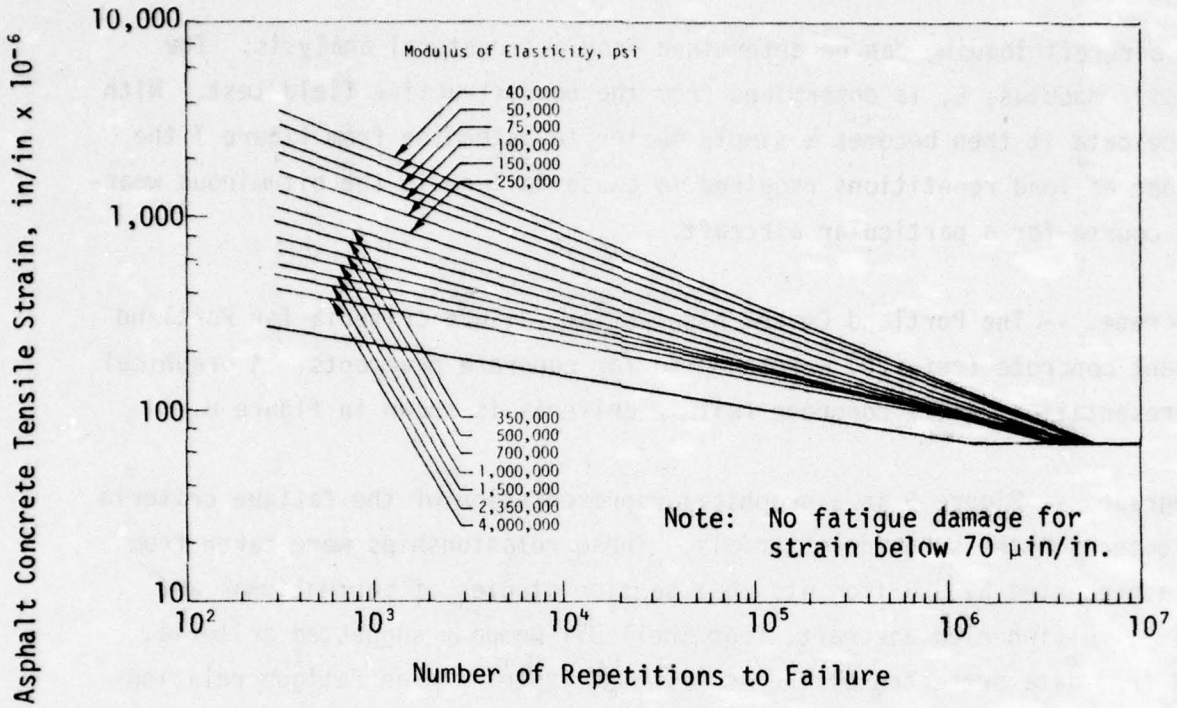

Figure 7. Fatigue Criteria for Bituminous Pavements [after Monismith (ref. 19)]

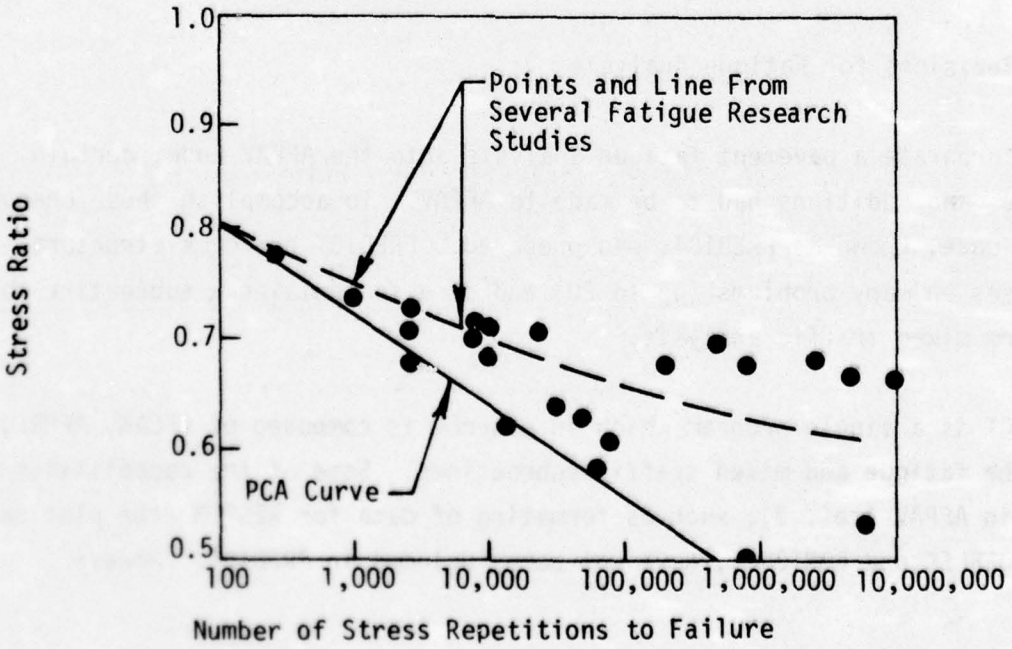

Figure 8. Fatigue Criteria for Concrete Pavements [after Packard (ref. 20)]

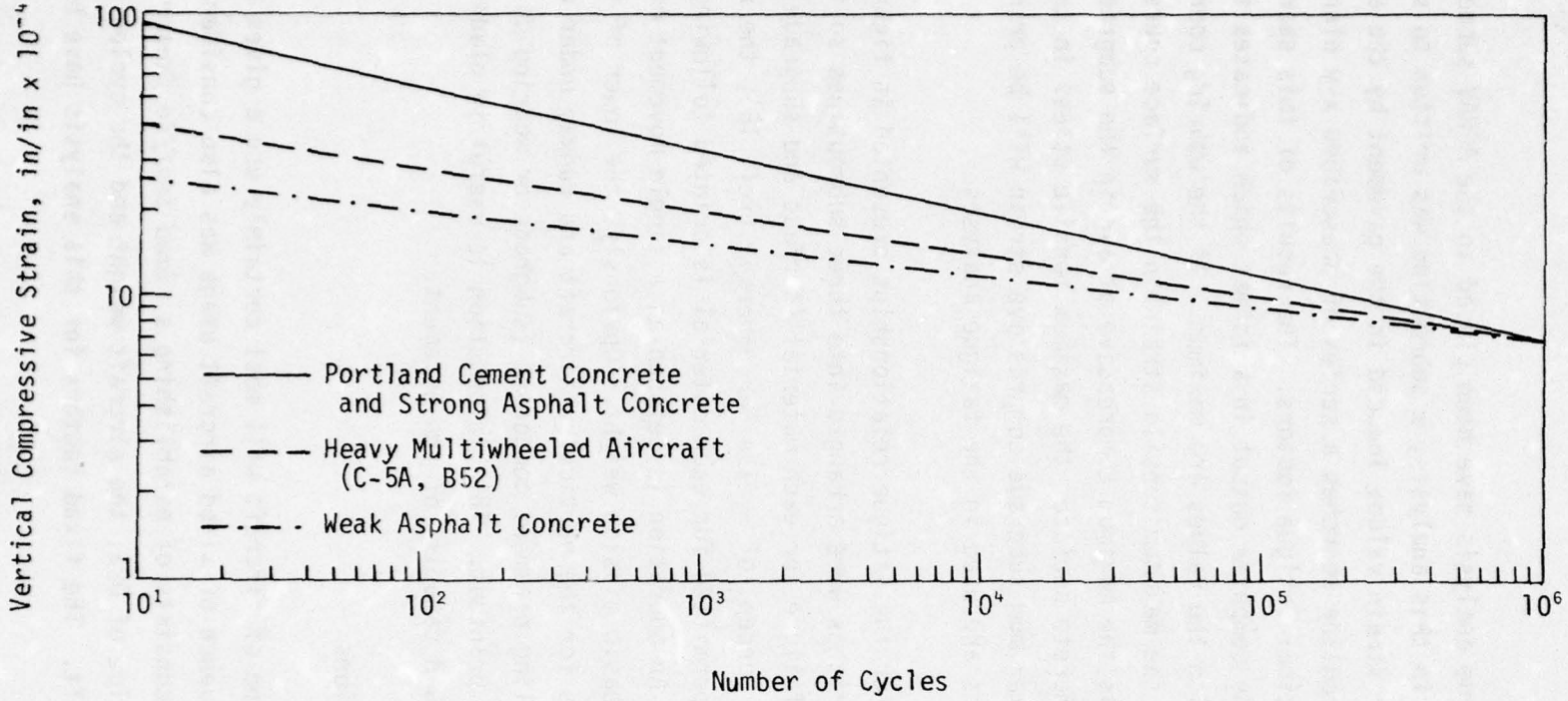

Figure 9. Fatigue Criteria for Subgrade Materials

PREDICT makes maximum use of previous developments associated with AFPAV and AFCAN.

All elements of the fatigue analysis have been placed in the AFPAV subroutine RESULT. As a first step in this analysis, a subroutine was written to search for the maximum stress or strain values induced in the pavement by the aircraft loading. This subroutine searches a series of prescribed x-y planes (z-stations) for the critical fatigue factors. The results of this search are printed as part of the computer output in a format which indicates the z-station (ZPLANE) at which the values are maximum. If the wearing course is a bituminous surface, the maximum tensile strain in the surface course will be printed as well as the maximum compressive strain in the subgrade; if the pavement has a concrete surface, the maximum tensile stress in the concrete as well as the maximum subgrade compressive strain will be printed. These stresses and strains are used in the fatigue analyses.

Algorithms were written for the fatigue relationships presented in figures 7, 8, and 9. These algorithms were arranged into three subroutines so that the number of cycles to failure for each material (surface and subgrade) can be calculated. With the concept of *cycles per coverage* (ref. 18), the number of operations (OPS) permitted for each material is printed following the stress and strain data. An operation is defined as a single movement of the aircraft (departure) at basic mission weight. Obviously, the lower of the two reported OPS controls for the particular aircraft and runway under consideration. The controlling pavement component (subgrade or wearing course) is also indicated on the printout. This information is useful in planning a program to upgrade the load capacity of the pavement.

Mixed Traffic Considerations

Because more than one type of aircraft will most certainly use a given runway or taxiway, the influence of mixed aircraft usage was also considered. The procedure developed consists of establishing a *mixed traffic factor* based on the limiting value of OPS, the aircraft weight and the cycles per coverage for each aircraft. The fixed factors for this analysis have been

placed in the aircraft subroutines in AFCAN. The controlling mixed traffic factor is printed in the computer output along with the stress/strain data and the OPS information. A typical computer summary is shown below:

```
SHAW AFB RW 22R SOUTH END
F4
        OPS-CONCRETE    OPS-ASPHALT   OPS-SUBGRADE
             85107.            0.       206943.
        MIXED TRAFFIC FACTOR FOR CONCRETE =    .0000008782
        MIXED TRAFFIC FACTOR FOR SUBGRADE =    .0000003612
        CONTROLLING OPERATIONS FOR F4         = CONCRETE
        CONTROLLING MIXED TRAFFIC FACTOR FOR F4        = CONCRETE


SHAW AFB RW 22R CENTER
F4
        OPS-CONCRETE    OPS-ASPHALT   OPS-SUBGRADE
                1.            0.        45692.
        MIXED TRAFFIC FACTOR FOR CONCRETE =    .0747384155
        MIXED TRAFFIC FACTOR FOR SUBGRADE =    .0000016357
           F4         CANNOT USE THIS FACILITY


SHAW AFB RW 22R NORTH END
F4
        OPS-CONCRETE   OPS-ASPHALT   OPS-SUBGRADE
          1338000.            0.      6690000.
        MIXED TRAFFIC FACTOR FOR CONCRETE =   .0000000559
        MIXED TRAFFIC FACTOR FOR SUBGRADE =   .0000000112
        CONTROLLING OPERATIONS FOR F4        = CONCRETE
        CONTROLLING MIXED TRAFFIC FACTOR FOR F4        = CONCRETE
```

To evaluate the effect of mixed traffic, the user simply multiplies the mixed traffic factor for each aircraft by the expected number of annual operations. The sum of all these multiplications must not exceed one. Each aircraft which is expected to use the runway must be processed through PREDICT.

If the critical stress or strain induced in the pavement by a particular aircraft falls below the endurance limit of the material, the number of repetitions to failure is as shown in table 3. These values are then converted to

operations. If the pavement is overstressed, a statement which indicates that the particular aircraft cannot use the facility is printed; if the computed number of operations is between 1 and 10, a statement which indicates that only emergency use is permitted is printed.

Table 3. Limiting Failure Criteria for Paving Materials

Factor	Material		
	Asphalt	Concrete	Subgrade
Endurance Limit	70×10^{-6} in/in	54 % Modulus of Rupture	7×10^{-4} in/in
Repetitions	10^6	10^5	5×10^5

SECTION 4
DATA INTERPRETATION PROCEDURE

INTRODUCTION

A study was undertaken to develop a procedure for interpreting phase angle/frequency plots and resulting dispersion curves. This procedure is to be used by AFCEC personnel, along with the NDPT van and PREDICT, to perform pavement evaluation studies.

A wave-propagation technique to determine the load-carrying capability of airfield pavements has been developed at CERF. This technique consists of placing a vibrator on the surface of a pavement and sweeping the load through a frequency range of 10 to 3500 Hz. The propagation velocity, which varies with frequency, is determined from measurements of the phase angle taken during the frequency sweep between accelerometers fixed to the surface of the pavement. This variation of stress wave velocity with frequency is termed *dispersion*. A dispersion curve shows how the propagation velocity changes with frequency. The curve usually is made up of various line segments, the terminal or peak points of which represent the critical velocities of the propagating stress waves. These velocities are used to determine the elastic properties of the different layers of the pavement system. These properties are then used in a multilayered, nonlinear, finite-element computer code to determine the structural response of the pavement to various aircraft loadings. The results of this analysis along with pavement fatigue data provide a means of predicting the remaining service life of the pavement.

PHASE ANGLE/FREQUENCY PLOTS

Data from several airbases tested with the NDPT van in April 1975 were used (ref. 21) in a study of phase angle/frequency plots. The phase

---

21. Nielsen, J. P., *Airfield Test Plan*, CERF Letter Report, Aerospace Facilities Branch, Air Force Weapons Laboratory, Kirtland Air Force Base, New Mexico, February 20, 1975.

angle/frequency plots were constructed by the laboratory-based, data-reduction system developed at CERF for AFCEC (ref. 22). This reduction system is essentially the same as that in the NDPT van (ref. 6), except that a larger X-Y recorder is used to plot the data.

Phase angle/frequency plots were obtained for different pairs of accelerometers to determine variations in the data at different distances from the vibrator. Accelerometers 1 and 2 were located side-by-side at a distance of 2 ft from the center of the vibrator; 3 and 4 were similarly placed 4 ft from the center of the vibrator; 5 and 6 were located 6 ft from the center of the vibrator (ref. 6). The accelerometers are positioned in pairs for two reasons: (1) for backup; i.e., in case an accelerometer should fail, data could still be obtained by the other, and (2) for calibration; i.e., assuming that a symmetrical or spherical plane wave is created by the vibrator, a phase angle of 0 deg should result between adjacent accelerometers and thus indicate that both accelerometers are responding to the same surface excitation.

Calibration curves for the three pairs of accelerometers are shown in figure 10 for the low-frequency sweep (10 to 350 Hz) and the high-frequency sweep (10 to 3500 Hz) on the Portland cement concrete pavement at Cannon Air Force Base. The calibration curves for the low-frequency sweep show a near 0-deg phase shift between the paired accelerometers. The data from accelerometers 3 and 4 show a greater deviation from the 0-deg phase shift line than the data from accelerometers 1 and 2 or 5 and 6. The high-frequency sweep data show that the best calibration is between accelerometers 1 and 2 and the poorest is between 5 and 6. This trend was observed on most of the data and can be used as an indicator of the quality of the data. Most isolated spikes are believed to be pavement and/or equipment resonant points; some simply cannot be explained.

Phase angle/frequency plots were prepared for 12 test locations along runway 03-21 at Cannon Air Force Base. Accelerometer pairs 1 and 3, and 2 and 3;

---

22. Nielsen, J. P., *Development of Pavement Evaluation System*, Progress Report No. 2 (T.D. 5.01/00), Civil Engineering Research Facility, Kirtland Air Force Base, New Mexico, January 31, 1976.

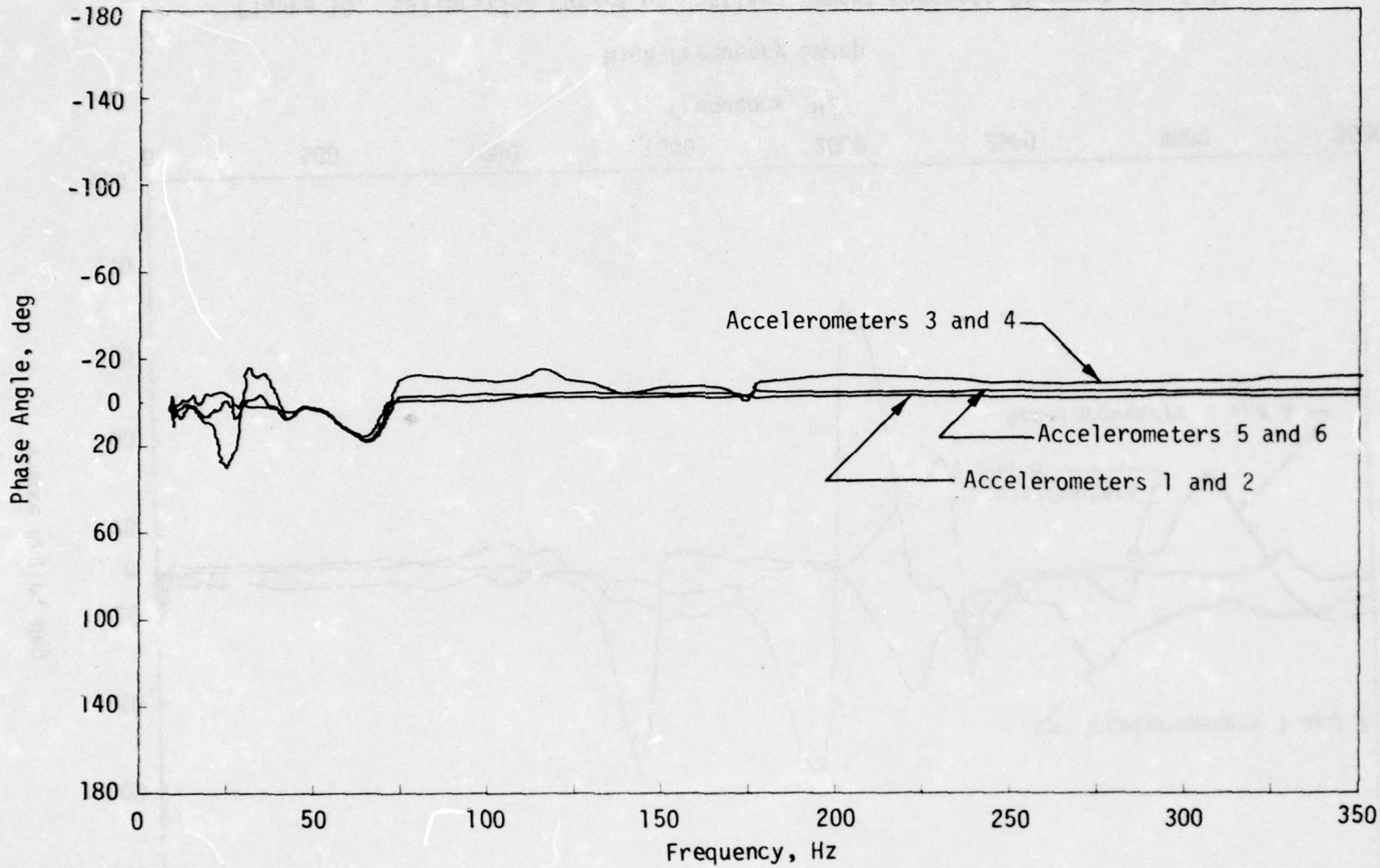

Low-Frequency Sweep

Figure 10. Calibration Curves on Portland Cement Concrete Pavement (1 of 2)

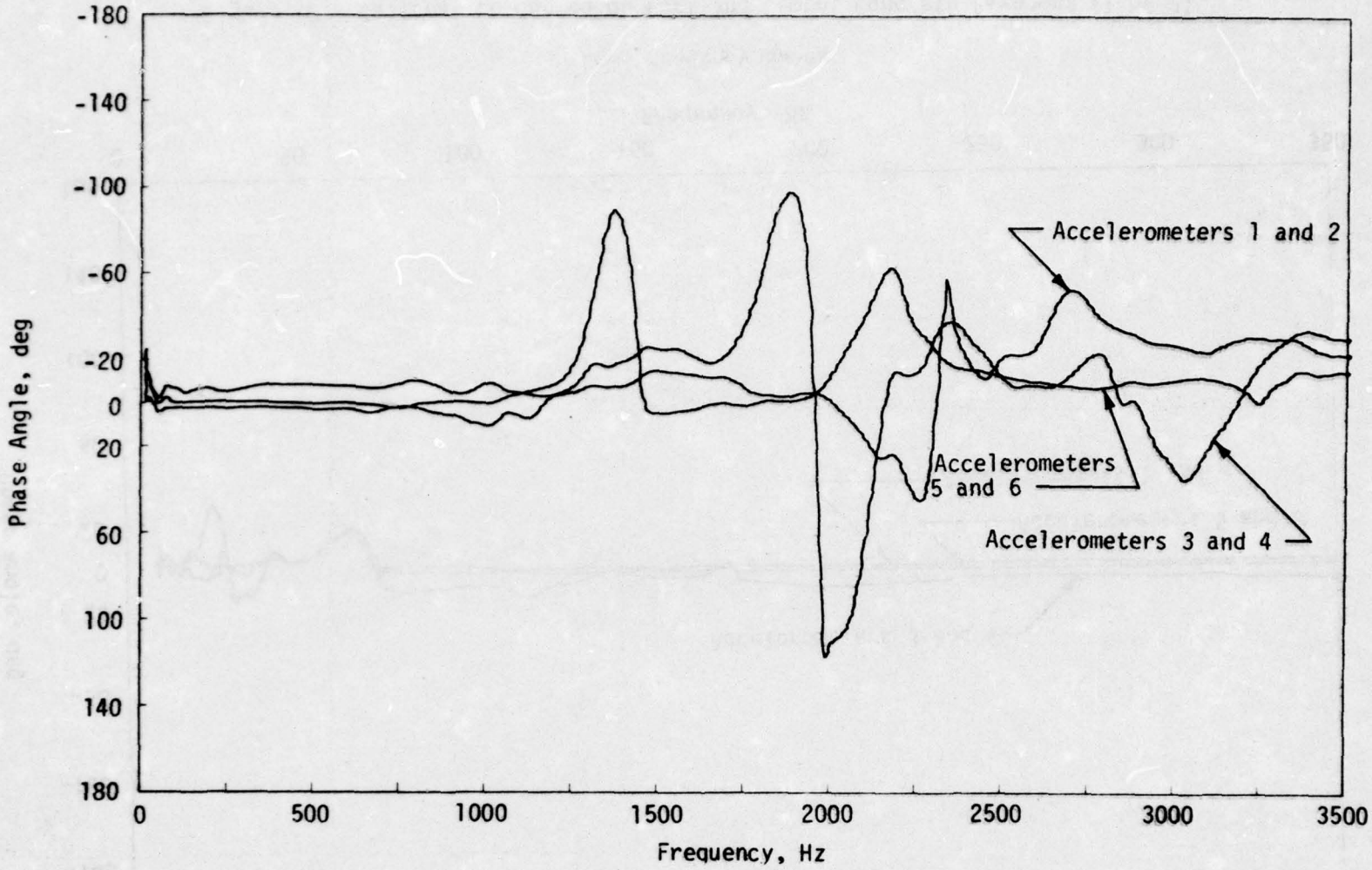

High-Frequency Sweep

Figure 10. Calibration Curves on Portland Cement Concrete Pavement (2 of 2)

3 and 5, and 4 and 5; and 1 and 5, and 2 and 5 were used. Typical low-frequency plots are shown in figure 11; figure 12 shows the high-frequency data. After considerable review it was decided to interpret these plots by following the general trend of the phase angle/frequency data by fairing through the spikes (noise). The final interpretation of the data is shown as a dashed line. These interpretations are based on an averaging of the data; the abrupt slopes where the plotter shifts through 360 deg were ignored. Data points along the interpreted curve were used to establish the dispersion curves shown in figures 13a, b, and c. (See section 5 for full details.)

As part of the phase angle/frequency plot interpretation, it was observed that the high-frequency (short wavelength) portion of the dispersion curves was more consistent for the data from accelerometers 1 and 3 and 2 and 3. More consistent low-frequency data, which represent subgrade conditions, resulted from accelerometers 1 and 5 and 2 and 5. If the low-frequency (25 to 125 Hz) data from accelerometers 1 and 5 are combined with the high-frequency (250 to 3500 Hz) data from accelerometers 1 and 3, a satisfactory dispersion curve can be developed (fig. 14). Because the high-frequency (short wavelength) vibrations are essentially contained in the surface and near-surface layers, it appears that the closer-spaced accelerometers (i.e., 1 and 3 or 2 and 3) provide a more accurate phase angle/frequency relationship for these material layers. A parallel rational was applied to the low-frequency data, which represent the deeper material layers. Thus, greater spacing is required between accelerometers (i.e., 4 ft for accelerometers 1 and 5 or 2 and 5) to obtain good subgrade data. This is similar to a conventional seismic field exploration in which data obtained by closely spaced geophones yield information concerning the shallow materials and those with a greater spacing give data on the deeper materials (ref. 23).

---

23. Dobrin, Milton B., *Introduction to Geophysical Prospecting*, 2nd Edition, McGraw-Hill, New York, 1960.

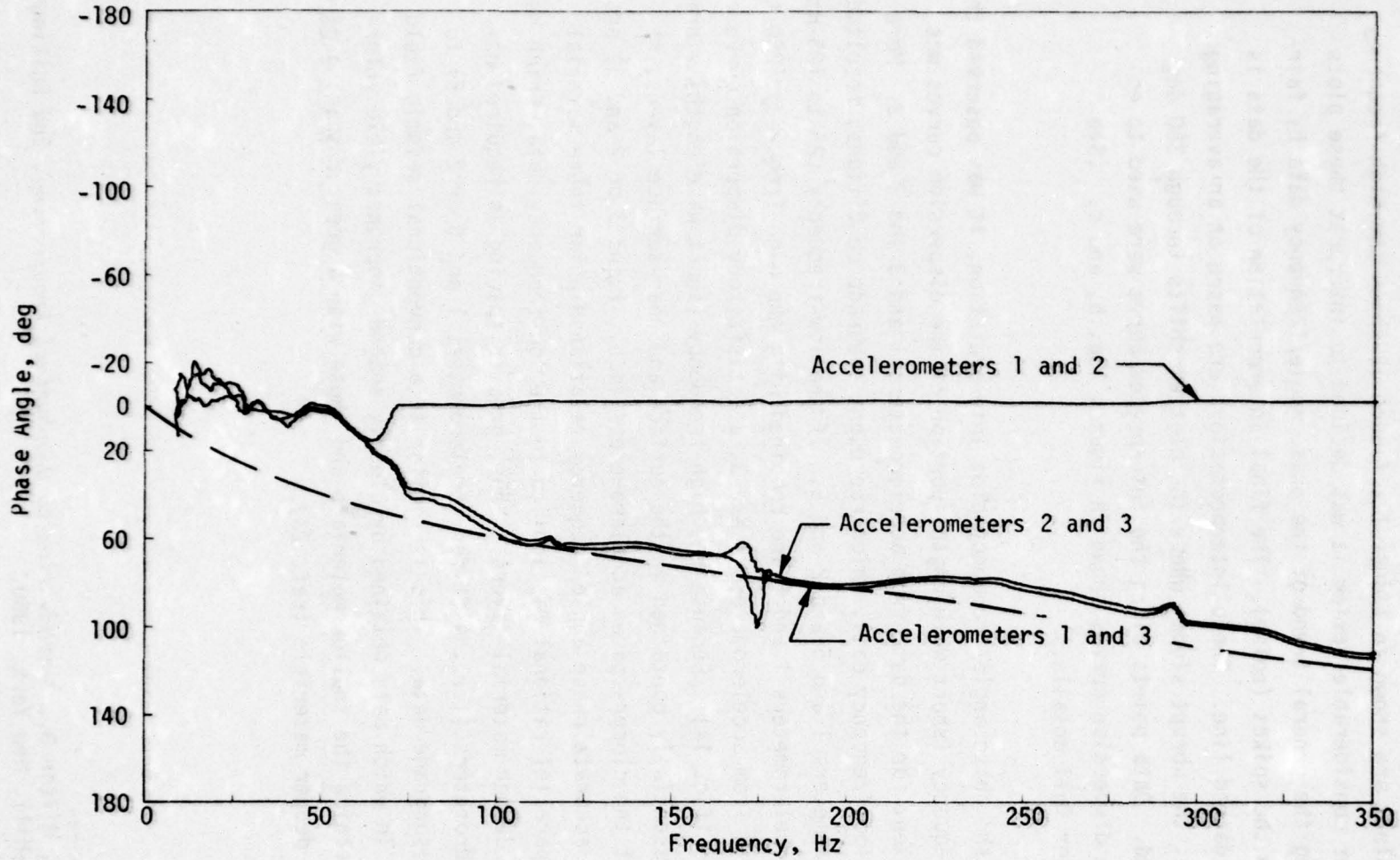

Figure 11. Typical Low-Frequency Phase Angle/Frequency Plots (1 of 3)

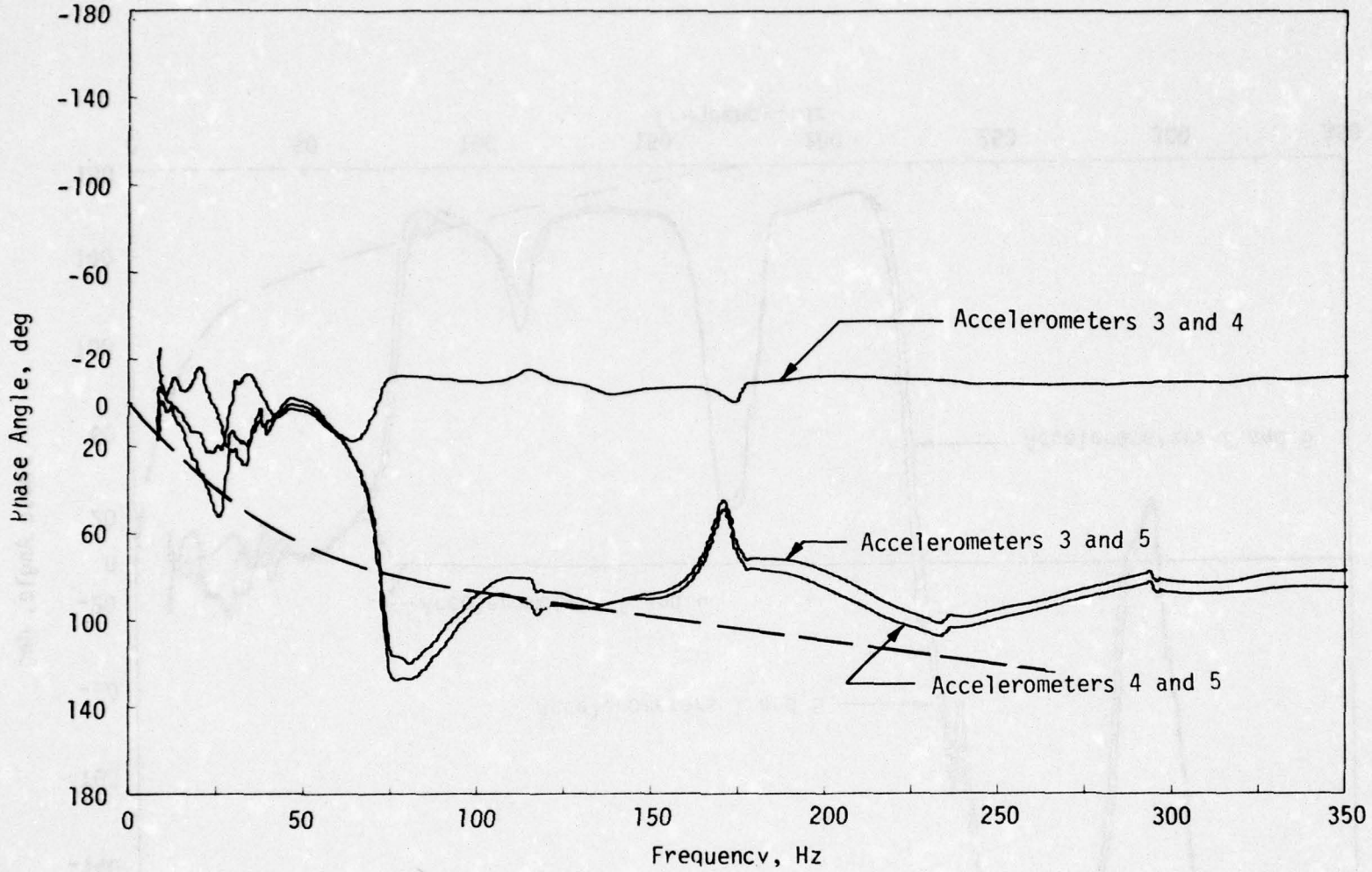

Figure 11. Typical Low-Frequency Phase Angle/Frequency Plots (2 of 3)

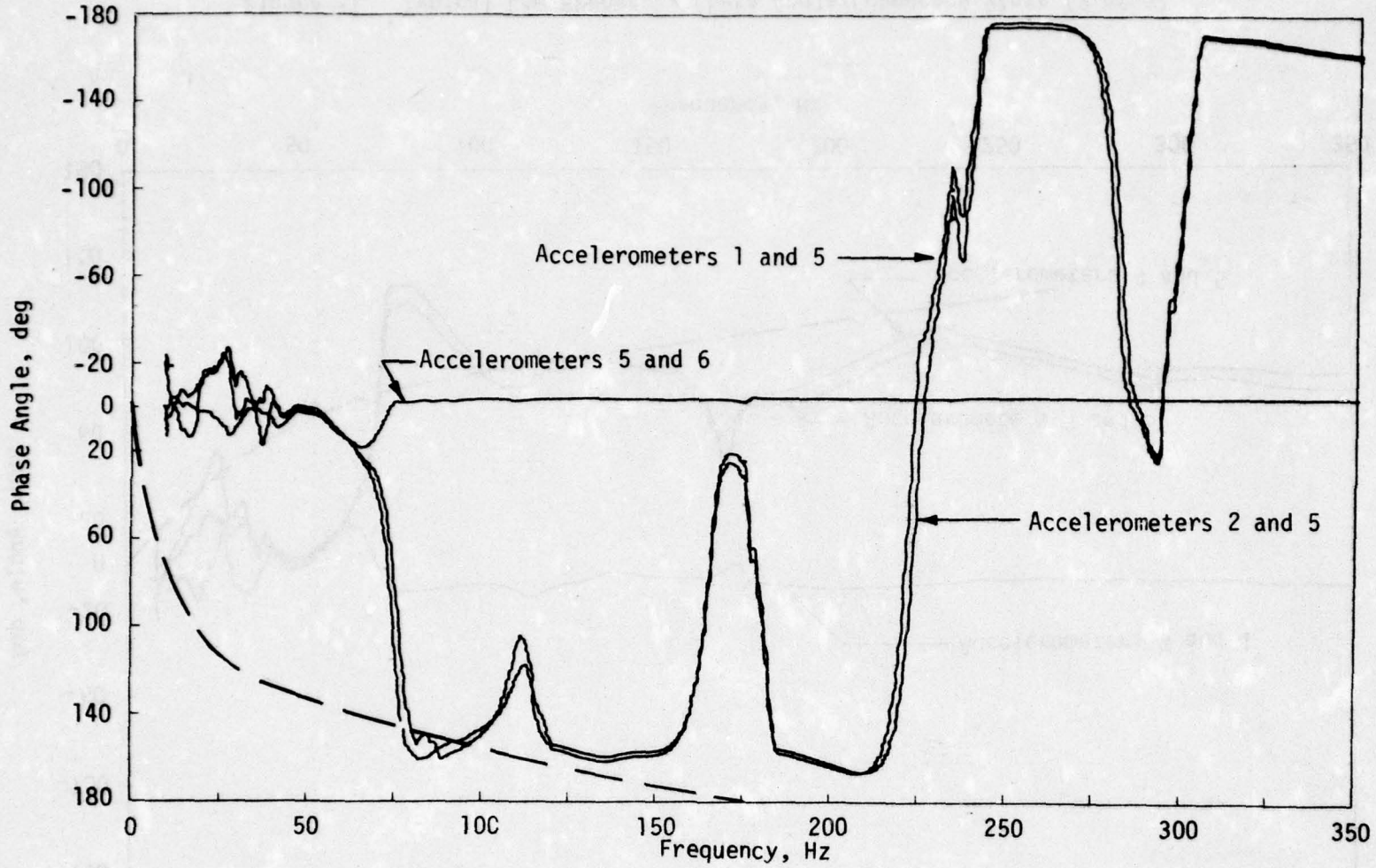

Figure 11. Typical Low-Frequency Phase Angle/Frequency Plots (3 of 3)

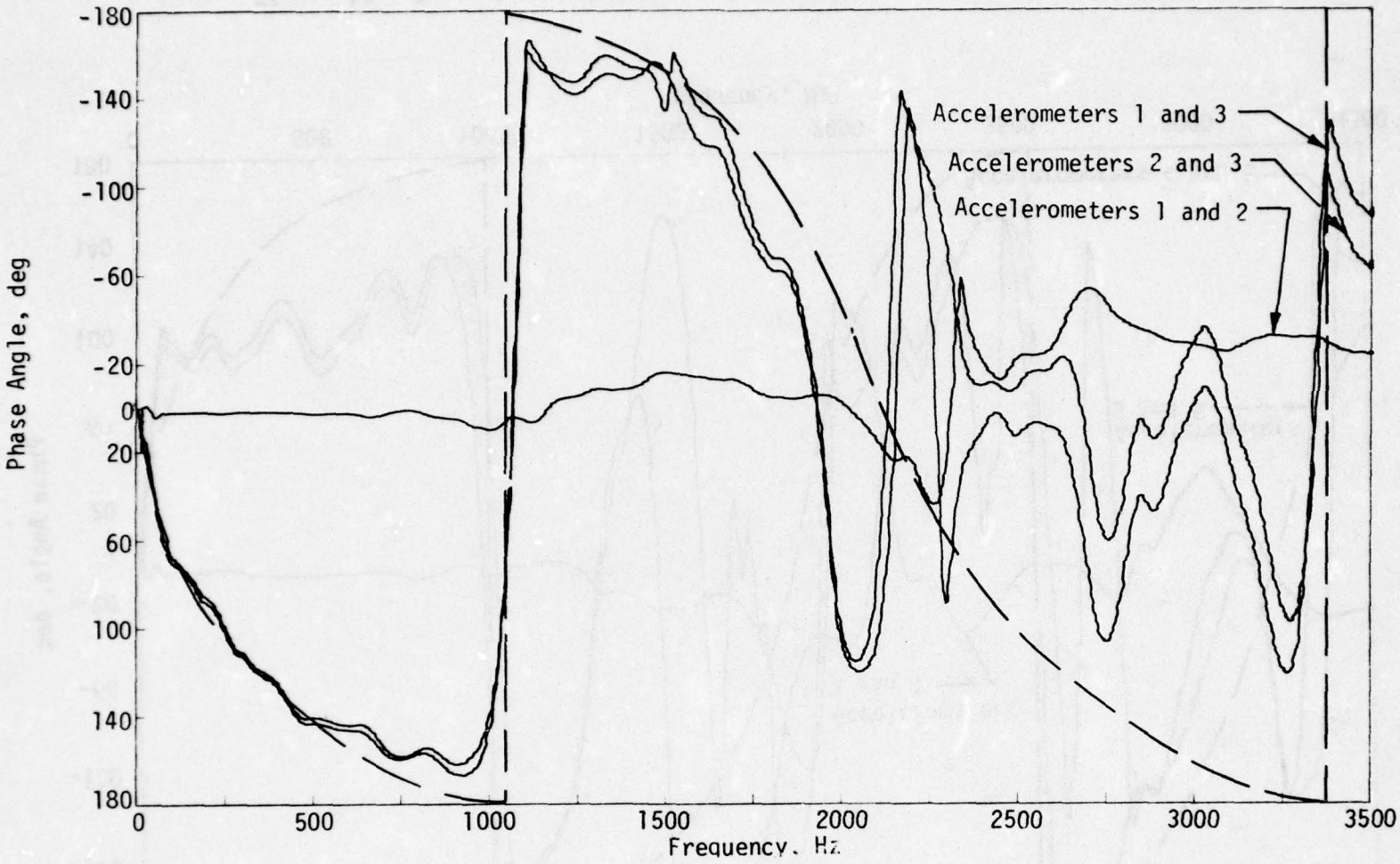

Figure 12. Typical High-Frequency Phase Angle/Frequency Plots (1 of 3)

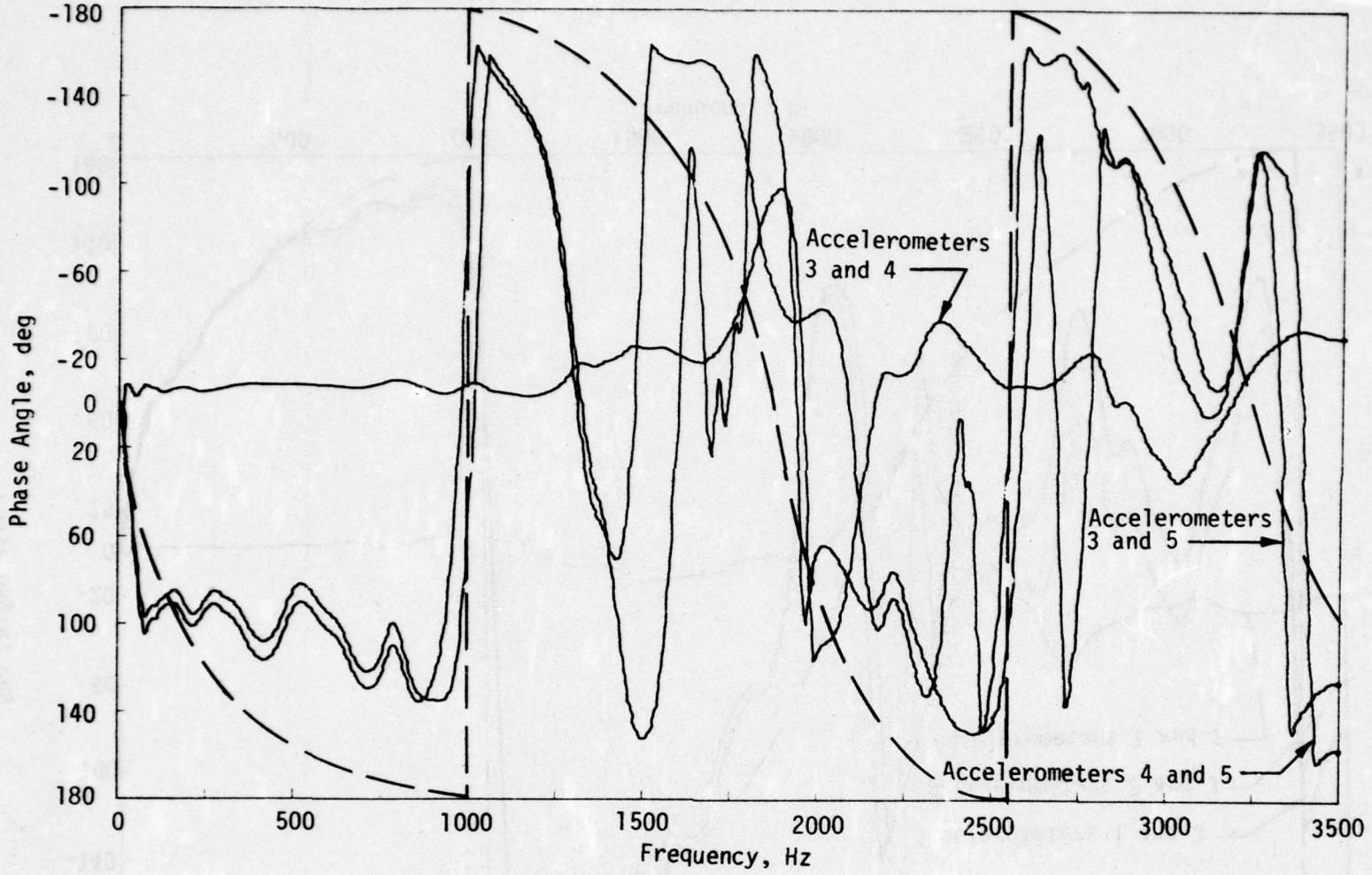

Figure 12. Typical High-Frequency Phase Angle/Frequency Plots (2 of 3)

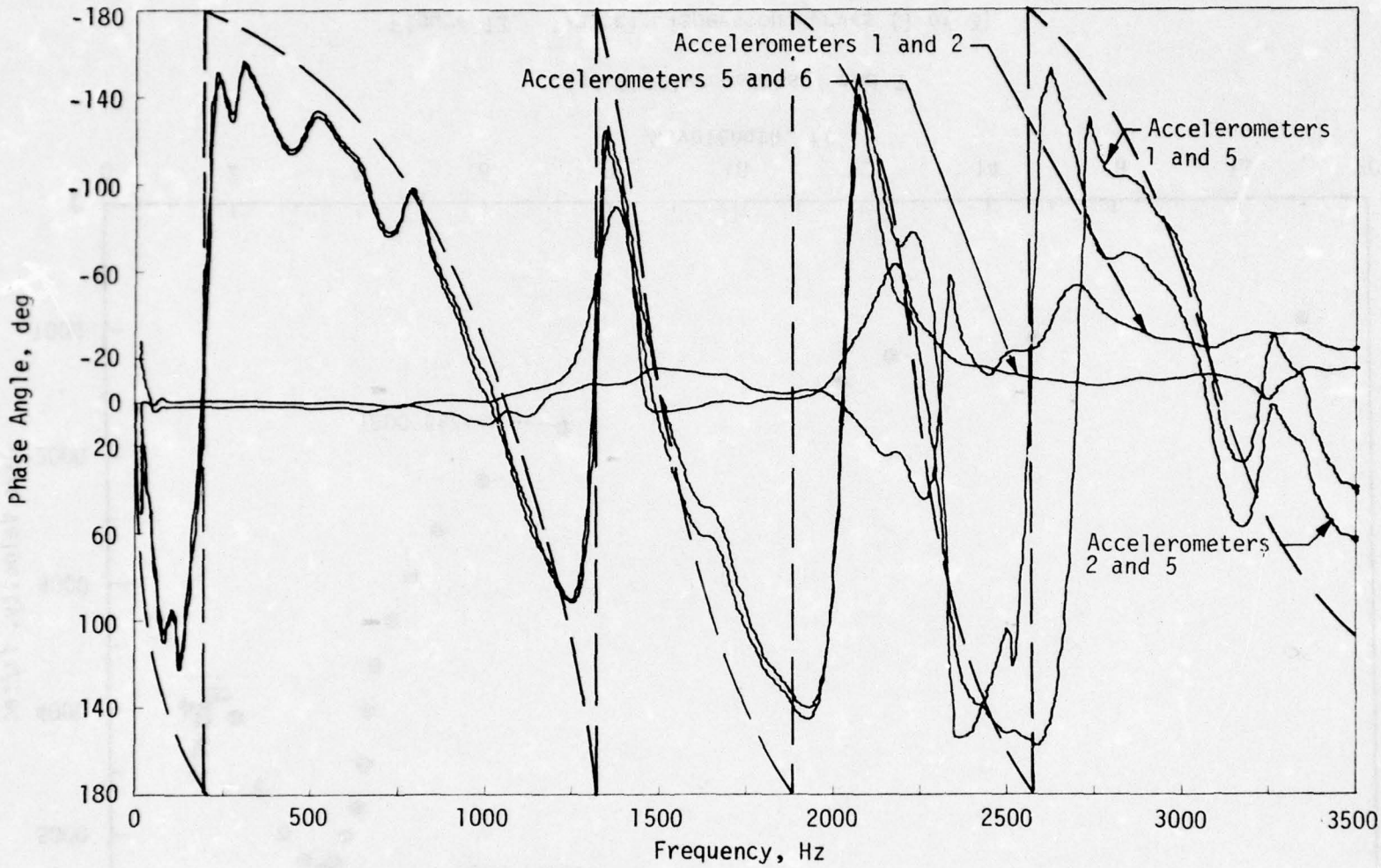

Figure 12. Typical High-Frequency Phase Angle/Frequency Plots (3 of 3)

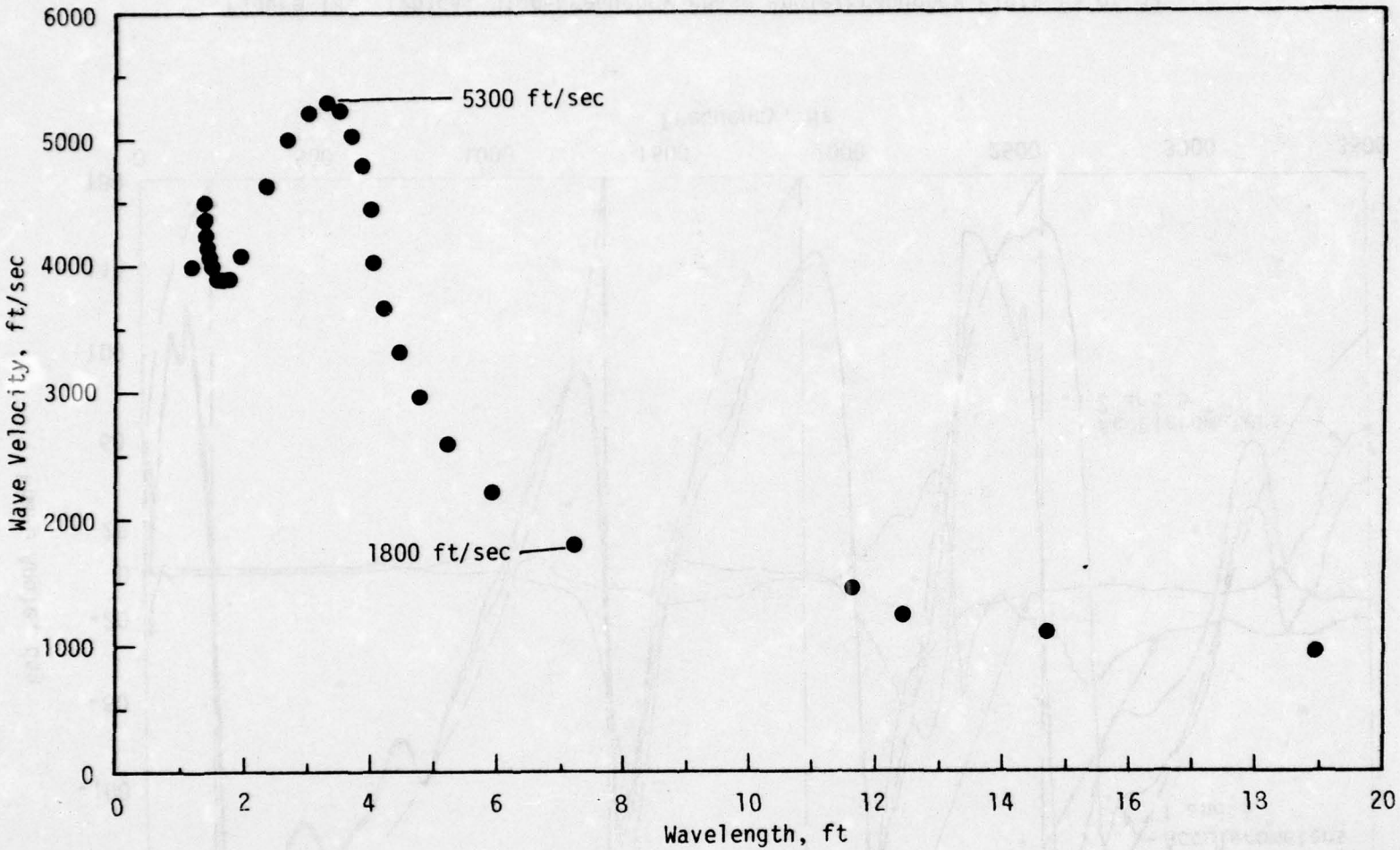

(a) Accelerometers 1 and 3

Figure 13. Typical Dispersion Curves (1 of 3)

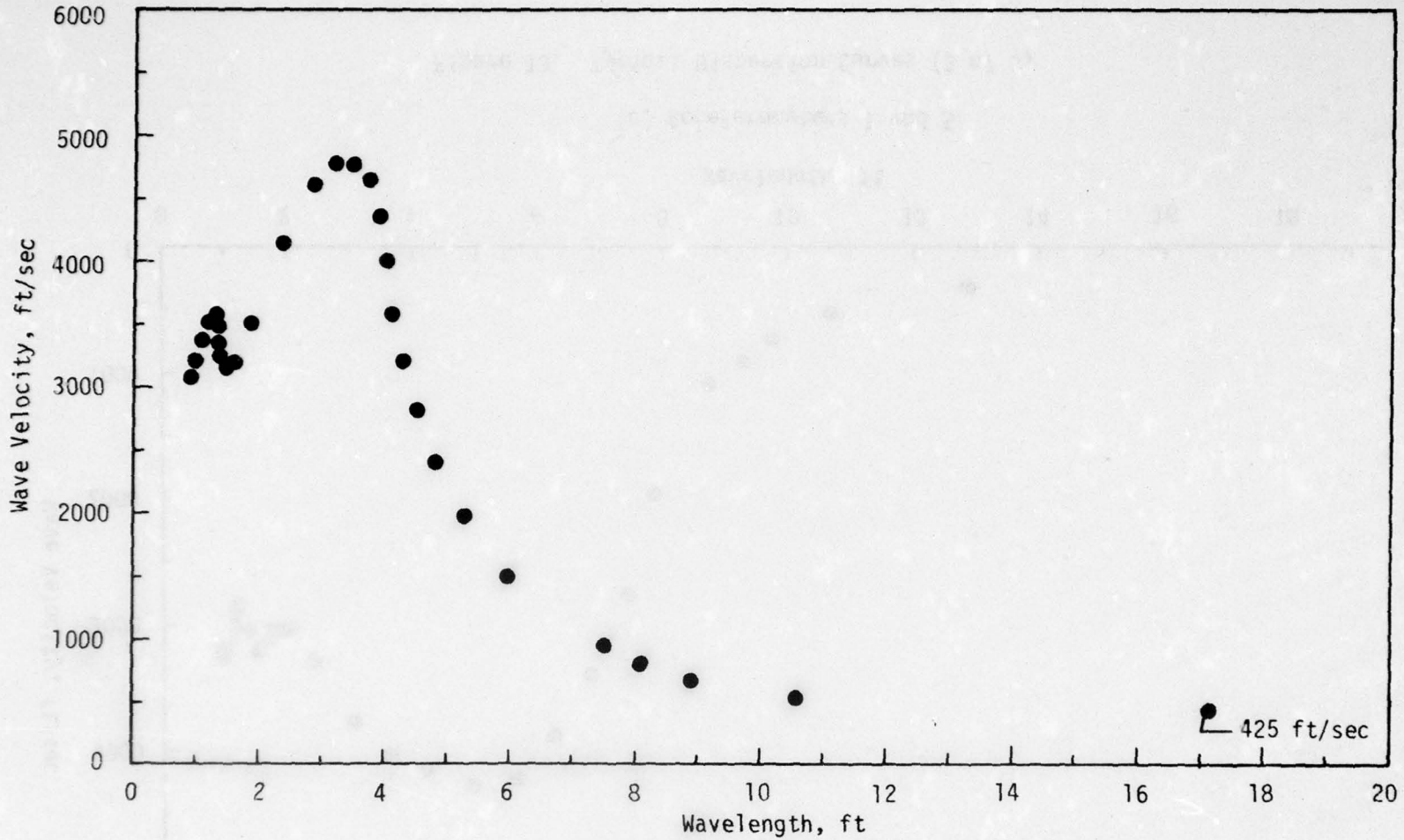

(b) Accelerometers 3 and 5

Figure 13. Typical Dispersion Curves (2 of 3)

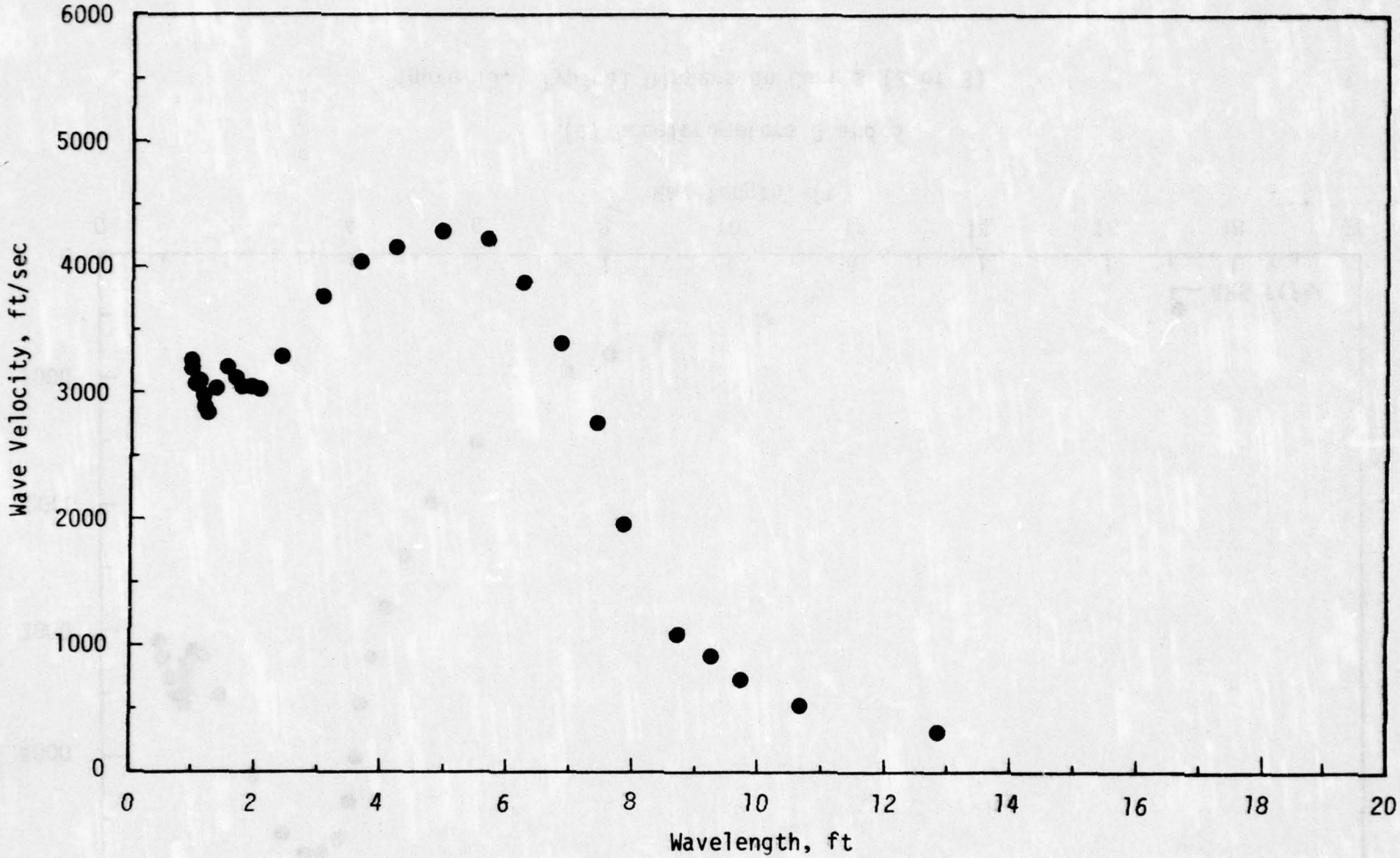

(c) Accelerometers 1 and 5

Figure 13. Typical Dispersion Curves (3 of 3)

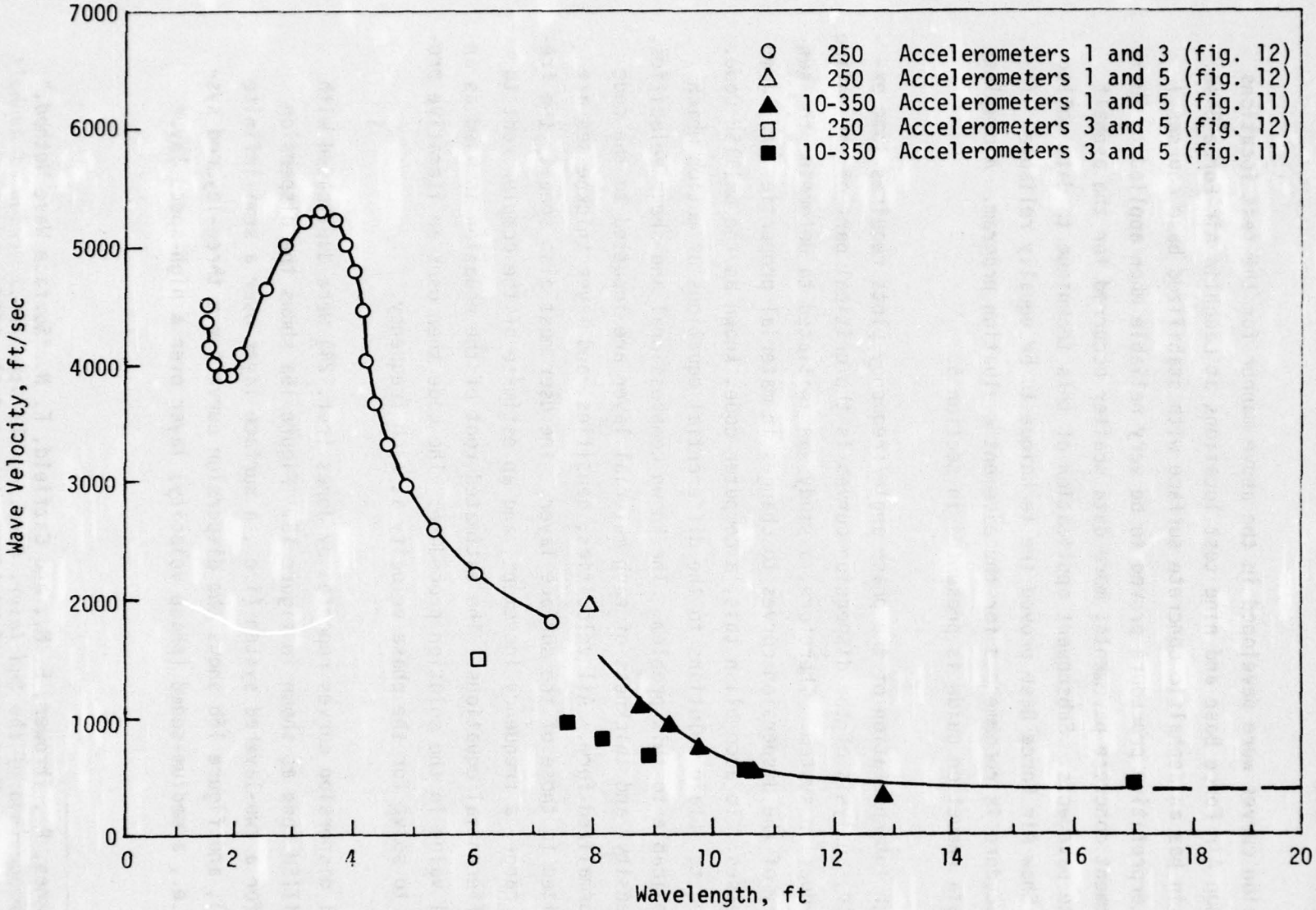

Figure 14. Composite Dispersion Curve

DISPERSION CURVES

Dispersion curves were developed in the above manner for the test locations at Cannon Air Force Base and nine test locations at Laughlin Air Force Base. (Laughlin has an asphaltic concrete surface with stabilized base courses.) The interpretative procedure proved to be very reliable when applied to Portland cement concrete pavements; more data scatter occurred for the asphalt concrete pavements. Subsequent application of this technique to data collected at Shaw Air Force Base proved the technique to be equally reliable. Thus, the procedure is recommended for the pavement evaluation program. A complete NDPT data reduction guide is presented in section 5.

Although interpretation of the phase angle/frequency plots requires some experience, analysis of the dispersion curves is the critical part of the entire data-reduction system. Therefore, a study was initiated to determine the sensitivity of the dispersion curves to changes in material properties and layer thicknesses. To accomplish this, a computer code, known as the BRITISH Code, was used to obtain solutions to the differential equations of motion which are applicable to this problem. The known compressional and shear velocities, mass density, and thickness of each material layer are inputted to the code in a normalized form. All velocities, densities, and layer thicknesses are normalized to those of the surface layer. The user must also specify the frequency range, a frequency increment, and an estimate of the complex root to the differential equations. The estimated root of the equation is used as an initial value in the solution procedure. The code then uses an iterative procedure to solve for the phase velocity at each frequency.

Several dispersion curves reported by Jones (ref. 24) were duplicated with the BRITISH Code as shown in figure 15. Figure 15a shows the dispersion curve for a two-layered system (i.e., a surface layer over a semi-infinite medium), and figure 15b shows the dispersion curve for a three-layered system (i.e., a medium-speed (phase velocity) layer over a high-speed layer

---

24. Jones, R., Thrower, E. N., and Gatfield, E. N. "Surface Wave Method," *Proceedings of the 2nd Inter. Conf. on the Structural Design of Asphalt Pavements*, University of Michigan, August 7-11, 1967.

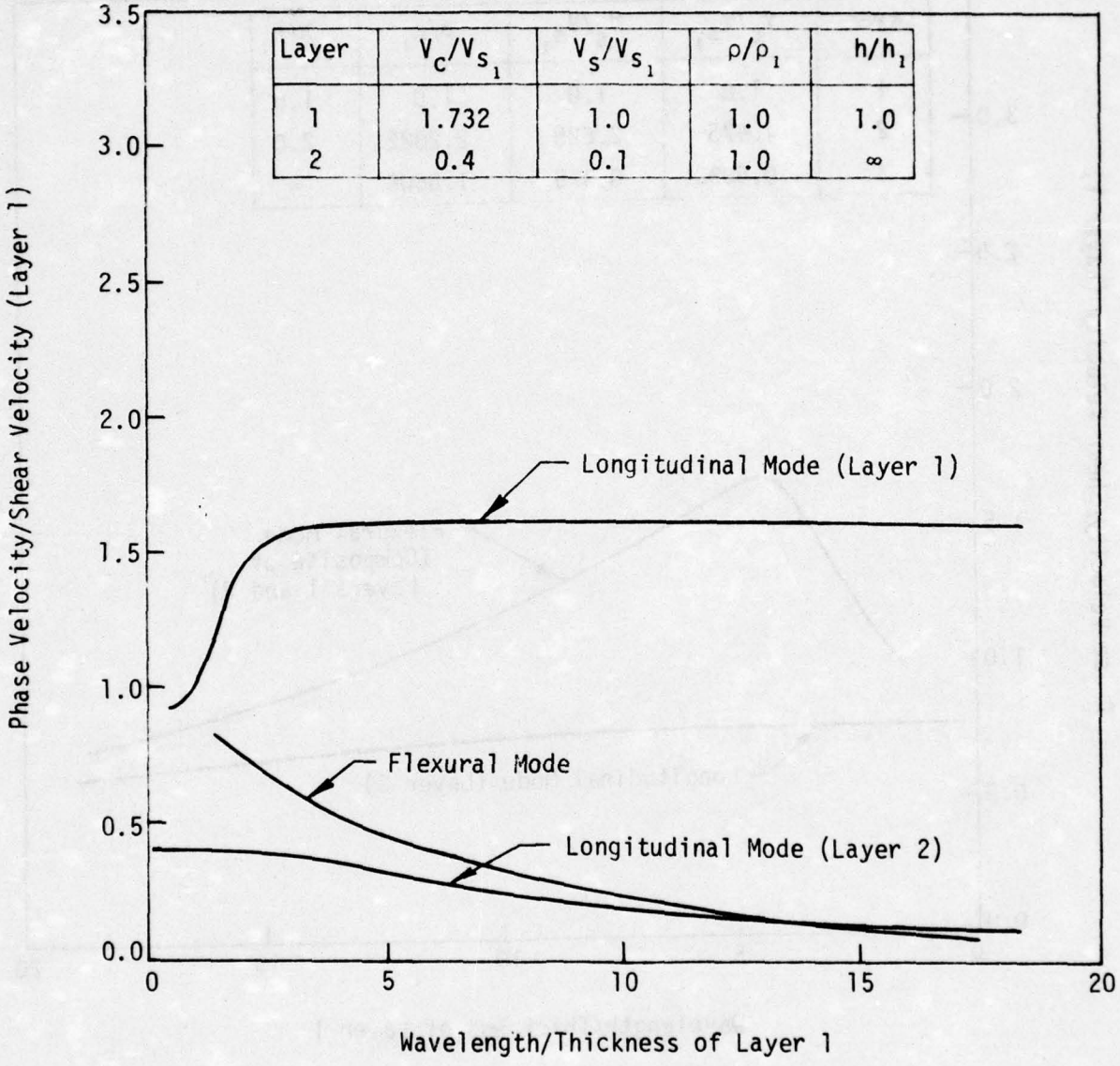

(a) Two-Layered System

Figure 15. Duplicate of Dispersion Curves by Jones (1 of 2)

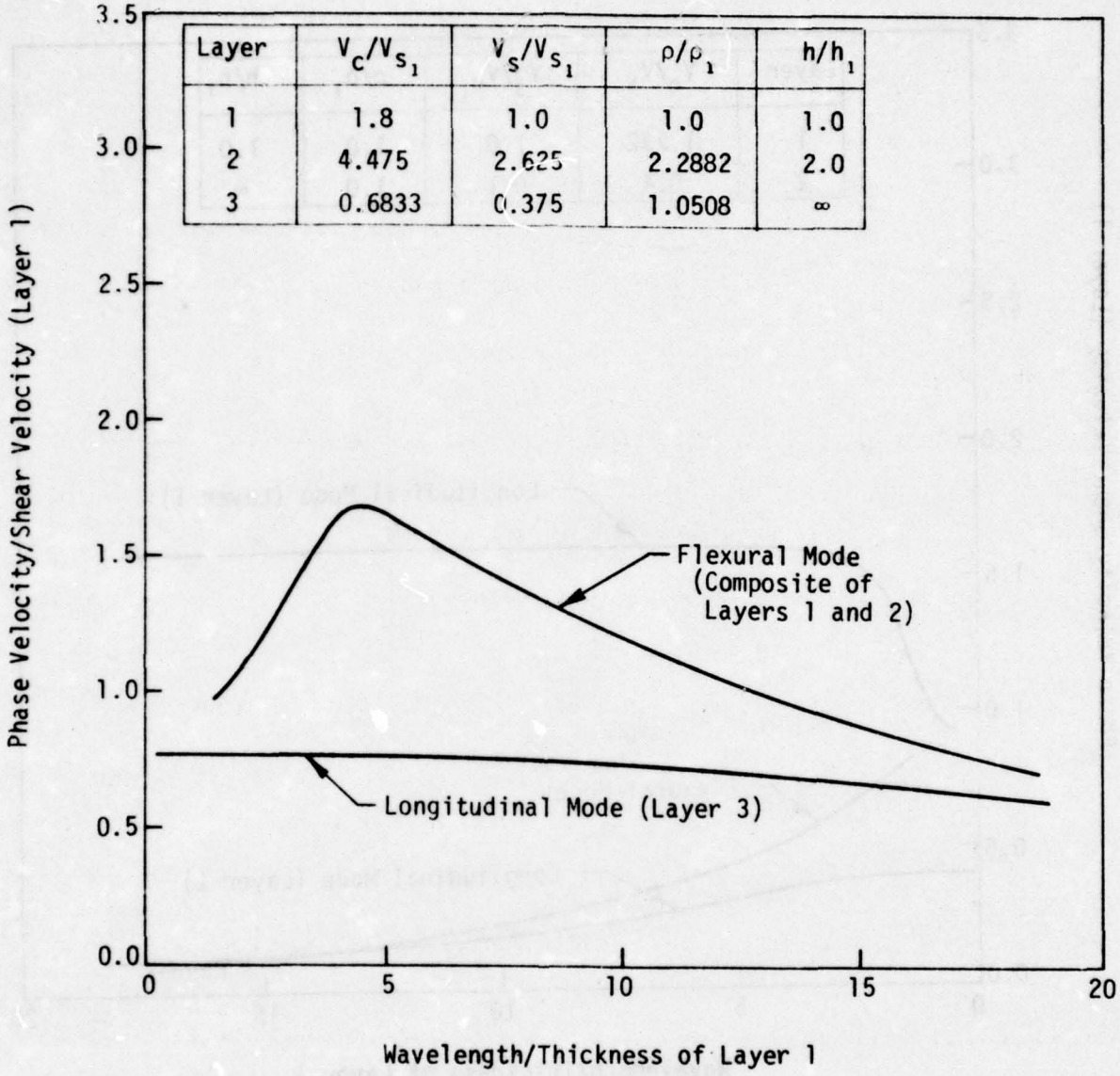

(b) Three-Layered System

Figure 15. Duplicate of Dispersion Curves by Jones (2 of 2)

over a low-speed, semi-infinite medium). These dispersion curves were obtained only after a considerable trial-and-error effort to satisfactorily duplicate Jones' curves. The dispersion curves were highly dependent on the input data, specifically the initial estimates of the roots of the equation. This is illustrated by the dispersion curve results (figs. 15b and 16). Figure 16 is the computed dispersion curve using data identical to that for figure 15b but with a different estimate of the imaginary root for the initial frequency. No analytical method could be developed by which the estimate of the input root could be improved so as to eliminate the problem revealed by these two figures. It became evident that consistent dispersion curves could not be obtained with the BRITISH Code in its present form. To further illustrate the inconsistent results from the code, the dispersion curve for a third problem involving a high-speed layer over a medium-speed layer over a low-speed layer is presented in figure 17 (ref. 24). Figure 18 shows the best solution that could be obtained for this problem with the BRITISH Code. The surface layer was then divided into four layers of equal thickness with identical material properties; the second layer was divided into two layers with identical properties. The total thickness of the system was not changed; but, the three-layered system was modified to appear as a seven-layered system. The input frequency and estimated roots were the same as those used to construct figure 18 (the three-layered solution). Figure 19 shows the dispersion curve for the seven-layered system. A considerable difference can be seen between these two plots.

Based on the foregoing results, it was decided that the BRITISH Code could not be used with confidence as a guide to interpret field dispersion curves. Other researchers (ref. 25) who have had considerable experience with other computer codes for calculating dispersion data have had little success in applying such codes to a system in which the stiffness decreases with depth (i.e., pavement). It appears that present codes are theoretically valid, but discrepancies result when these codes are applied to a pavement system. In addition, there is some concern about the theoretical basis of these

---

25. Personal communication with Professor John Lysmer, Civil Engineering Department, University of California, Berkeley, California, February 4, 1976.

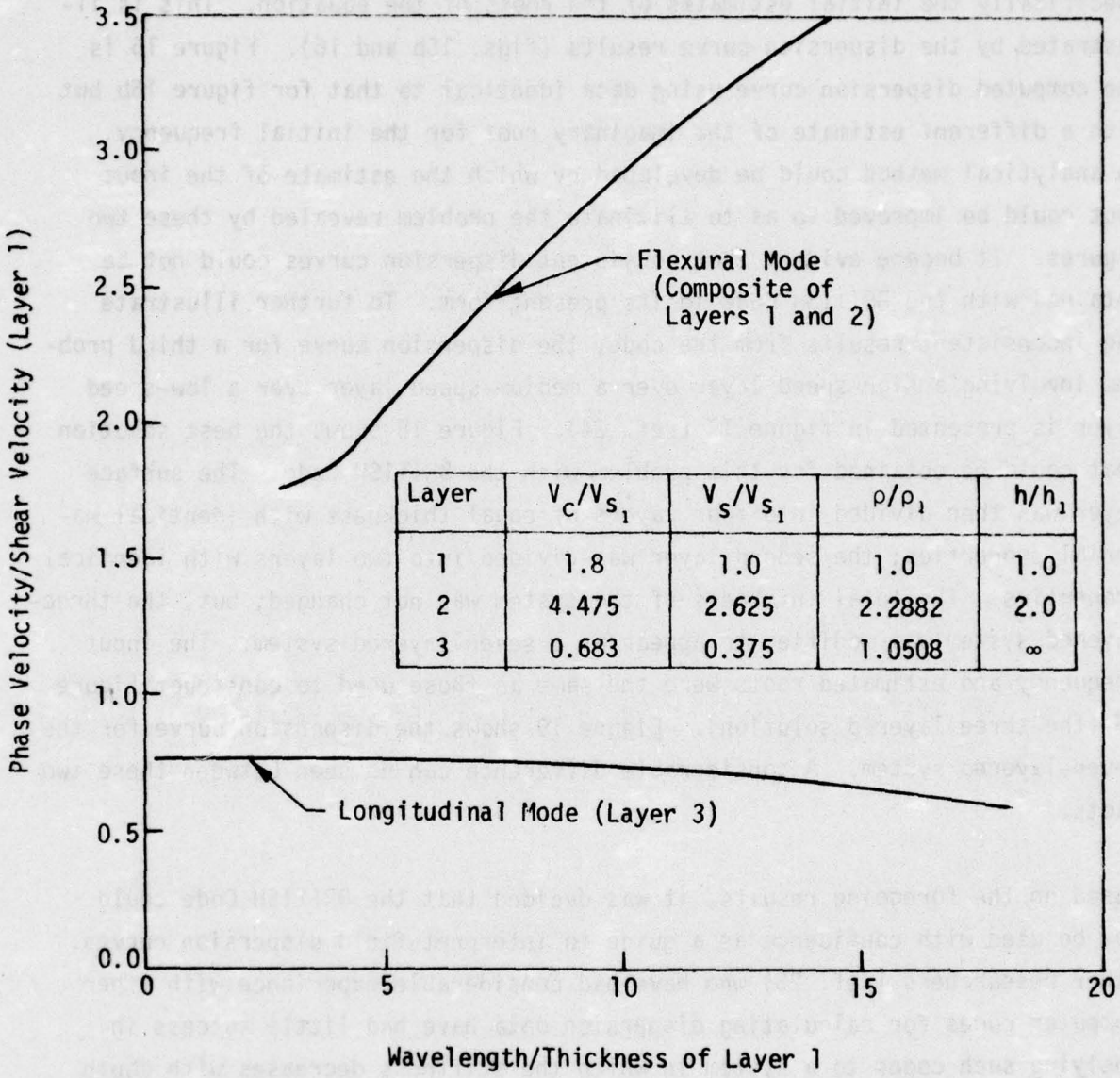

Layer	V_c/V_{s_1}	V_s/V_{s_1}	ρ/ρ_1	h/h_1
1	1.8	1.0	1.0	1.0
2	4.475	2.625	2.2882	2.0
3	0.683	0.375	1.0508	∞

Figure 16. Alternate Solution for Three-Layered System for Different Initial Estimate of Imaginary Root

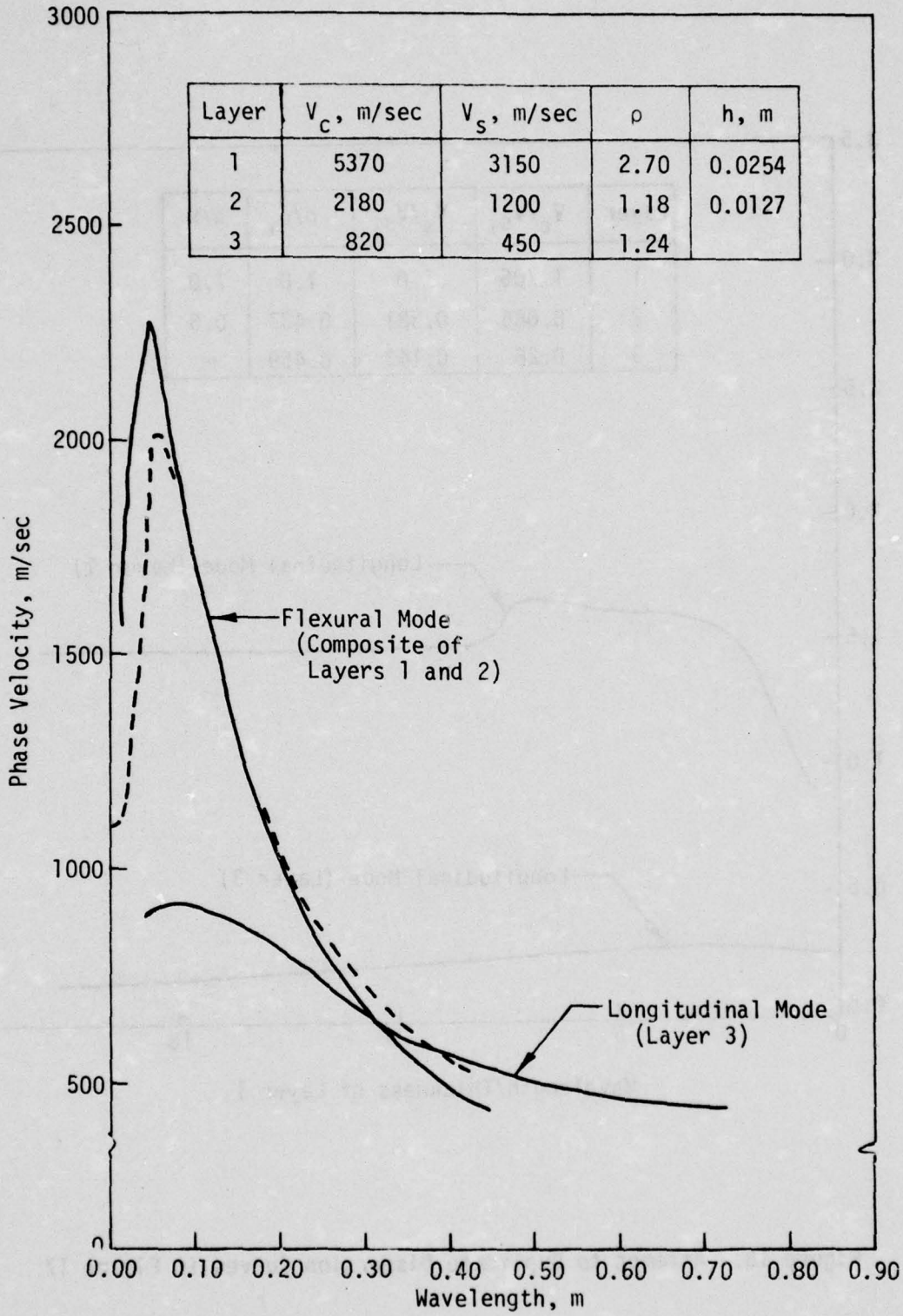

Figure 17. Dispersion Curves for Two-Layered System [after Jones (ref. 24)]

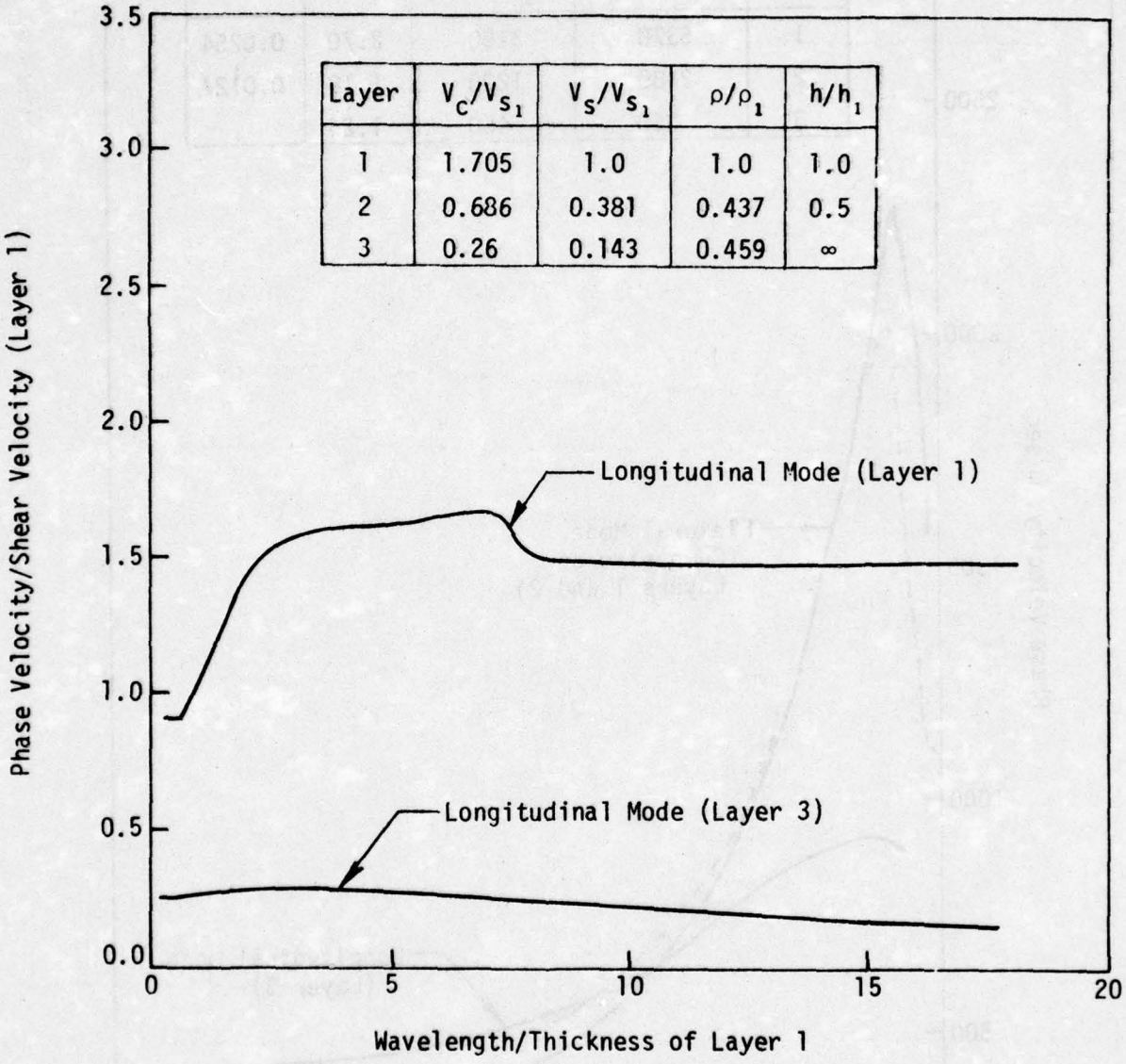

Figure 18. Attempt to Duplicate Dispersion Curves in Figure 17

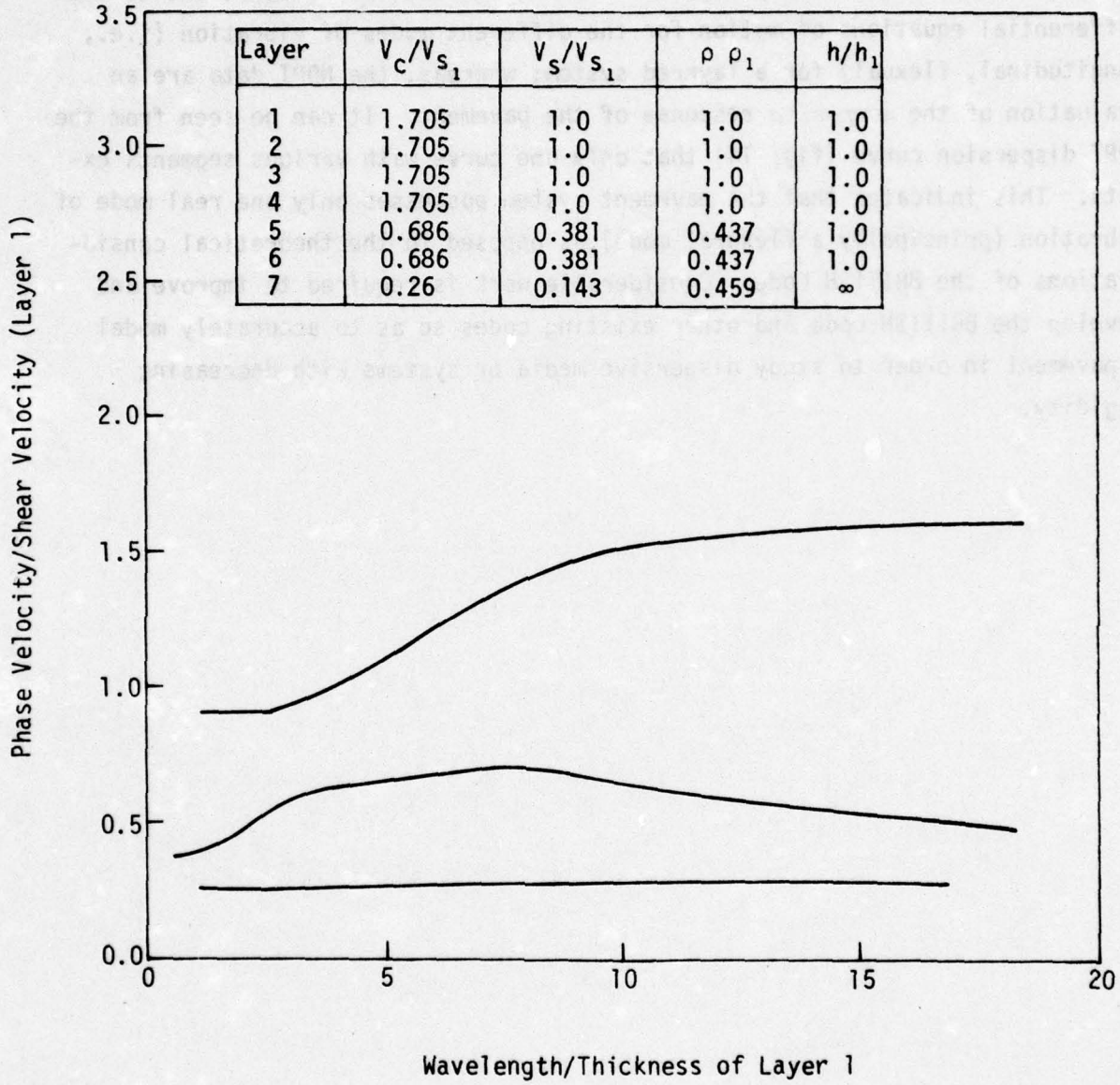

Figure 19. Dispersion Curves for Seven-Layered Representation of System Considered in Figure 18

codes as it relates to the NDPT method developed by CERF. A comparison of the successful dispersion curves computed by the BRITISH Code (figs. 15, 16, 18, and 19) and those computed from the NDPT data (figs. 13 and 14) indicates very different responses of the pavement. The BRITISH Code finds solutions to the differential equations of motion for the different modes of vibration (i.e., longitudinal, flexual) for a layered system; whereas, the NDPT data are an evaluation of the *composite* response of the pavement. It can be seen from the NDPT dispersion curve (fig. 14) that only one curve with various segments exists. This indicates that the pavement system possesses only one real mode of vibration (principally a flexural mode) as opposed to the theoretical considerations of the BRITISH Code. Considerable work is required to improve and develop the BRITISH Code and other existing codes so as to accurately model a pavement in order to study dispersive media or systems with decreasing rigidity.

SECTION 5
DATA-REDUCTION TECHNIQUES

PHASE ANGLE/FREQUENCY PLOTS

Phase angle/frequency plots must be obtained with either the NDPT electronics in the van or the laboratory, data-reduction instrumentation. Plots for reduction should include the following:

Plot No.	Frequency Range, Hz	Accelerometer Pairs
1	10 to 350	1 and 3, 2 and 3, 1 and 2
2	10 to 350	1 and 5, 2 and 5, 5 and 6
3	10 to 3500	1 and 3, 2 and 3, 1 and 2
4	10 to 3500	1 and 5, 2 and 5, 5 and 6

In addition, plots of the phase angle in the ±180-deg format and the 0 to 360-deg format should be made to aid with the data interpretation.* Only plots 2 and 3 are used for analysis, but plots 1 and 4 can be helpful when poor data are encountered. Interpretation of these plots can be accomplished with a minimum background in the analysis and trends of the data. A detailed example of the procedures used in interpreting phase angle/frequency plots is presented in appendix B.

Once the plots have been interpreted, the phase angle, ϕ, must be determined and recorded for certain frequencies. (CERF has designed transparent templates which expedite this process.) The phase angle must be continuously accumulated from 0 deg at zero Hz to 3500 Hz. On the ±180-deg plot, the phase angle is read directly over the frequency range for which $\phi \leq 180$ deg. When +180 deg is reached (at the bottom of the plot) the trace *flops over* to the top of the graph and progresses downward to the bottom of the plot again. The phase angle at any frequency past the first *flopover* is equal to 180 deg

*See reference 6 for full details on the electronic procedures for producing these graphs.

plus the angle represented by the distance from the top of the graph to the point on the interpretation curve. See figure 20a for examples of phase angles at different points along the curve. If a 0 to 360-deg plot is used, a phase angle of 0 deg is at the top of the plot and 360 deg is at the bottom. The phase angle increases to 360 deg, at which point a *flopover* occurs, and the trace begins again at the top of the plot (0 deg). Phase angles past the 360-deg *flopover* point are equal to 360 deg plus the angle represented by the distance from the top of the graph to the point on the interpretation curve. See figure 20b for examples of phase angles at different points along the curve. The maximum phase angle depends on the interpretation of the phase angle/frequency plot and which accelerometers are used for analysis.

DISPERSION CURVES

The following equations are used to compute the wavelengths and phase velocities for the dispersion curve:

$$\lambda = \frac{360d}{\phi}$$

and

$$v = f\lambda$$

where

λ = wavelength (ft)
d = distance between compared accelerometers (ft)
ϕ = phase angle (deg)
v = phase velocity (ft/sec)
f = frequency (Hz)

The wavelength equation was proven valid by previous researchers involved with the NDPT van and its development (ref. 7). Similarly, the equal accelerometer spacing of 2 ft was found adequate for most pavements tested (ref. 26). A computer program, NDTPLOT, computes wavelengths and phase

---

26. Rao, H. A. B., *Results of Nondestructive Tests at Webb Air Force Base*, Letter Report III, Civil Engineering Research Facility, Albuquerque, New Mexico, August 1973.

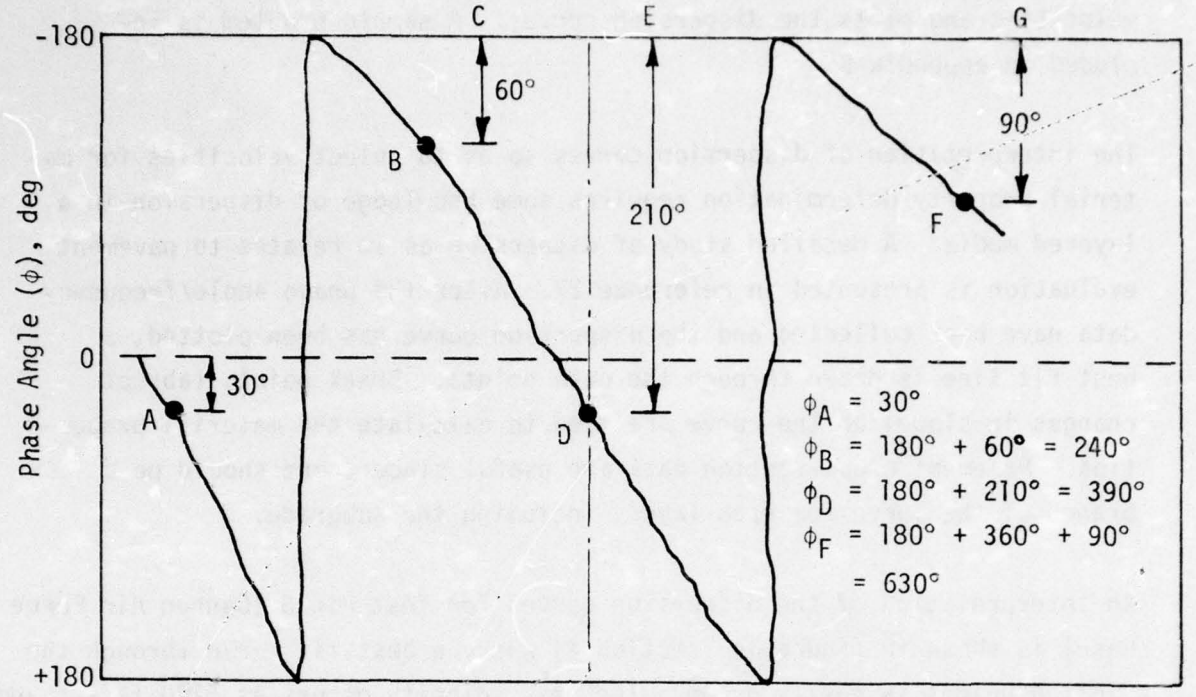

(a) ± 180-deg Format

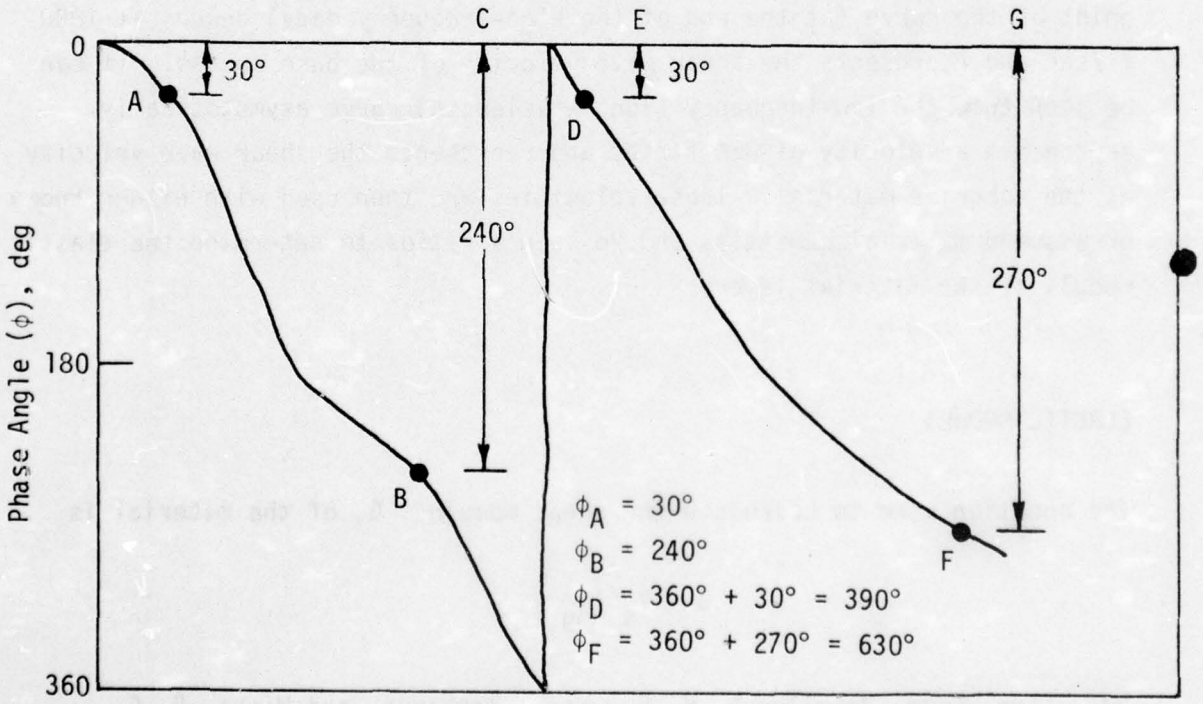

(b) 0-360-deg Format

Figure 20. Interpretation of Phase Angle/Frequency Plot

velocities and plots the dispersion curves. A sample problem is included in appendix B.

The interpretation of dispersion curves so as to select velocities for material property determination requires some knowledge of dispersion in a layered media. A detailed study of dispersion as it relates to pavement evaluation is presented in reference 27. After the phase angle/frequency data have been collected and the dispersion curve has been plotted, a best fit line is drawn through the data points. Break points (abrupt changes in slope) on the curve are used to calculate the material properties. Pavement cross-section data are useful since there should be a branch of the curve for each layer, including the subgrade.

An interpretation of the dispersion curves for Test Pit 6 (Cannon Air Force Base) is shown in figure 14 (section 4) where a best-fit curve through the plotted points is easily drawn. The peak velocity occurs at 5280 ft/sec and represents the Rayleigh wave velocity for the surface course. The break point of the curve (at the end of the high-frequency data) occurs at 1800 ft/sec and represents the shear wave velocity of the base course. It can be seen that the low-frequency (long wavelength) curve asymptotically approaches a velocity of 330 ft/sec and represents the shear wave velocity of the subgrade material. These velocities are then used with either known or assumed material densities and Poisson's ratios to determine the elastic moduli of the material layers.

ELASTIC MODULI

The equation used to calculate the shear modulus, G, of the material is

$$G = V_s^2 \left(\frac{\gamma}{g}\right)$$

27. Finn, Fred, McCullough, B. F., Nair, Keshavan, and Hicks, R. G., *Plan for Development of Nondestructive Method for Determination of Load-Carrying Capacity of Airfield Pavements*, Final Report No. 1062-2(F), Materials Research and Development, Inc., Oakland, California, November 1966.

where

V_s = shear wave velocity (ft/sec)

γ = unit weight of material (lb/ft^3)

g = acceleration constant (32.2 ft/sec)

Young's modulus, E, is computed by

$$E = 2(1 + \nu) G$$

where

ν = Poisson's ratio (usually assumed to be a reasonable value)

The shear-wave velocities for all materials except the surface course can be inputted into these equations for modulus determinations. However, the Rayleigh wave velocity for the surface course requires a correction before the shear-wave velocity can be computed. The equation used to compute the shear-wave velocity from the Rayleigh-wave velocity is

$$V_s = \frac{V_R}{a}$$

where a is a function of Poisson's ratio and varies from 0.875 for $\nu = 0$ to 0.955 for $\nu = 0.5$ (ref. 27).

When the peak velocities of the dispersion curve are used to calculate elastic moduli, very acceptable values are obtained for Portland cement concrete; however, high modulus values are obtained for asphaltic concrete surfaces. Because of the rigid interparticle contact and bonding in Portland cement concrete, the stress wave in such a layer propagates through the material without any damping effects. However, in asphaltic concrete pavements, the viscous damping properties of the asphalt binder at high frequencies retard the phase angle shift and this results in high calculated velocities. Asphaltic concrete moduli have been observed by others to increase with the testing frequency (ref. 28). Therefore, the calculated moduli must be reduced so as to more accurately model the conditions in the field. CERF has found that a modulus reduction factor of 50 percent is reasonable for asphaltic concrete surfaces of average thickness (3 to 6 in). A different

28. Yoder, E. J., and Witczak, M. W., *Principles of Pavement Design*, 2nd Edition, John Wiley and Sons, New York, 1975.

analysis must be performed when the pavement is Portland cement concrete overlaid with asphaltic concrete. In this situation the velocity of propagation of the Portland cement concrete dominates, and the asphaltic concrete velocity cannot be determined accurately. This is especially true with thin overlays; here the asphaltic concrete modulus must be estimated on the basis of the general competency of the surfacing.

Typical moduli for various types of paving materials, determined by plate-bearing tests performed at CEL (ref. 29), are given in table 4. When moduli are computed for the base and subgrade layers from dispersion curve data, the values obtained are also too high and must be corrected. Correction procedures based on theoretical considerations are used to adjust the NDPT moduli to acceptable values.

Two different procedures are employed to correct the base course moduli depending on the type of pavement surface. A theoretical approach is used for Portland cement concrete pavements. From the theory of wave propagation through layered media, the velocity should increase as a stress wave travels from a lower-speed, less-dense material (i.e., base course) to the higher-speed, more-dense material (i.e., Portland cement concrete pavement). The governing equation for propagation of a shear wave through media is

$$V_s = \sqrt{\frac{G}{\rho}} = \sqrt{\frac{Gg}{\gamma}}$$

Thus, the shear wave velocity in the base course (layer 2) is defined by

$$V_{s_2} = \sqrt{\frac{G_2 g}{\gamma_2}}$$

so that the velocity increase as the wave travels into the Portland cement concrete pavement (layer 1) is

$$V'_{s_2} = \sqrt{\left(\frac{G_1}{\gamma_1}\right)\left(\frac{\gamma_2}{G'_2}\right)} \quad V_{s_2}$$

---

29. Nielsen, J. P., *Layered Pavement Systems: Analysis Related to Design*, Technical Report R-594, Civil Engineering Laboratory, Port Hueneme, California, September 1968.

Table 4. Typical Moduli for Paving Materials

Material	Modulus Range, psi
Portland Cement Concrete	$2.0 - 5.0 \times 10^6$
Asphaltic Concrete	$0.1 - 1.0 \times 10^6$
Well-Graded Crushed Stone Base	$30 - 90 \times 10^3$
Cement-Treated Base (SM, SC)	$25 - 40 \times 10^3$
Well-Graded Gravels (GW) Silty Gravels (GM)	$10 - 25 \times 10^3$
Silty Sand (SM) Sandy Clay (SC) Clays (CL)	$3 - 10 \times 10^3$

where

V'_{S_2} = shear velocity in the base course as indicated by the dispersion curve

V_{S_2} = actual in-situ shear velocity in the base course

G_1 = shear modulus of the surface layer

G'_2 = shear modulus of the base course as derived from V'_{S_2}

The above equation can be solved for V_{S_2}, and thus the in-situ shear modulus can be determined from $G = V_{S_2}^2 \rho$. This analysis was performed on the Cannon Air Force Base data and yielded a corrected velocity range of 625 to 825 ft/sec for a stabilized base course. These velocities correspond to Young's moduli of 30,000 to 50,000 psi, which are satisfactory values for a base course.

The following sample calculation is performed with data from Test Pit 2 at Cannon Air Force Base:

V_{R_1} = 6200 ft/sec (surface Rayleigh wave, a = 0.90)

V_{S_1} = 6889 ft/sec

V'_{S_2} = 2130 ft/sec (dispersion curve data)

γ_1 = 145 lb/ft^3

γ_2 = 135 lb/ft^3

ν_1 = 0.20

ν_2 = 0.30

$$G_1 = (6889)^2 \left(\frac{145}{32.2}\right)\left(\frac{1}{144}\right) = 1.48 \times 10^6 \text{ psi}$$

$$G'_2 = (2130)^2 \left(\frac{135}{32.2}\right)\left(\frac{1}{144}\right) = 1.32 \times 10^5 \text{ psi}$$

$$V_{S_2} = \sqrt{\frac{(1.32 \times 10^5)(145)}{(1.48 \times 10^6)(135)}}\ (2130) = 659 \text{ ft/sec}$$

$$G_2 = (659)^2 \left(\frac{135}{32.2}\right)\left(\frac{1}{144}\right) = 12{,}650 \text{ psi}$$

$$E_2 = 32{,}900 \text{ psi}$$

An alternate and simpler approach is to use the approximate equation

$$E_2 = \frac{(E'_2)^2}{E_1}$$

where

E_2 = adjusted Young's modulus

E'_2 = Young's modulus obtained from the dispersion curve shear-wave velocity for the base course

E_1 = Young's modulus of Portland cement concrete

When this approach is used, the following results are obtained:

$$E'_2 = (1.32 \times 10^5)(2)(1 + 0.30) = 3.43 \times 10^5 \text{ psi}$$

$$E_1 = (1.48 \times 10^6)(2)(1 + 0.20) = 3.55 \times 10^6 \text{ psi}$$

$$E_2 = \frac{(3.43 \times 10^5)^2}{(3.55 \times 10^6)} = 33{,}160 \text{ psi}$$

When the pavement surface is asphaltic concrete, a 50-percent reduction is applied to the base course modulus value. Although past experience with asphaltic concrete pavements has indicated that this factor is appropriate, no theoretical development can be presented to validate this. However, as with the correction procedure for the surface modulus, it appears that the viscous damping properties of the asphaltic concrete interfere with the determination of the actual velocities of propagation. An empirical correction factor, therefore, is deemed necessary.

Subgrade modulus values are corrected based on an empirical correction factor of 50 percent for both asphaltic concrete and Portland cement concrete pavements. This value was arrived at through the studies at Cannon and Laughlin Air Force Bases. When applied to the data, the subgrade moduli were corrected to an acceptable range of 3,000 to 10,000 psi. A summary of the modulus correction procedure is presented in table 5.

Table 5. Modulus Correction Procedure

Pavement Layer	Correction
Surface	
Portland Cement Concrete	Use actual value determined.
Asphaltic Concrete	Reduce by 50 percent.
Base/Subbase with:	
PCC Surface	Corrected $E_2 = E_2^2/E_1$
AC Surface	Reduce by 50 percent
AC/PCC Surface	Reduce by 50 percent
Subgrade with:	
PCC Surface	Reduce by 50 percent
AC Surface	Reduce by 50 percent
AC/PCC Surface	Reduce by 50 percent

(The reverse of this page is blank)

APPENDIX A

OPERATIONAL INSTRUCTIONS FOR LABORATORY DATA-REDUCTION INSTRUMENTATION

INTRODUCTION

This appendix provides brief instructions for the operation of the laboratory-based, data-reduction instrumentation shown in figure A1. This equipment is similar to that installed in the NDPT van. These instructions have been written with the understanding that operators of this equipment are thoroughly familiar with the equipment in the van; hence, these instructions lack the details provided in the user's manual for the van (ref. 6).

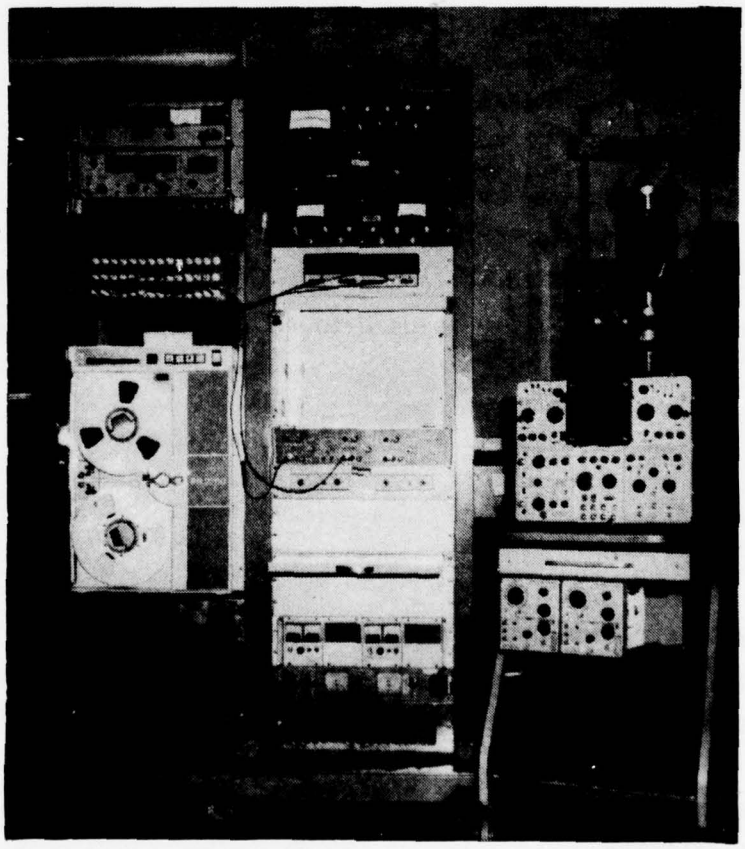

Figure A1. Laboratory-Based Data-Reduction Instrumentation

INITIAL SETUP

(1) Turn on the main power (lower left section of rack). Indicator lights above the left and right racks should be lit.

(2) Clean the tape deck record/reproduce heads with cleaning fluid according to the instructions and recommendations included in the manufacturer's operation manual. Clean heads with Ampex head cleaner. Clean capstan (puck) with denatured alcohol only.

(3) Turn on the tape deck power.

(4) Install a scratch tape in the tape deck and depress the STOP READY Button.

(5) Insure that other equipment is receiving power and that power switches are on.

(6) Verify that the power supply for the punch panel indicator lights (lower right section of rack) registers 12 Vdc. Adjust if necessary.

Allow a 30-min warmup period before performing any calibrations. During this time, field notes and audio tape documentations should be reviewed to determine the exact channels to be used to record the field data.

EQUIPMENT CALIBRATION

Differential Amplifiers

All necessary calibration procedures are outlined in detail in the manufacturer's manuals. However, once these calibrations have been completed, the following must be performed before other system calibrations are made:

(1) Turn the AMPLIFIER OUTPUT Switches (on punch panel) for Channels 1 and 2 to FILTERED.

(2) Turn the REFERENCE FREQ. and ANALOG FREQ. Switches to DIRECT.

(3) Turn the FILTER Switches for both amplifiers to 10 kHz.

(4) Turn the VAR GAIN (variable gain) Switches for both amplifiers counter-clockwise to DETENT (calibrate).

Phase Computer

(1) Remove softwire connections to the phase computer inputs for Channels A and B before calibration.

(2) Push the METER RANGE Switch to ± 180°.

(3) Push the FILTER SELECTION Switch to 1 (latched). This indicates a minimum amount of signal smoothing.

(4) Turn the NORMAL/180 Switch to NORMAL (released).

(5) Turn the 3mV-5V/x100 Switch to 3mV-5V (released) for both channels.

(6) With no signal applied, and adjusting the PHASE ZERO Control Potentiometer, correct the digital phase indicator to read ± 180.0°.

(7) Depress the 0-360 METER RANGE Switch and verify that the indicator reads 360.0°.

NOTE

An exact reading of 360° may not show on the indicator; the reading may deviate a few tenths of a degree depending on the ± 180° calibration.

(8) Return the METER RANGE Switch to + 180°.

(9) Replace softwire connections to the phase computer inputs for Channels A and B.

Carrier Generator

NOTE

Refer to the manufacturer's manual for laboratory calibration.

(1) Turn the OPER CAL Switch to CAL.

(2) Verify that the needle is in the green area on the tuning amplitude meter. If it is not, refer to the manufacturer's manual for the proper calibration procedure.

NOTE

Periodically during the test, check that the tuning amplitude meter needle is reading in the green area; adjust if necessary using the TUNING AMPL (tuning amplitude) Potentiometer with the OPER CAL Switch on OPER.

Tracking Filter

(1) Verify that the OPER CAL Switch on the carrier generator is on CAL.

(2) Turn the RANGE Switch for Channels 1 and 2 to CAL.

(3) Turn the RELATIVE RANGE Vernier for both channels to CAL.

(4) Turn the METER MULTIPLIER Switch for both channels to CAL.

(5) Verify that the FILTER SELECTION Switch on the phase computer is on 1.

(6) Turn the MODE SELECTION Switch to SINE AVG (SEC) 1.

(7) Using the FREQ Trim Potentiometer of the carrier generator, adjust for maximum signal strength of both channels (indicated by the signal strength meters of the tracking filter).

NOTE

It may be necessary to adjust one of the channels to a maximum signal and fine tune the other as indicated in step 8.

(8) Using the CAL Trim Potentiometer for Channel 1 Filter 1, adjust the Channel 1 signal meter to read 10 (full range).

(9) Repeat step 8 using Channel 2 Filter 1 CAL Trim Potentiometer and Channel 2 signal meter.

(10) Turn the carrier generator OPER CAL Switch to OPER.

(11) Turn the RANGE Switch for Channels 1 and 2 to 3Vrms.

(12) Turn the METER MULTIPLIER Switches of the tracking filter to 1.

(13) Input a calibration signal to both channels to adjust the tracking filter. The Spectral Dynamics Sweep Oscillator Servo (upper left rack) is used for this purpose. The SOS signal is hardwired to the patch panel CAL SIGNAL OUT Terminal and softwire connections are made to input this signal to the tracking filter (fig. A2). Adjust the sweep oscillator as follows:

(a) Set FUNCTION Switch to SINE WAVE.

(b) Set LEVEL Potentiometer to 6 (relative gain setting).

(c) Switch MODE SELECTION Switch to LINEAR SWEEP SINGLE.

(d) Switch Multiplier A to 10.

(e) Set Multiplier B to 10.

(f) Set sweep rate (30 to 50 Hz/sec is recommended).

(g) Sweep up to 3500 Hz and hold at this frequency.

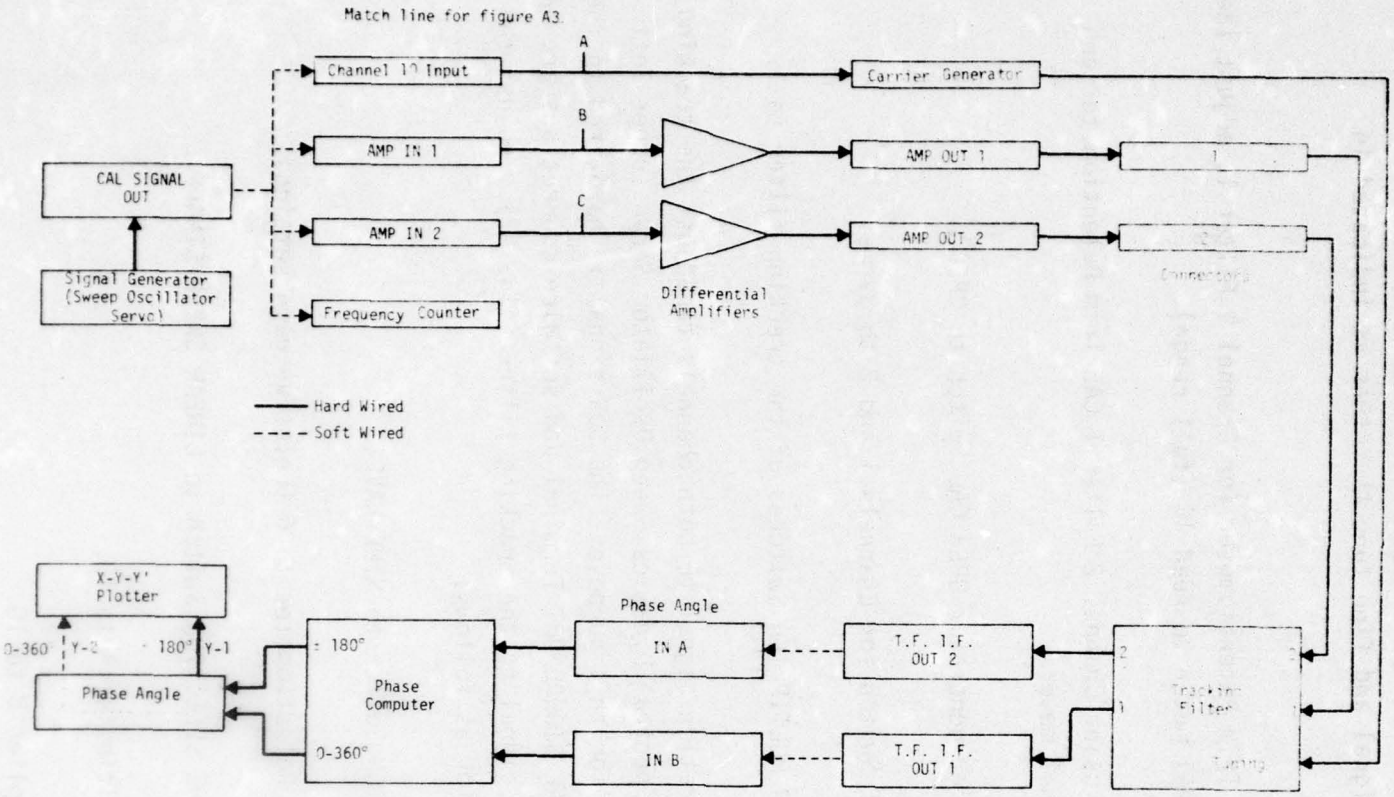

Figure A2. Wiring Scheme for Calibration

(14) Adjust the TUNING AMPL Trim Potentiometer of the carrier generator until the meter reads mid-scale in the green area.

(15) Set the GAIN Switches of the differential amplifiers so that the signal-strength meters of the tracking filter indicate approximately the same mid-scale reading.

NOTE

The GAIN Switches should be set at identical positions.

(16) Adjust the Channel 1 Filter 1 Trim Potentiometer on the tracking filter to indicate a system phase angle of 0° (± 0.2°) on the phase meter.

AMPEX PR-2200 Tape Recorder/Reproducer

For calibration procedures refer to the manufacturer's operation manual. Knowledge of the quality level of recording is necessary to properly calibrate and adjust the reproduce amplifiers for data reduction. Only a qualified technician should perform the calibrations given in the manufacturer's manual.

The tape deck is equipped with special reproduce heads which can be adjusted to correct for skew, which could introduce errors into the phase angle computation. The following procedure is required to adjust the tape deck skew between different channels for accurate phase-angle determinations of field data.

(1) Press the TAPE SPEED Switch (i.e., 7 1/2 in/sec).

(2) Disconnect CAL SIGNAL OUT from amplifier input terminals (AMP IN 1 and AMP IN 2) on patch panel and connect to tape deck channel inputs which correspond to Accelerometers 1 and 5 of the field data as shown in figure A3.

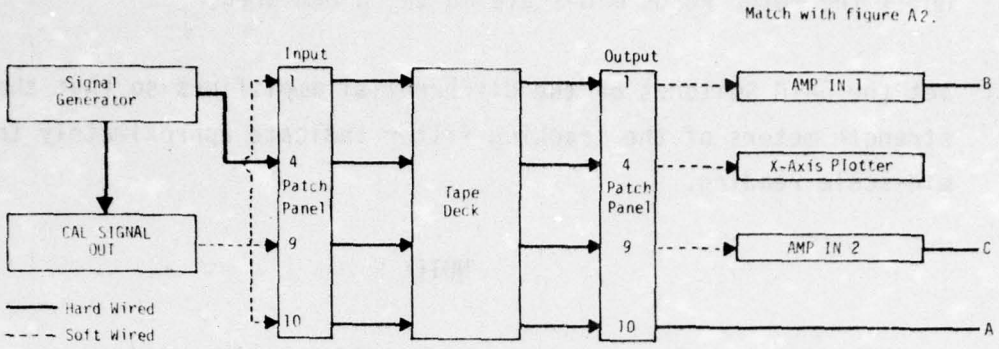

Figure A3. Supplement Wiring for Calibration of Tape Deck Skew

(3) Connect Channels 1 and 9 tape output to amplifier input AMP IN 1 and AMP IN 2, respectively.

(4) Turn the REFERENCE FREQ and ANALOG FREQ Switches on the punch panel to PLAYBACK.

(5) Place tape deck in record forward mode by simultaneously depressing the RECORD and FWD Buttons.

(6) Adjust the TUNING AMPL Trim Potentiometer on the carrier generator until the TUNING AMPLITUDE Meter is in the green area.

CAUTION

Adjustments should be very minor; do not overextend the range of the skew adjusting screw. Damage to the tape

heads can result if the screws are extended past their normal range.

(7) While monitoring the digital phase indicator, adjust the skew adjusting screw for the odd-numbered tape channels to minimize the skew error between channels indicated by the phase reading.

NOTE

The adjusting screws are labeled O and E for the odd-and even-numbered tape heads, respectively. The digital phase indicator should show a phase angle of 0° when calibrated properly.

(8) Check other channel combinations on the same head to verify calibrations.

NOTE

The same procedure must be performed for the even-numbered channels with the E skew adjusting screw.

(9) Stop the tape deck.

(10) Disconnect the following:

(a) Signal generator output from tape deck inputs (i.e., Channels 1 and 9) on the patch panel.

(b) Signal generator output from carrier generator (Channel 10) on the patch panel.

(c) Generator signal from CAL SIGNAL OUT on the patch panel.

(11) Turn off signal generator.

(12) Remove scratch tape.

(13) Install field test data tape.

X-Y-Y' Plotter

The X-Y-Y' plotter is capable of recording two different signals on the Y-axis. This capability is used to calibrate the plotter and to create two different plots. One axis is used to plot the ± 180° plot and the other is used to plot the 0-360° plot. By using the two different axis of the plotter, recalibration of the plotter is unnecessary when both plots are desired.

(1) Place plot paper on plotter and turn the CHART Switch to HOLD.

(2) Properly install plotter pens in pen carriages (see instruction manual) and turn the PEN Switch to LIFT.

(3) Turn RESPONSE Switches (3) to SLOW.

(4) Turn on SERVO Switch.

Y-1 Axis

The Y-1 axis of the plotter is used to create the ± 180° plot. The following calibration of the Y-1 axis is required for this plot.

(1) With no voltage applied to the Y-1 input, adjust the pen to register on the center of the plot using the ZERO Adjust knob.

(2) Observing standard signal polarity, input + 1.8 Vdc from a precision power supply (e.g., DIAL-A-VOLT) to the Y-1 axis of the plotter.

(3) Turn the Y-1 RANGE SELECTOR Switch to .1V/in.

(4) Turn the POLARITY Switch to -UP.

(5) Using the Y-1 RANGE CAL Vernier, adjust the Y-1 axis to read + 180° on the plot (i.e., bottom of the plot).

(6) Flip the POLARITY Switch to +UP and verify that the plotter indicates - 180° (i.e., top of the plot).

(7) After calibration, turn the POLARITY Switch to -UP. (This will result in a plot of + 180° at the bottom of the plot and - 180° at the top.)

(8) Disconnect calibration input voltage.

Y-2 Axis

The Y-2 axis of the plotter is used to create the 0-360° plot. The following calibration of the Y-2 axis is required for this plot.

(1) With no voltage applied to the Y-2 input, adjust the axis using the Y-2 ZERO Adjust Knob of the plotter to correspond to 0° at the top of the plot.

(2) Observing standard signal polarity, input + 3.6 Vdc from a precision power supply to the Y-2 axis of the plotter.

(3) Turn the Y-2 RANGE SELECTOR Switch to .1V/in.

(4) Turn the Y-2 POLARITY Switch to -UP.

(5) Using the Y-2 RANGE CAL Vernier, adjust the plot to 360° (i.e., bottom of plot).

(6) Disconnect calibration input voltage.

(7) Reconnect phase output to appropriate axis.

X-Axis

(1) Set the RANGE SELECTOR Switch of the X-axis to an appropriate range for the recorded test data.

(2) Turn the POLARITY Switch to +RT (right). (This will plot with the frequency increasing to the right.)

(3) Proceed to low end of test (i.e., 10 Hz).

(4) Using the analog frequency from the data tapes, set the lower frequency limit (i.e., 10 Hz) with the ZERO Adjust Knob of the X-axis.

(5) Proceed to the beginning of the test (i.e., 350 or 3500 Hz).

(6) Using the RANGE CAL Vernier of the X-axis, adjust the upper frequency limit (i.e., 350 or 3500 Hz).

(7) Turn the three RESPONSE Switches to FAST.

(8) Rewind tape to beginning of recorded field test data.

PLOTTING OF FIELD DATA

(1) Connect phase angle output on patch panel to Y-1 input of plotter for a $\pm$ 180° plot. (If a 0-360° plot is desired, the phase angle output should be connected to the Y-2 input.)

(2) Verify that the METER RANGE Switch of the phase computer is on $\pm$ 180°. (If a 0-360° plot is desired, the METER RANGE Switch should be on 0-360°.)

(3) Verify that the NORMAL/180 Switch is on NORMAL (released).

(4) Verify that the 3mV-5V/x100 Switch is on 3mV-5V (released).

(5) Verify that the X-axis is connected to the analog frequency tape output channel (i.e., Channel 4).

(6) Turn IRIG MODE SELECTOR Switch to TRANS.

(7) Turn SYNC Switch of IRIG generator/reader to IRIG B.

(8) Turn INPUT Switches on the IRIG generator/reader to + and FWD.

NOTE

The position of the FILTER Switch of the IRIG generator/reader is determined by the quality of the recorded IRIG signal.

(9) Connect accessory equipment for data monitoring (i.e., frequency counter, oscilloscope, etc.) to proper channels, utilizing the tape outputs.

(10) Verify that the following switches located on the punch panel are in the indicated positions:

Switch	Position
Panel Power	ON
Analog Frequency	PLAYBACK
Reference Frequency	PLAYBACK
Amplitude 1 Output	FILTERED
Amplitude 2 Output	FILTERED
IRIG Reader	B

(11) Connect desired accelerometer channels to proper amplifier input. (The inboard accelerometer should be connected to the AMP IN 1 Terminal; the outboard accelerometer should be connected to the AMP IN 2 Terminal.)

(12) Insure that the SERVO Switch on the plotter is on STAND BY.

(13) Play back data in the forward mode by pressing the FWD Button on the recorder.

(14) Check tracking filter signal level and adjust gain levels to provide mid-scale readings.

(15) Flip the SERVO Switch on the plotter to ON.

(16) Turn the PEN Switch to RECORD when frequency sweep begins.

(17) When the frequency sweep is completed, turn PEN Switch to LIFT.

(18) Flip the SERVO Switch to STAND BY.

(19) If other accelerometer data are desired, rewind the tape to beginning of test and connect the desired accelerometer channels to the AMP IN Terminals and repeat steps 2, and 11 through 18. If data from another test are desired, proceed to next test tape position and repeat steps 2, and 11 through 18.

SHUTDOWN

(1) Rewind the data tape and remove it from the tape deck.

(2) Turn off the tape deck power and allow the internal timing sequence to turn off the tape deck.

(3) Turn off instrumentation rack power and accessory equipment.

APPENDIX B
SAMPLE DATA-REDUCTION PROBLEM

This appendix outlines the recommended procedure for reducing the phase angle/frequency plots, constructing the dispersion curves, and determining modulus values. Actual field data from Shaw Air Force Base are utilized in the example.

The actual phase angle/frequency plots for Shaw are shown in figures B1 and B2 for the low-frequency and high-frequency sweeps, respectively. The general trend (interpretation) of the plots is shown by the heavy, solid, smooth line. In figure B1, the trend of the data can easily be seen and no problem exists in interpretation above 125 Hz. However, below 125 Hz, the data show no trend and the interpretation shown was arrived at by examination of other data at Shaw and through previous experience with phase angle/frequency data. The trend from point A through point E is the appropriate interpretation. An interpretation based on a straight line from the zero position to 180 deg at 125 Hz is not accurate and contrary to trends observed from other NDPT data. It should be pointed out that the interpretations of the data must be *forced* through a phase angle of 180 deg or multiples thereof. The actual field data never plot to exactly 180 deg. This is due to the effect of the sampling rate of the phase computer. The sampling rate could be increased (i.e., make shorter time intervals between phase computations) but the amount of noise (illustrated by the erratic traces) would also be increased. Therefore, the data were forced through 180 deg at 125 Hz. Below this frequency, the interpretation represents a typical pavement response. Figure B1 may be used as a model for the general trend of the low-frequency data, independent of pavement type. Specific points on the interpretation curves are labeled with the corresponding phase angles.

The phase angle/frequency coordinates of points A through E can be read directly from the plot (fig. B1); those of points F through I can also be read directly from the plot (fig. B2); but points J through P require some explanation. If the interpretation line is followed beginning at 0 Hz (fig. B2),

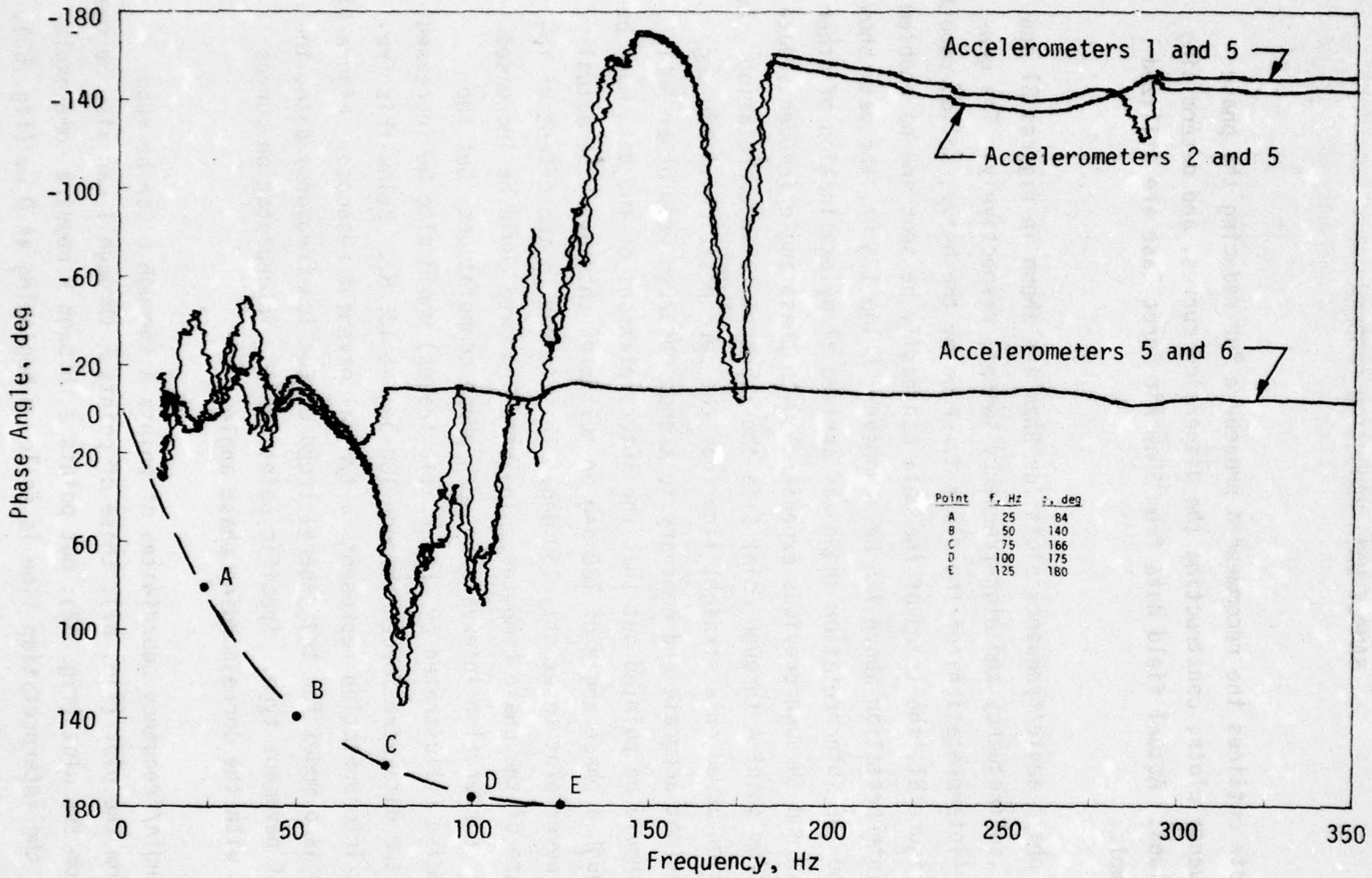

Figure B1. Low-Frequency Phase Angle/Frequency Data for Shaw Air Force Base

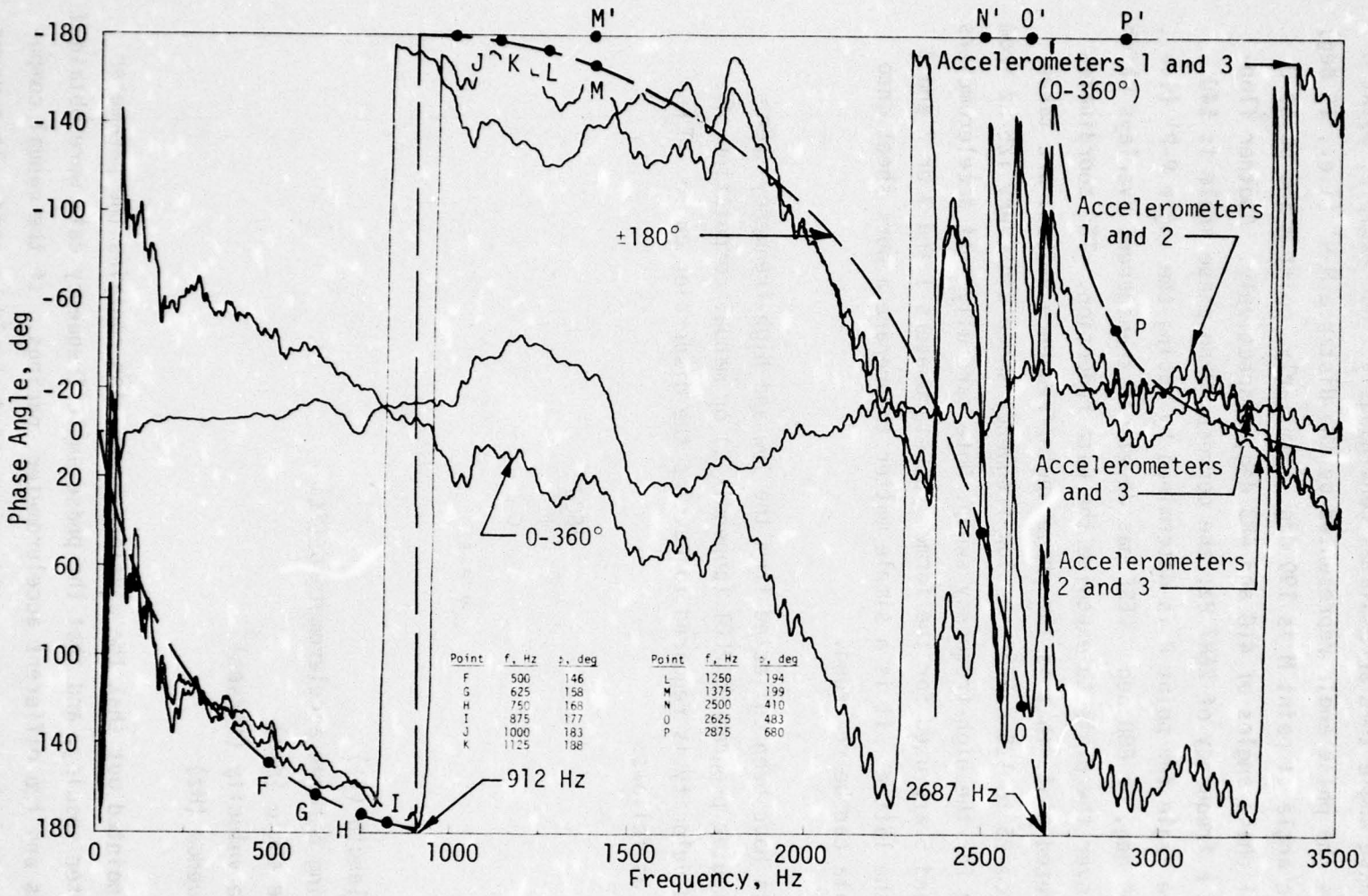

Figure B2. High-Frequency Phase Angle/Frequency Data for Shaw Air Force Base

the phase angle increases to 180 deg at a frequency of 912 Hz, where a flopover occurs. The phase angle then accumulates continuously. For example, point M is 180 deg plus the phase angle represented by the distance M-M' (i.e., 19 deg). The total phase angle at point M is 199 deg. Similarly, point N and point O represent total phase angles of 410 and 483 deg, respectively. Another flopover occurs at a frequency of 2687 Hz; the corresponding phase angle is 540 deg. The phase angle for point P is determined by adding the angle P-P' (i.e., 140 deg) to 540 deg, or 680 deg. CERF has developed transparent overlays which can be placed over the plots to expedite the data reduction. The coordinates of the interpreted plot, that is the phase angle/frequency values, are taken every 25 Hz from 25 to 125 Hz for the low-frequency sweep and every 125 Hz from 250 to 3500 Hz for the high-frequency sweep. Note carefully that accelerometers 1 and 5 or 2 and 5 are used for the former; accelerometers 1 and 3 or 2 and 3 are used for the latter. It is a simple matter to prepare a work sheet onto which these data can be recorded.

When these data have been collected from the low-and high-frequency sweep plots, the computer program NDTPLOT (appendix C) or manual computation of wavelength and velocity is required to develop the dispersion curve. The equations are as follows:

$$\lambda = \frac{360d}{\phi}$$

$$v = f\lambda$$

where

λ = wavelength (ft)
d = spacing between accelerometers (ft)
ϕ = phase angle (deg)
v = phase velocity (ft/sec)
f = frequency (Hz)

It should be pointed out that the wavelength equation contains the parameter d, accelerometer spacing, and that the phase angle/frequency data were obtained from two plots and two different accelerometer spacings. If the manual computation method is used, the appropriate values of d should be used. This means that d = 2 ft for the high-frequency (250 to 3500 Hz) data and d = 4 ft for the

low-frequency (25 to 125 Hz) data. However, with NDTPLOT, the phase angle for the low-frequency data is divided by two and then inputted to the program along with the high-frequency data. A spacing of 2 ft is then inputted to the program because the program is incapable of using different accelerometer spacings for two sweeps placed on the same plot. Thus, it is necessary to divide the actual phase angle by two for the low-frequency data only.

The phase angle/frequency data and the resulting dispersion curve are shown in figures B3 and B4, respectively. Figure B3 illustrates the format used to input the phase angles for selected frequencies to the NDTPLOT program. The frequencies are inputted to the program by a data statement incorporated in the program. Therefore, care must be taken to insure that the phase angle values are positioned on the Fortran coding form so that they correspond to the proper frequencies (appendix C). Notice that the phase angles indicated in figure B1 corresponding to frequencies of 25, 50, 75, 100, and 125 Hz have been divided by two on the coding form.

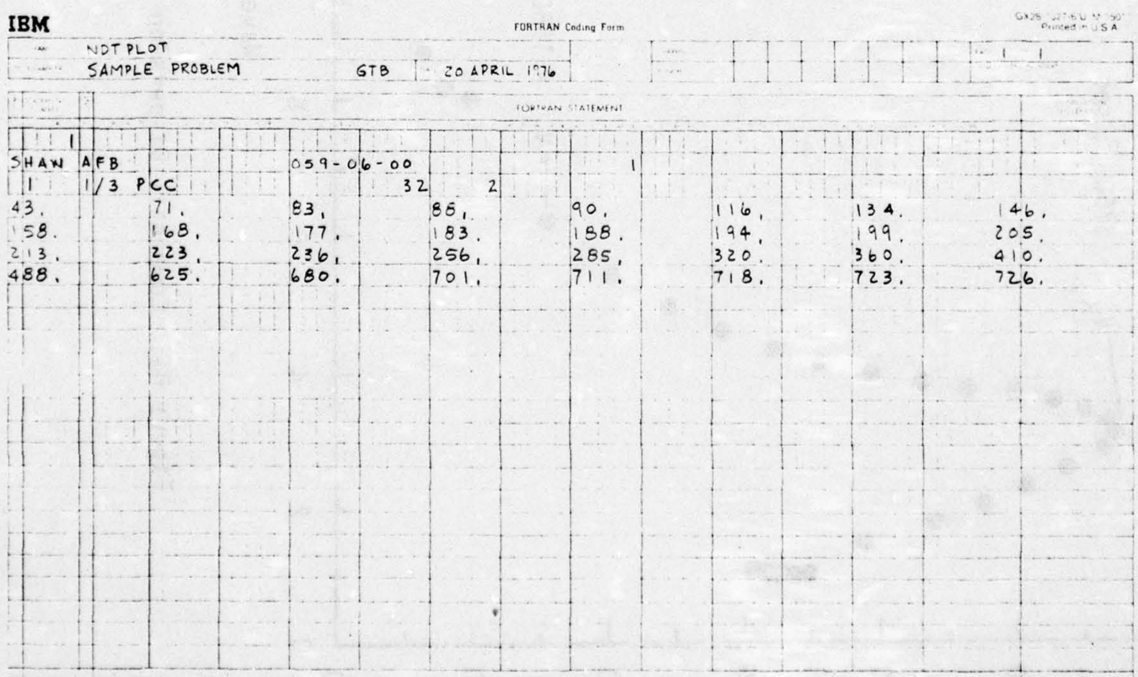
IBM FORTRAN Coding Form

NDT PLOT
SAMPLE PROBLEM GTB 20 APRIL 1976

FORTRAN STATEMENT

Card								
A	1							
B	SHAW AFB		059-06-00		1			
C	1 1/3 PCC		32	2				
D1	43.	71.	83.	86.	90.	116.	134.	146.
D2	158.	168.	177.	183.	188.	194.	199.	205.
D3	213.	223.	236.	256.	285.	320.	360.	410.
D4	488.	625.	680.	701.	711.	718.	723.	726.

Figure B3. Sample NDTPLOT Fortran Coding Form

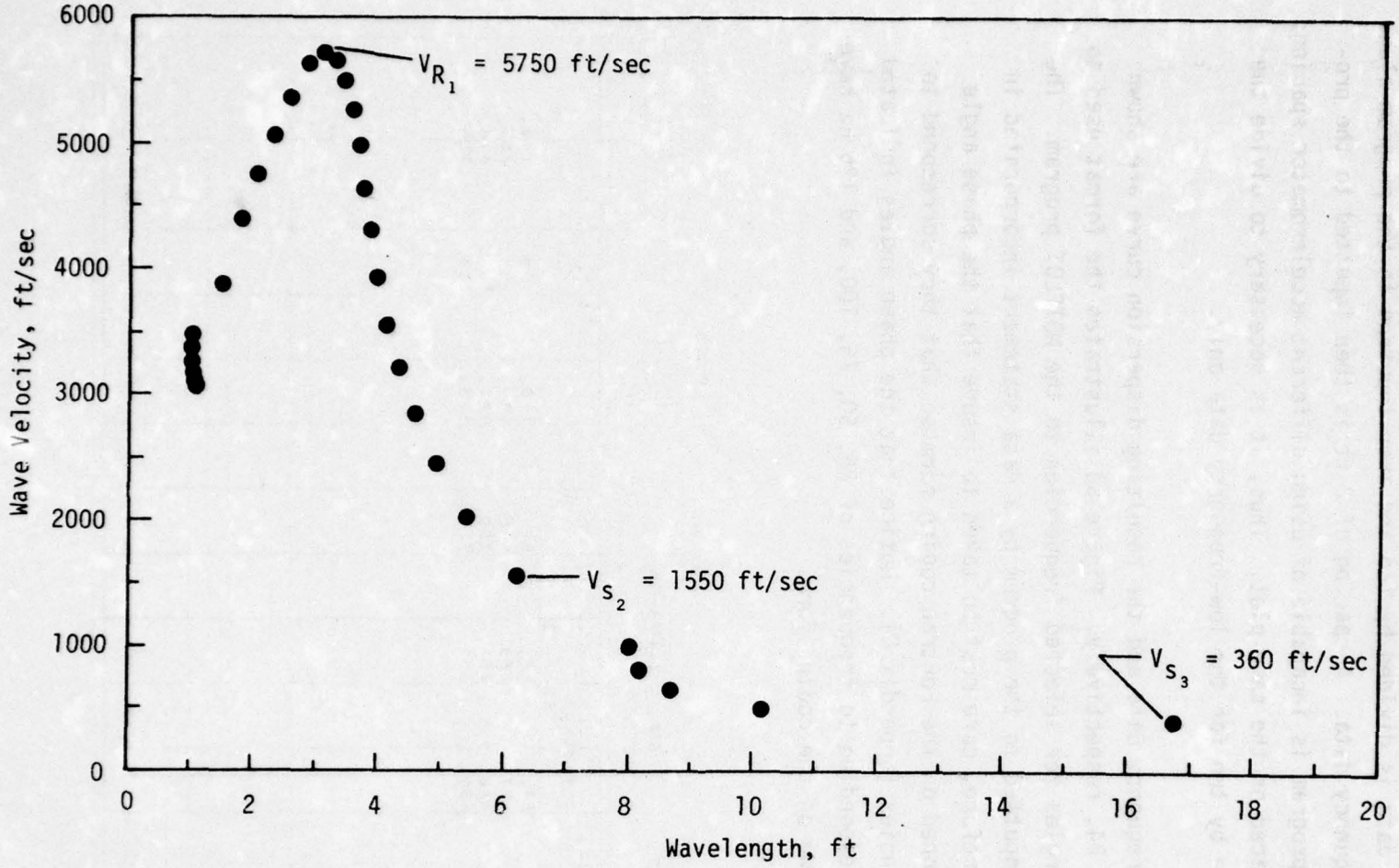

Figure B4. Composite Dispersion Curves for Shaw Air Force Base

Interpretation of the dispersion curve can easily be made and the critical velocities can be obtained. The Rayleigh peak velocity of the surface course of the Portland cement concrete pavement is 5750 ft/sec; the shear wave velocity of the base course is 1550 ft/sec; and the subgrade shear wave velocity is 360 ft/sec. Next, the uncorrected moduli are calculated by

$$G = V_s^2 \left(\frac{\gamma}{g}\right)$$

where

G = shear modulus (lb/ft^2)
V_s = shear wave velocity (ft/sec)
γ = unit weight (lb/ft^3)
g = acceleration constant (32.2 ft/sec/sec)

The Rayleigh velocity of 5750 ft/sec must be converted to a shear velocity by dividing by 0.9 (used for both Portland cement concrete and asphaltic concrete). This yields a shear wave velocity of 6389 ft/sec, which corresponds to a Young's modulus of 3.06×10^6 psi. A summary of the calculations is as follows:

	V_s, ft/sec	γ, lb/ft^3	ν	Uncorrected Moduli G, psi	Uncorrected Moduli E, psi
Portland Cement Concrete	6389	145	0.25	1.28×10^6	3.19×10^6
Base Course	1550	120	0.35	6.22×10^4	1.68×10^5
Subgrade	360	105	0.38	2.93×10^3	8.10×10^3

The modulus for the base course is very high when the dispersion curve velocity of 1550 ft/sec is used. However, the modulus can be corrected with the correction procedure presented in section 5.

$$E_2 = \frac{(E_2')^2}{E_1}$$

where

E_2 = corrected Young's modulus (psi)

AD-A043 003 NEW MEXICO UNIV ALBUQUERQUE ERIC H WANG CIVIL ENGINE--ETC F/G 13/2
PAVEMENT EVALUATION SYSTEM.(U)
OCT 76 J P NIELSEN, G T BAIRD F29601-76-C-0015
UNCLASSIFIED CERF-AP-20 AFCEC-TR-76-28 NL

2 OF 2
AD
A043003

END
DATE
FILMED
9-77
DDC

E'_2 = uncorrected Young's modulus based on dispersion curve velocity (psi)

E_1 = Young's modulus of surface course (psi)

$$E_2 = \frac{(1.68 \times 10^5)^2}{(3.19 \times 10^6)} = 8847 \text{ psi}$$

The subgrade modulus is reduced 50 percent from the calculated value (i.e., 8100 psi) to a corrected value of 4050 psi.

The structural analysis of the pavements is accomplished by implementing PREDICT. Appendix D contains a user's manual for PREDICT.

APPENDIX C

PROGRAM NDTPLOT USER'S MANUAL

```
                    NDTPLOT USERS MANUAL
     CERF VERSION 15 APRIL 1976
     WRITTEN FOR AFCEC REDUCTION OF NDPT DATA

A CARD    FORMAT (I5)
     COLUMN  VARIABLE   DESCRIPTION
       1-5     NOTS    TOTAL NUMBER OF TEST STATIONS
B CARD    FORMAT (4A10,3X,I2)
     COLUMN  VARIABLE   DESCRIPTION
       1-20   TITLE    NAME OF FACILITY (EG.NELSON AFB)
      21-40             RUNWAY OR TAXIWAY NUMBER AND STATION OR TEST POINT
                         NUMBER (EG.RW 03R-21L STA.41+00)
      44-45   IPAIRS   NUMBER OF ACCELEROMETER PAIRS PER TEST STATION
                         (COL.45 = 1)
C CARD    FORMAT (I2,3X,2A10,I5,F5.0)
     COLUMN  VARIABLE   DESCRIPTION
       1-2    IAPAIR    ACCELEROMETER PAIR DESIGNATION NUMBER
                        (COL.2 - 1)
       6-25   TITLEI    CAN BE USED TO DOCUMENT TEST DATA
                        (WILL APPEAR ON PLOT TITLE)
      26-30   NMPT      NUMBER OF PHASE ANGLE POINTS
                        (MUST CORRESPOND TO THE NUMBER OF POINTS INPUT ON
                        (D CARDS. COL.29-30 = 32)
      31-35   SPACE     SPACING BETWEEN ACCELEROMETERS
                        (COL.35 = 2)
D CARD    FORMAT (8F10.0)
     COLUMN  VARIABLE   DESCRIPTION
       1-10    PHI      PHASE ANGLE
      11-20
      21-30
      ETC.
          (THE PHASE ANGLES INPUT ON THE D CARDS MUST CORRESPOND TO THE
          (FOLLOWING FREQUENCIES 25,50,75,100,125,250,375,500,625,750,
          (875,1000,1125,1250,1375,1500,1625,1750,1875,2000,2125,2250,
          (2375,2500,2625,2750,2875,3000,3125,3250,3375,3500.
          (IF ANY PHASE ANGLE IS OMITTED FOR ANY OF THE ABOVE FREQUENCIES
          (A PHASE ANGLE =0. MUST BE ENTERED FOR THOSE FREQUENCIES IN THE
          (APPROPRIATE COLUMNS.  FOUR D CARDS ARE REQUIRED TO INPUT ALL
          (PHASE ANGLES FOR THE ABOVE FREQUENCIES.  IE. 32 VALUES
(B,C,D CARDS MUST BE REPEATED FOR NOTS NUMBER OF TEST STATIONS
```

```
      PROGRAM NOTPLOT(INPUT,OUTPUT,TAPE2,TAPE5=INPUT,TAPE6=OUTPUT)
C     ************************************************************
C     *     THIS PROGRAM, WRITTEN FOR THE AIR FORCE WEAPONS LABORATORY *
C     *BY AMN, P. H. BAKER, USES DATA GATHERED WITH THE NON-DESTRUCTIVE*
C     *PAVEMENT TEST APPARATUS TO CALCULATE THE WAVELENGTH AND VELOCITY*
C     * OF A SHOCK WAVE TRAVELING THROUGH A PAVEMENT TEST SECTION.  THE*
C     *PROGRAM THEN PLOTS THESE VALUES ON RECTILINEAR PAPER TO OBTAIN A*
C     *DISPERSION CURVE, AND PRINTS THE VALUES OF WAVELENGTH AND VELO  *
C     *CITY IN A TABULAR FORM.                                         *
C     *CERF VERSION --- REVISED BY BILL MOORE MAY 1975.                *
C     *                                                               *
C     *                                                               *
C     *NOTS   = NUMBER OF TEST STATIONS ON A RUNWAY OR TAXIWAY        *
C     *IAPAIR = NUMBER USED TO IDENTIFY WHICH PAIRS OF ACC WILL BE USED*
C     *IPAIRS = NUMBER OF ACC PAIRS AT A PARTICULAR STATION OR TEST PIT*
C     *         TO PLOT THE DISPERSION CURVES                         *
C     *TITLE  = NAME OF FACILITY, RUNWAY OR TAXI-WAY                  *
C     *TITLE1 = ACC PAIR (FX,4/6) APPEARS ON PLOT TITLE               *
C     *NMPT   = NUMBER OF DATA POINTS USED                            *
C     *SPACE  = SPACING BETWEEN TEST ACCELEROMETERS USED              *
C     *FREQ   = FREQUENCY OF VIBRATION                                *
C     *PHI    = PHASE ANGLE                                          *
C     *WAVLGT = WAVELENGTH                                           *
C     *WAVVEL = WAVE VELOCITY                                        *
C     ************************************************************
      DIMENSION FREQ(150),PHI(150),WAVLGT(150),WAVVEL(150)
      DIMENSION MAXWL(12),MAXWV(12),MINWL(12),MINWV(12)
      DIMENSION LGT1(6,150),VEL1(6,150)
      DIMENSION WVPLT(150),WLPLT(150)
      DIMENSION TITLE(4),TITLE1(2),SAVE(6)
      REAL MAXWL,MAXWV,MINWL,MINWV,LGT1
      DATA FREQ /25.,50.,75.,100.,125.,250.,375.,500.,625.,
     1750.,875.,1000.,1125.,1250.,1375.,1500.,1625.,1750.,
     21875.,2000.,2125.,2250.,2375.,2500.,2625.,2750.,2875.,
     33000.,3125.,3250.,3375.,3500./
      CALL PLOTS(    0,0,2)
      WRITE(6,7000)
      XSCALE = 10./20.
      YSCALE = 8. / 8000.
      READ(5,103) NOTS
      WRITE(6,103) NOTS
      DO 888 K=1,NOTS
      DO 15 J=1,6
      DO 20 I=1,150
      LGT1(J,I)=VEL1(J,I)=0.
   20 CONTINUE
   15 CONTINUE
      READ(5,105) TITLE,IPAIRS
      WRITE(6,105) TITLE,IPAIRS
      DO 10 L=1,IPAIRS
      READ(5,110) IAPAIR,TITLE1,NMPT,SPACE
      WRITE(6,111) IAPAIR,TITLE1,NMPT,SPACE
      SAVE(L)=IAPAIR
      READ(5,140) (PHI(I),I=1,NMPT)
      WRITE(6,140) (PHI(I),I=1,NMPT)
      MAXWL(IAPAIR) = MAXWV(IAPAIR) = 0.
      MINWL(IAPAIR) = MINWV(IAPAIR) = 9999.
      DO 100  I = 1,NMPT
C     ***  CALCULATE WAVELENGTH  ***
      IF(PHI(I).EQ.0.) GO TO 401
      WAVLGT(I) = 360 * SPACE / PHI(I)
      GO TO 402
  401 CONTINUE
```

```
      WAVLGT(I)=0.
  402 CONTINUE
      IF(WAVLGT(I).LT.MINWL(IAPAIR))MINWL(IAPAIR) = WAVLGT(I)
      IF(WAVLGT(I).GT.MAXWL(IAPAIR))MAXWL(IAPAIR) = WAVLGT(I)
C     ***  CALCULATE WAVE VELOCITY  ***
      WAVVEL(I) = FREQ(I) * WAVLGT(I)
      IF(WAVVEL(I).GT.8000.) WAVVEL(I)=8000.
      IF(WAVVEL(I).GT.MAXWV(IAPAIR))MAXWV(IAPAIR) = WAVVEL(I)
      IF(WAVVEL(I).LT.MINWV(IAPAIR))MINWV(IAPAIR) = WAVVEL(I)
      LGT1(IAPAIR,I) = WAVLGT(I)
      VEL1(IAPAIR,I) = WAVVEL(I)
  100 CONTINUE
C     ***  DRAW AXES FOR PLOT  ***
      CALL AXIS(0.,1.,0.,20.,-5,1.,2.,4HF4.0,0.,10HWAVELENGTH,10)
      CALL AXIS(0.,1.,0.,8000.,-001,500.,1000.,4HF5.0,90.,13HWAVE VELOCI
     1TY,13)
      CALL SYMBOL(6.0,8.5,0.14,TITLE(1),0.0,20)
      CALL SYMBOL(6.0,8.25,0.14,TITLE(3),0.0,20)
      CALL SYMBOL(6.0,8.0,0.14,TITLE1(1),0.0,20)
      DO 500  I = 1,NMPT
      WVPLT(I) = YSCALE * (WAVVEL(I)) + 1.
      IF(WAVLGT(I).GT.20.) WAVLGT(I)=20.
      WLPLT(I) = XSCALE * (WAVLGT(I))
C     ***  PLOT WAVE VELOCITY AS A FUNCTION OF WAVELENGTH  ***
      CALL SYMBOL(WLPLT(I),WVPLT(I),.10,3,0.0,-1)
  500 CONTINUE
      CALL PLOT (15.,0.,-3)
C     ***  TABULATE RESULTS  ***
      WRITE(6,200)
      WRITE(6,210)
      WRITE(6,215)
      WRITE(6,220)((LGT1(J,I),VEL1(J,I),J = 1,6),FREQ(I),I=1,NMPT)
      WRITE(6,230)
      WRITE(6,240)(MAXWL(J),MAXWV(J),J = 1,6)
      WRITE(6,250)
      WRITE(6,260)(MINWL(J),MINWV(J),J = 1,6)
   10 CONTINUE
      IF(IPAIRS.EQ.1) GO TO 888
      CALL AXIS(0.,1.,0.,20.,-5,1.,2.,4HF4.0,0.,10HWAVELENGTH,10)
      CALL AXIS(0.,1.,0.,8000.,-001,500.,1000.,4HF5.0,90.,13HWAVE VELOCI
     1TY,13)
      CALL SYMBOL(6.0,8.5,0.14,TITLE(1),0.0,20)
      CALL SYMBOL(6.0,8.25,0.14,TITLE(3),0.0,20)
      CALL SYMBOL(6.0,8.0,0.14,9HCOMPOSITE,0.0,9)
      DO 600 KK=1,IPAIRS
      J=SAVE(KK)
      DO 610 I=1,NMPT
      WVPLT(I)=YSCALE*(VEL1(J,I))+1.
      WLPLT(I)=XSCALE*(LGT1(J,I))
      CALL PLOT(WLPLT(I),WVPLT(I),3)
      CALL PLOT(WLPLT(I),WVPLT(I),2)
  610 CONTINUE
  600 CONTINUE
      CALL PLOT(15.,0.,-3)
  888 CONTINUE
      CALL PLOT(0.,0.,999)
      STOP 0
  103 FORMAT(I5)
  105 FORMAT(4A10,3X,I2)
  106 FORMAT(//2X,4A10,3X,I2)
  110 FORMAT(I2,3X,2A10,I5,F5.0)
  111 FORMAT(2X,I2,3X,2A10,I5,F5.0)
  140 FORMAT(8F10.0)
  200 FORMAT(1H1,8X,*1/3*,17X,*2/4*,17X,*3/5*,17X,*4/6*,17X,*1/5*,17X,*2
     1/6*)
```

```
  210 FORMAT(1H0,2X,*LGT(1)*,4X,*VFL(1)*,4X,*LGT(2)*,4X,*VFL(2)*,4X,*LGT
     1(3)*,4X,*VFL(3)*,4X,*LGT(4)*,4X,*VFL(4)*,4X,*LGT(5)*,4X,*VFL(5)*,
     24X,*LGT(6)*,4X,*VFL(6)*,4X,*FREQ*)
  215 FORMAT(1H , )
  220 FORMAT(13F10.3)
  230 FORMAT(1H ,1X,*MAXWL(1)*,2X,*MAXWV(1)*,2X,*MAXWL(2)*,2X,*MAXWV(2)*
     1,2X,*MAXWL(3)*,2X,*MAXWV(3)*,2X,*MAXWL(4)*,2X,*MAXWV(4)*,2X,*MAXWL
     2(5)*,2X,*MAXWV(5)*,2X,*MAXWL(6)*,2X,*MAXWV(6)*)
  240 FORMAT(12F10.3)
  250 FORMAT(1H ,1X,*MINWL(1)*,2X,*MINWV(1)*,2X,*MINWL(2)*,2X,*MINWV(2)*
     1,2X,*MINWL(3)*,2X,*MINWV(3)*,2X,*MINWL(4)*,2X,*MINWV(4)*,2X,*MINWL
     2(5)*,2X,*MINWV(5)*,2X,*MINWL(6)*,2X,*MINWV(6)*)
  260 FORMAT(12F10.3)
 7000 FORMAT(*1*)
      END
      SUBROUTINE AXIS(X,Y,VI,VF,SCALE,TIC,DLBL,FMT,THETA,LBL,NC)
C
C        LATEST CHANGE  --  AUGUST 7, 1973.
C
      DATA DTR,IBLANK/0.0174532925,1H /
      CTH=COS(THETA*DTR)
      TCC=0.05*CTH
      STH=SIN(THETA*DTR)
      TCS=0.05*STH
      N=(VF-VI)/TIC + 1.000001
      CALL PLOT(X,Y,3)
      M=DLBL/TIC + 0.000001
      XX=X
      YY=Y
      XINC=CTH*TIC*SCALE
      YINC=STH*TIC*SCALE
      DO 10 I=1,N
      F=1+(M-MOD(I-1,M))/M
      CALL PLOT(XX,YY,2)
      CALL PLOT(XX-F*TCS,YY+F*TCC,2)
      CALL PLOT(XX+F*TCS,YY-F*TCC,2)
      CALL PLOT(XX,YY,2)
      XX=XX+XINC
   10 YY=YY+YINC
      CALL PLOT(X+CTH*(VF-VI)*SCALE,Y+STH*(VF-VI)*SCALE,2)
      CALL PLOT(X,Y,2)
      XINC=CTH*DLBL*SCALE
      YINC=STH*DLBL*SCALE
      N=(VF-VI)/DLBL+1.000001
      DELX=-STH*SIGN(0.50,THETA)-0.30
      DELY= CTH*SIGN(0.15,THETA)-0.05
      IF (THETA .EQ. 0.) DELY=-.20
      DO 20 I=1,N
      F=I-1
      V=VI+F*DLBL
      XX=X+F*XINC+DELX + .25
      YY=Y+F*YINC+DELY
   20 CALL NUMBER(XX,YY,0.10,V,0.,-1)
      IF (NC .LT. 11 .AND. LBL .EQ. IBLANK) RETURN
      XX=0.5*SCALE*(VF-VI)-0.06*NC
      YY=SIGN(1./(2.-ABS(STH)),THETA)
      IF (THETA .EQ. 0.) YY=-0.50
      EPS=0.001                    $     IF (ABS(THETA) .GT. 360.) EPS=-0.001
      N=(IABS(INT(THETA-EPS))+90)/180 * SIGN(1.,THETA)
      ANG=THETA-180.*N
      IF (MOD(N,2) .NE. 0) XX=XX+0.12*NC
      XXX=X+XX*CTH-YY*STH    $      YYY=Y+XX*STH+YY*CTH
      CALL SYMBOL(XXX,YYY,0.15,LBL,ANG,NC)
      RETURN
      END
```

APPENDIX D

PROGRAM PREDICT USER'S MANUAL

```
C                  PREDICT DATA CARD SPECIFICATIONS
C                       (CERF VERSION)
C
C
C A.TITLE AND SOLUTION TYPE CARD (  A8,17A4,1X,A2)
C    COLUMN   VARIABLE    DESCRIPTION
C
C      1-8    TITLE(1)    AIRCRAFT NAME(LEFT JUSTIFIED)
C
C      9-76   TITLE(2)    NAME OF AIRBASE
C                          RUNWAY OR TAXIWAY NUMBER
C                          DATE OR OTHER PERTINENT DATA
C
C     78-79   LRWIP       RUNWAY TYPE
C                          T = CHANNELIZED TRAFFIC AREAS (LEFT JUSTIFIED)
C                          RA = NON-CHANNELIZED TRAFFIC AREAS
C
C
C B. LOAD FACTORS AND PRINT CONTROLS (12,1X,F3.0,2(1X,I1),5X,F10.0,I5)
C     COLUMN  VARIABLE    DESCRIPTION
C
C     1-2     NUMLAY      NUMBER OF MATERIAL LAYERS (MAX = 10)
C                         (MUST BE GREATER THAN ZERO BUT .LE. 10)
C
C
C     4-6     PSI         TIRE PRESSURE (PSI)
C                         0 = DEFAULTS TO STANDARD AFCAN VALUE
C                         (USER VALUE MUST BE BETWEEN 70 AND 350 PSI)
C
C     8       KPPRE       PRINT CONTROL FOR AFPRE OUTPUT
C                         (ALWAYS USE 1)
C
C     10      KPPAV       PRINT CONTROL FOR AFPAV OUTPUT
C                         (ALWAYS USE L)
C
C     16-25   WLOAD       SINGLE TIRE LOAD (POUNDS)
C                         1 = DEFAULTS TO STANDARD AFCAN VALUE
C                         (USER VALUE MUST BE .GT. 0.)
C
C     26-30   LCONCOP     CONCRETE SPLIT TENSILE STRENGTH IN PSI
C                         ( WHEN MATERIAL TYPE IS CONCRETE,LCONCOP MUST
C                           BE GREATER THAN ZERO BUT .LE. 1500 )
C
C C. LAYER MATERIAL PROPERTIES CARD
C     (F4.0,1X,A1,I1,F8.0,1X,F3.2,5X,F1.0,5X,F5.3,2X,F3.0,2X,F3.0)
C
C     ( NOTE- ONE C-CARD IS REQUIRED FOR EACH LAYER, THAT IS NUMBER
C       OF C-CARDS MUST EQUAL NUMLAY )
C
C     COLUMN  VARIABLE    DESCRIPTION
C
C      1-4    THICK       LAYER THICKNESS (INCHES)
C                         ( THE SUM OF THICK FOR ALL LAYERS MUST
C                         EQUAL 144 INCHES)
C
C      6      MATID       MATERIAL IDENTIFICATION CODE
C                         C = PORTLAND CEMENT CONCRETE
C                         A = ASPHALT WEARING SURFACE
C                         B = BASE OR SUBBASE
C                         S = SUBGRADE
```

```
C                              X = SPECIAL MATERIAL
C
C      7          MATCHSR      MATERIAL PROPERTIES CHECK
C                              0 = PROPTY(1) MUST FALL WITHIN AFCAN
C                                  ACCEPTABLE RANGE
C                              1 = PERMITS PROPTY(1) VALUES OUTSIDE
C                                  AFCAN ACCEPTABLE RANGE
C
C                              ( AFCAN ACCEPTABLE RANGES FOR PROPTY(1) )
C
C                              ASPHALT - .GE. 20000 BUT .LE. 2000000
C                              CONCRETE - .GE. 2000000 BUT .LE. 5000000
C                              BASE OR SUBBASE - .GE. 5000 BUT .LE. 100000
C                              SUBGRADE - .GE. 500 BUT .LE. 20000
C                              SPECIAL MATERIAL - .GE. 500
C
C      8-15       PROPTY(1)    CORRECTED ELASTIC MODULUS FROM THE
C                              NDPT VAN
C
C      17-19      PROPTY(2)    POISSONS RATIO
C                              0 = DEFAULTS TO STANDARD AFCAN VALUE
C                              (USER VALUE MUST BE BETWEEN 0. AND .5)
C
C      25         STYPE        LAYER SOIL TYPE
C                              1 = NON-PLASTIC WITH FINES AND LOW PLASTICITY
C                              2 = HIGH-PLASTICITY,LL ABOVE 50
C                              3 = CLEAN SANDS
C                              4 = CLEAN GRAVELS, POORLY GRADED SAND/GRAVEL
C                                  MIXTURES
C                              5 = WELL-GRADED SAND/GRAVEL
C                              (WHEN MATERIAL TYPE IS ASPHALT OR CONCRETE,
C                              STYPE MUST EQUAL 0.)
C
C      31-35      ERATIO       LAYER VOID RATIO,EXPRESSED AS A DECIMAL
C                              (WHEN MATERIAL TYPE IS ASPHALT OR CONCRETE,
C                              ERATIO MUST EQUAL 0.)
C                              (WHEN MATERIAL TYPE IS B,S,OR X,ERATIO
C                              MUST BE BETWEEN .2 AND 2.)
C
C      38-40      SATUR        LAYER SATURATION,EXPRESSED AS A PERCENT
C                              (WHEN MATERIAL TYPE IS ASPHALT OR CONCRETE,
C                              SATUR MUST EQUAL 0.)
C                              (WHEN MATERIAL TYPE IS B,S,OR X, SATUR MUST
C                              BE BETWEEN 0 AN+ 100)
C
C      43-45      PI           LAYER PLASTICITY INDEX,EXPRESSED AS A PERCENT
C                              (WHEN MATERIAL TYPE IS ASPHALT OR CONCRETE PI
C                              MUST EQUAL 0.)
C                              (WHEN MATERIAL TYPE IS B,S, OR X, PI MUST BE
C                              BETWEEN 0 AND 100)
C
C  D. END CARD (A3)
C      COLUMN     VARIABLE     DESCRIPTION
C
C      1-3        TITLE(1)     COLUMNS 1-3 MUST HAVE END IN THEM
C
C      (NOTE-ONLY ONE D-CARD IS REQUIRED. IT WILL ALWAYS BE THE LAST
C      CARD IN THE DATA DECK.)
C
```

```
C
C     REPEAT A,B, AND C CARDS FOR EACH PROBLEM
C
C
C     SAMPLE PROBLEMS
C
C                                        COLUMN NUMBER
1    5    10        20        30        40        50        60        70        80
          -----                          ----                ---------
F111      WEAK ASPHALT-CONCRETE                                                RA
 4      1 1           30000
    4 A1   150000
    4 B1    88700 .30      5        .22
    8 B1    32100 .35      5        .25
  128 B1    15000 .40      1        .45    80    13
F111      STRONG ASPHALT-CONCRETE                                              RA
 4      1 1                1 3000
    4 A1   500000
    4 B1    88700 .30      5        .22
    8 B1    32100 .35      5        .25
  128 B1    15000 .40      1        .45    80    13
B52       ASPHALT TEST PROBLEM--MULTIWHEEL                                     RA
 4      1 1                1
    8 A1   721600 .38
    4 B1    88700          5        .22
    8 B     32100 .35      5        .25
  124 B     15000          1        .45    80    13
END
```


(The reverse of this page is blank)

REFERENCES

1. Nielsen, J. P., Rational Pavement Evaluation - Review of Present Technology, AFWL-TR-69-9, Air Force Weapons Laboratory, Kirtland Air Force Base, New Mexico, Vol. I, October 1969; Vol. II, May 1970.

2. Crawford, J. E., An Analytical Model for Airfield Pavement Analysis, AFWL-TR-71-70, Air Force Weapons Laboratory, Kirtland Air Force Base, New Mexico, May 1972.

3. Nielsen, J. P., AFPAV Computer Code for Structural Analysis of Airfield Pavements, AFWL-TR-75-151, Air Force Weapons Laboratory, Kirtland Air Force Base, New Mexico, October 1975.

4. Crawford, J. E., Software for Everyday Usage of AFPAV, Technical Memorandum M-51-76-06, Civil Engineering Laboratory, Port Hueneme, California, March 1976.

5. Hardin, B. O., Constitutive Relationships for Airfield Subgrade and Base Course Materials, Technical Report UKY 32-71-CE5, College of Engineering, University of Kentucky, Lexington, Kentucky.

6. Baird, [illegible] T., et al., Instruction Manual for Mobile Nondestructive Vibra[illegible]est Equipment, AFWL-TR-74-301, Air Force Weapons Laboratory, Kirt[illegible] Force Base, New Mexico, August 1975.

7. Rao, H. A. B., Nondestructive Evaluation of Airfield Pavements (Phase I), AFWL-TR-71-75, Air Force Weapons Laboratory, Kirtland Air Force Base, New Mexico, December 1971.

8. O'Brien, Ken and Associates, Distress Criteria for Pavement Systems, AFWL-tr-73-226, Air Force Weapons Laboratory, Kirtland Air Force Base, New Mexico, April 1974.

9. Hammitt, G. M., et al., Multiple-Wheel Heavy Gear Load Pavement Tests, AFWL-TR-70-113, Vol. IV, Air Force Weapons Laboratory, Kirtland Air Force Base, New Mexico, November 1971.

10. Hall, J. W. and J. L. Green, Nondestructive Vibratory Testing of Airport Pavements, Vol. I, Evaluation Methodology and Experimental Test Results, FAA Report, US Department of Transportation, Federal Aviation Administration, Washington, D.C., December 1973.

11. Lysmer, J., Vertical Motion of Rigid Footings, Contract Report No. 3-115, University of Michigan, ORA Project 05366, Ann Arbor, Michigan, June 1975.

12. Nielsen, J. P., Develop Pavement Evaluation System, Progress Report No. 3 (T.D. 5.11/00), Civil Engineering Research Facility, University of New Mexico, Albuquerque, New Mexico, December 30, 1974.

13. Nielsen, J. P., CERF letter to Major George D. Ballentine, AFWL/DEZ, Kirtland Air Force Base, New Mexico, February 20, 1975.

14. Nielsen, J. P. and Glenn T. Baird, Air Force System for Nondestructive Testing of Pavements, Symposium on Nondestructive Test and Evaluation of Airport Pavements, Waterways Experiment Station, Corps of Engineers, Vicksburg, Mississippi, November 1975.

15. Nielsen, J. P. and Glenn T. Baird, Nondestructive Pavement Load Rating, Thirteenth Paving Conference, University of New Mexico, Albuquerque, New Mexico, January 1976.

16. Crawford, J. and R. Pichumani, Finite-Element Analysis of Pavement Structures Using AFPAV Code (Nonlinear Elastic Analysis), AFWL-TR-74-71, Air Force Weapons Laboratory, Kirtland Air Force Base, New Mexico, April 1975.

17. Crawford, J. E., Unpublished user's manual on AFCAN. Contract report to be prepared for AFCEC by CEL. Publication date unknown.

18. Hay, D. R., Aircraft Characteristics for Pavement Design and Evaluation, AFWL-TR-69-54, Air Force Weapons Laboratory, Kirtland Air Force Base, New Mexico, October 1969.

19. Monismith, C. L. and D. B. McLean, "Structural Design Considerations," Proceedings, Association of Asphalt Paving Technologists, Cleveland, Ohio, 1966.

20. Packard, R. G., "Design of Concrete Airport Pavement," Engineering Bulletin, Portland Cement Association, 1973.

21. Nielsen, J. P., Airfield Test Plan, CERF Letter Report, Aerospace Facilities Branch, Air Force Weapons Laboratory, Kirtland Air Force Base, New Mexico, February 20, 1975.

22. Nielsen, J. P., Development of Pavement Evaluation System, Progress Report No. 2 (T.D. 5.01/00), Civil Engineering Research Facility, Kirtland Air Force Base, New Mexico, January 31, 1976.

23. Dobrin, Milton B., Introduction to Geophysical Prospecting, 2nd Edition, McGraw-Hill, New York, 1960.

24. Jones, R., Thrower, E. N. and E. N. Gatfield, "Surface Wave Method," Proceedings of the 2nd Inter. Conf. on the Structural Design of Asphalt Pavements, University of Michigan, August 7-11, 1967.

25. Personal communications with Professor John Lysmer, Civil Engineering Department, University of California, Berkeley, California, February 4, 1976.

26. Rao, H. A. B., Results of Nondestructive Tests at Webb Air Force Base, Letter Report III, Civil Engineering Research Facility, Albuquerque, New Mexico, August 1973.

27. Finn, Fred, McCullough, B. F., Nair, Keshaven and R. G. Hicks, Plan for Development of Nondestructive Method for Determination of Load-Carrying Capacity of Airfield Pavements, Final Report No. 1062-2(F), Materials Research and Development, Inc., Oakland, California, November 1966.

28. Yoder, E. J. and M. W. Witczak, Principles of Pavement Design, 2nd Edition, John Wiley and Sons, New York, 1975.

29. Nielsen, J. P., Layered Pavement Systems: Analysis Related to Design, Technical Report R-594, Civil Engineering Laboratory, Port Hueneme, California, September 1968.

ABBREVIATIONS, ACRONYMS, AND SYMBOLS

E	elastic modulus (Young's)
$\{F\}$	force vector
F_{u_i}	force at node i which produces a displacement in the y-direction
G	shear modulus
V_R	Rayleigh wave velocity
V_s	shear wave velocity
d	distance between compared accelerometers
f	frequency
$f(z)$	tire pressure defined over tire length
g	acceleration constant
n	number of terms
p	half-period of function
v	phase velocity
γ	unit weight of material
λ	wavelength
υ	Poisson's ratio
σ_x, σ_y	boundary stresses
ϕ	phase angle

INITIAL DISTRIBUTION

Hq USAF/PRE	1
AFISC/PQUAL	1
Hq AFSC/DE	1
Hq AFSC/DLCAM	1
Hq TAC/DEE	1
Hq SAC/DEE	1
Hq AFLC/DEE	1
Hq ADCOM/DEE	1
Hq AUL/LDE	1
Hq AAC/DEE	1
AFIT/Tech Lib	1
AFIT/CES	1
Hq USAFE/DEE	1
Hq PACAF/DEE	1
USAFA/DFCE	1
ASD/DEE	1
SAMSO/DEE	1
ESD/DEE	1
AFATL/DLOSL	1
Hq ADTC/DEE	1
Hq ATC/DE	1
RADC/DEE	1
USAF Reg Civil Eng	2
Chief of Eng/DAEN-RDM	1
AFCEC/EMR	5
CERL	1
Hq MAC/DEMP	1
Dir, USAF Eng WW Exp Stn	1
AFCEC/PR	1
AFCEC/EMP	10
CEL/Naval Const Battalion Ctr	1
DDC	12

(The reverse of this page is blank)